

2-28-18
62208630

This is to certify that the
dissertation entitled

Design And Fabrication Of A Micro-Impedance Biosensor For
Detecting Pathogenic Bacteria

presented by

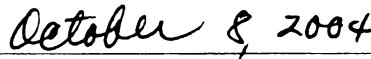
Stephen M. Radke

has been accepted towards fulfillment
of the requirements for the

Ph.D. degree in Biosystems Engineering



Major Professor's Signature



Date

**LIBRARY
Michigan State
University**

PLACE IN RETURN BOX to remove this checkout from your record.
TO AVOID FINES return on or before date due.
MAY BE RECALLED with earlier due date if requested.

DATE DUE	DATE DUE	DATE DUE

**DESIGN AND FABRICATION OF A MICRO-IMPEDANCE BIOSENSOR
FOR DETECTING PATHOGENIC BACTERIA**

By

Stephen M. Radke

A DISSERTATION

**Submitted to
Michigan State University
in partial fulfillment of the requirements
for the degree of**

DOCTOR OF PHILOSOPHY

Department of Biosystems and Agricultural Engineering

2004

ABSTRACT

DESIGN AND FABRICATION OF A MICRO-IMPEDANCE BIOSENSOR FOR DETECTING PATHOGENIC BACTERIA

By

Stephen M. Radke

A biosensor for bacterial detection was developed based on microelectromechanical systems (MEMS), heterobifunctional crosslinkers and immobilized antibodies. The sensor detected the change in impedance caused by the presence of bacteria immobilized on interdigitated gold electrodes. Fabricated from (100) silicon with a 2 μ m layer of thermal oxide as an insulating layer, the sensor active area was 9.6mm² and consisted of two interdigital gold electrode arrays each measuring 0.8mm x 6mm. *Escherichia coli* specific antibodies were immobilized to the silicon oxide between the electrodes to create a biological sensing surface. The electrical impedance across the interdigital electrodes was measured at frequencies between 100Hz to 10MHz after immersing the biosensor in a neutral buffer. Bacterial cells present in the sample solution attached to the antibodies and became tethered to the sensor surface thereby causing a change in measured impedance. The biosensor was tested using pathogenic and non-pathogenic *E. coli* strains and was able to discriminate between different cellular concentrations from 10⁵ - 10⁷ CFU/mL (colony-forming units per milliliter) in pure culture. The design, fabrication and testing of the biosensor is discussed along with the implications of these findings towards developing a biosensor for the detection of foodborne pathogens.

© Copyright By
STEPHEN M. RADKE
2004

ACKNOWLEDGEMENTS

I would like to express my gratitude to my fellow coworkers Lisa Marie Kindschy, Finny Papachan Mathew, Zarini Binti Muhammad-Tahir and Maria Ivelisse Rodriguez and also to those undergraduates who have worked in our laboratory over the years. I also wish to thank Dr. Evangelyn C. Alocilja for being a constant source of motivation, encouragement and support. Lastly, I would like to thank the USDA for financial support in the way of a National Needs Doctoral Fellowship. Thank you.

TABLE OF CONTENTS

LIST OF TABLES.....	vii
LIST OF FIGURES.....	viii
CHAPTER 1. INTRODUCTION.....	1
1.1 Objectives and Goals.....	1
1.2 Foodborne Pathogens and Food Safety.....	1
1.3 Market Analysis for Pathogen Detection.....	3
1.4 Biosecurity and Agroterrorism.....	4
1.5 Routes of Infection.....	6
1.6 Use of Biosensors and Rapid Detection Methods.....	7
1.7 Novelty of Research.....	14
1.8 Hypothesis and Specific Aims.....	15
CHAPTER 2. LITERATURE REVIEW.....	16
2.1 Overview of the Biosensor.....	16
2.2 Lipid Bilayer Membrane Theory.....	18
2.3 Biological Recognition.....	20
2.4 Membrane Impedance Theory.....	22
2.5 Impedance Measurements.....	25
2.6 Circuit Elements.....	27
2.7 Electrode Spacing Model.....	33
2.8 Immobilization Methods.....	35
2.9 Microfabrication.....	37
CHAPTER 3. MATERIALS AND METHODS.....	41
3.1 Microfabrication of the Biosensor.....	42
3.2 Functionalizing the Biosensor Surface.....	44
3.3 Validation of the Biosensor.....	47
3.4 Signal Measurement.....	49
3.5 Statistical Analysis.....	49
3.6 Specificity Study.....	50
3.7 Testing in Complex Media.....	52
3.8 Facilities and Equipment.....	52
CHAPTER 4. RESULTS AND DISCUSSION.....	53
4.1 Simulation Results.....	53
4.2 Fabrication Results.....	60
4.3 Results and Discussion of Pure Culture Testing.....	67
4.3.1 Frequency Dependence.....	67
4.3.2 Effect of Non-Pathogenic and Pathogenic Bacteria.....	71

4.4 Results and Discussion of Specificity Study.....	77
4.5 Summary and Conclusions.....	82
4.6.1 Summary of Lower Detection Limits.....	82
4.6.2 Innovation and Future Possibilities.....	83
APPENDICES.....	84
Appendix A: US Foodborne Disease Outbreak Data.....	85
Appendix B: Materials, Methods and Bill of Process Supplemental.....	86
Appendix C: Results and Discussion.....	94
Appendix D.1: Testing in Complex Media.....	103
D.1.1 Testing of Romaine Lettuce.....	103
D.1.2 Testing of Ground Beef.....	104
D.1.3 Testing of Bovine Feces.....	105
Appendix D.2: Results and Discussion of Testing in Complex Media.....	106
D.2.1 Results for Romaine Lettuce Testing.....	106
D.2.2 Results for Ground Beef Testing.....	109
D.2.3 Results for Bovine Feces Testing.....	112
Appendix D.3: Summary and Conclusions.....	116
D.3.1 Summary of Lower Detection Limits.....	116
Appendix E: Business Plan.....	118
BIBLIOGRAPHY.....	141

LIST OF TABLES

Table 1.1 Food illness in the US caused by major foodborne pathogens.....	2
Table 1.2 Sample of recent product recalls due to pathogen contamination.....	3
Table 1.3 US food industry total microbial tests per sector.....	3
Table 1.4 Novelty of research compared to existing electrochemical biosensors.....	14
Table 3.1 Specificity testing matrix.....	51
Table 4.1 Comparison matrix of simulation sizes.....	58
Table A.1 Reported and estimated cases of foodborne illness by agent type in the US.....	84
Table A.2 Reported and estimated cases of foodborne illness by surveillance type in the US.....	85
Table B.1 Bill of process for microfabrication of the biosensor.....	86
Table B.2 Bill of process for surface functionalization of the biosensor.....	87
Table B.3 Bill of process for testing in ground beef samples.....	87
Table B.4 Bill of process for testing in romaine lettuce samples.....	88
Table B.5 Bill of process for testing in bovine feces samples.....	88
Table B.1 Bill of process for reagents used in the research.....	89

LIST OF FIGURES

Figure 1.1 A Schematic of the food supply chain showing potential entry points for contamination of foodborne pathogens.....	8
Figure 2.1 Schematic of biosensor detection theory.....	16
Figure 2.2 Electric field between: (a) interdigital electrode array; (b) cross-section of interdigital array with immobilized bacteria on the surface.....	18
Figure 2.3 Cross-section of lipid bilayer membrane showing charged hydrophilic phospholipid head groups and hydrophobic fatty acid tail groups.....	19
Figure 2.4 Antibody schematic.....	21
Figure 2.5 Schematic of dispersion in a cell at low (a) and high (b) frequencies.....	24
Figure 2.6 Idealized spectrum of the dielectric properties of cell suspensions.....	25
Figure 2.7 Impedance spectrum of ideal RC circuit showing reactive and resistive components.....	27
Figure 2.8 Schematic of the electrode-solution interface showing inner and outer Helmholtz planes.....	29
Figure 2.9 Equivalent circuit of the impedance measurement system with electrodes in solution.....	30
Figure 2.10 Circuit model for the impedance of bacteria immobilized between two interdigitated electrodes.....	32
Figure 2.11 Calculated electric field lines (a) above interdigital electrodes; (B) as a function of electrode spacing ratio.....	34
Figure 2.12 Antibody immobilization method.....	36
Figure 2.13 The sequence of a typical lift off process.....	39
Figure 3.1 (3-Mercaptopropyl) trimethyloxysilane (MTS) used for silanization.....	45
Figure 3.2 <i>N</i> - γ -maleimidobutyryloxy succinimide ester (GMBS) for crosslinking.....	45
Figure 3.3 Process of antibody attachment to the silicon oxide.....	46

Figure 3.4 Biosensor test apparatus in raised and lowered position.....	48
Figure 4.1 Simulation results for different electrode widths and spacing: (a) 1 μ m x 1 μ m array; (b) 6 μ m x 6 μ m array; (c) 5 μ m x 10 μ m array and (d) 10 μ m x 5 μ m array.....	54
Figure 4.2 Electric field simulation of 4 μ m x 3 μ m electrode array: (top) electric field magnitude; (bottom) vector representation of electric field.....	56
Figure 4.3 Surface plot of the electric field distribution at 2 μ m from electrode array.....	57
Figure 4.4 Percentage of electric field above sensor surface.....	57
Figure 4.5 Simulation of 3 μ m x 4 μ m array with immobilized bacteria: (top) electric field magnitude; (bottom) vector representation of electric field.....	59
Figure 4.6 Maxwell 3D simulation of the electric field on sensor surface.....	59
Figure 4.7 A 4" Silicon wafer before (left) and after (right) processing.....	60
Figure 4.8 CAD Drawing of Biosensor: (left) biochip layout; (top-right) close-up of electrode arrays; (bottom-right) detail of electrode arrays.....	61
Figure 4.9 Die shot of biosensor; high density electrode arrays; close up of electrodes...	62
Figure 4.10 Quality control diagram showing likely locations for damaged dies.....	64
Figure 4.11 AFM of electrodes; bacteria immobilized to surface.....	65
Figure 4.12 CLSM showing antibody immobilized to electrode and oxide.....	65
Figure 4.13 The effects of surface modification: (left) clean biosensor surface; (right) silanized biosensor surface.....	66
Figure 4.14 Impedance for a frequency distribution from 10Hz-10MHz for non-pathogenic <i>E. coli</i>	68
Figure 4.15 Impedance for a Frequency Distribution from 10Hz-10MHz for a Pure Culture of <i>E. coli</i> O157:H7.....	69
Figure 4.16 Comparison of <i>E. coli</i> and <i>E. coli</i> O157:H7 at selected frequencies: (top) 1kHz; (middle) 100kHz; (bottom) 10MHz.....	72
Figure 4.17 Cole-Cole plot showing the real and imaginary impedance with time.....	74

Figure 4.18 SEM micrographs of bacteria bound to the sensor surface: (a) sample of 10^2 CFU/mL; (b) sample of 10^6 CFU/mL.....	76
Figure 4.19 Statistical significance of mean differences between concentrations for pure culture.....	77
Figure 4.20 Impedance for a frequency distribution from 100Hz - 10MHz for a pure culture of <i>S. infantis</i>	78
Figure 4.21 Impedance for a frequency distribution from 100Hz - 10MHz for a mixed culture of <i>S. infantis</i> and <i>E. coli</i> O157:H7.....	79
Figure 4.22 Comparison of <i>E. coli</i> O157:H7, <i>S. infantis</i> , and mixed culture at selected frequencies: (top) 1kHz; (middle) 100kHz; (bottom) 10MHz.....	80
Figure 4.23 Statistical significance of mean differences between concentrations for specificity study.....	82
Figure B.1 Screen capture of user interface for LabVIEW 6.1.....	90
Figure B.2 Screen capture of circuit diagram for LabVIEW 6.1.....	90
Figure B.3 Clamp without biochip.....	91
Figure B.4 Clamp with biochip in locating chuck.....	91
Figure B.5 Apparatus setup.....	92
Figure B.6 Apparatus setup engaged in specimen testing.....	92
Figure B.7 Detail of contact mating to biochip.....	93
Figure B.8 Wiring schematic showing HP 4192A impedance analyzer connected to biosensor.....	93
Figure C.1 Vector representation of electric field simulation of $1\mu\text{m} \times 1\mu\text{m}$ array.....	94
Figure C.2 Surface plot of the electric field distribution at a $2\mu\text{m}$ distance from a $1\mu\text{m} \times 1\mu\text{m}$ electrode array.....	95
Figure C.3 Vector representation of electric field simulation of $10\mu\text{m} \times 5\mu\text{m}$ array.....	96
Figure C.4 Surface plot of the electric field distribution at a $2\mu\text{m}$ distance from a $10\mu\text{m} \times 5\mu\text{m}$ electrode array.....	97
Figure C.5 Vector representation of electric field simulation of $5\mu\text{m} \times 10\mu\text{m}$ array.....	98

Figure C.6 Surface plot of the electric field distribution at a 2 μ m distance from a 5 μ m x 10 μ m electrode array.....	99
Figure C.7 Vector representation of electric field simulation of 6 μ m x 6 μ m array.....	100
Figure C.8 Surface plot of the electric field distribution at a 2 μ m distance from a 6 μ m x 6 μ m electrode array.....	101
Figure C.9 3-D rendering of CAD layout file depicting biosensor.....	102
Figure D.1 Representative samples of romaine lettuce, ground beef and bovine feces.....	103
Figure D.2 Impedance for a frequency distribution from 100Hz - 10MHz for lettuce samples inoculated with <i>E. coli</i> O157:H7.....	107
Figure D.3 Comparison of romaine lettuce samples inoculated with <i>E. coli</i> O157:H7 at selected frequencies: (top)1kHz; (middle)100kHz; (bottom)10MHz.....	108
Figure D.4 Impedance for a frequency distribution from 100Hz - 10MHz for ground beef samples inoculated with <i>E. coli</i> O157:H7.....	110
Figure D.5 Comparison of ground beef samples inoculated with <i>E. coli</i> O157:H7 at selected frequencies: (top) 1kHz; (middle) 100kHz; (bottom) 10MHz.....	111
Figure D.6 Impedance for a frequency distribution from 100Hz - 10MHz for a manure samples inoculated with <i>E. coli</i> O157:H7.....	114
Figure D.7 Comparison of bovine feces samples inoculated with <i>E. coli</i> O157:H7 at selected frequencies: (top) 1kHz; (middle) 100kHz; (bottom) 10MHz.....	115
Figure D.8 Statistical significance of mean differences between concentrations for complex media study.....	116

Chapter 1. Introduction

1.1 Objectives and Goals

The long term goal of this research is to develop a field-deployable portable biosensor for the real-time detection of Category B disease agents transmissible through food and water. This is to be accomplished by using a new biosensor architecture, which combines the use of microelectromechanical systems (MEMS) fabrication methods and a biological sensing surface. The model disease agent for this research, aimed to demonstrate proof of concept, is *Escherichia coli* O157:H7. The biosensor, designed to detect whole cell organisms in a liquid volume, will consist of a reagent-coated MEMS biochip for detecting the analyte. The biosensor is designed to enable health care professionals, bioterrorism rapid-response teams, and food safety monitoring personnel to quantify results in less than 5 minutes.

The short term goal of this research is to construct a prototype biosensor. The biosensor will be evaluated for its ability to detect *E. coli* O157:H7 in liquid media. It represents an innovative approach to detecting infectious disease agents due to the biosensor's large sample size, minimal sample processing and 10 minute detection time from sample application to results.

1.2 Foodborne Pathogens and Food Safety

Pathogenic bacteria and other microorganisms are ubiquitous in the environment. Bacterial pathogens are found in soil, animal intestinal tracts and in fecal-contaminated water. Human beings, on average, harbor more than 150 types of bacteria inside and

outside of the body (Madigan et al., 1997). Although many microorganisms are harmless, some are known to be the causative agent of many different infectious diseases including botulism, cholera, diarrhea, emesis, pneumonia and typhoid fever (Doyle et al., 1997). More than 200 known diseases are transmitted through food and drink alone (Mead et al., 1999). A table of outbreak incidents is included in Appendix A.

Although recent data suggests naturally occurring cases of foodborne disease outbreaks are declining in the US (CDC, 2002), it is estimated that foodborne diseases cause approximately 76 million illnesses, including 325,000 hospitalizations and 5,000 deaths in the US each year (Mead et al., 1999). Of these, known pathogens account for an estimated 14 million illnesses, 60,000 hospitalizations, and 1,800 deaths indicating that these pathogens are a substantial source of infectious disease. Outbreaks caused by the four major foodborne pathogens, *Campylobacter*, *Salmonella*, *Listeria monocytogenes*, and *E. coli* O157:H7 are characterized in Table 1.1.

Table 1.1 Food illnesses in the US caused by major foodborne pathogens (CDC, 1999)

Pathogen	Number of Cases	Hospitalizations	Deaths
<i>Campylobacter</i>	1,963,141	10,539	99
<i>E. coli</i> O157:H7	62,458	1,843	52
<i>L. monocytogenes</i>	2,498	2,298	499
<i>Salmonella</i>	1,342,532	16,102	556

To demonstrate the scope of the contamination problem, selected recall data due to contamination of pathogens is shown in Table 1.2. The United States Department of Agriculture (USDA) estimates \$2.9 billion to \$6.7 billion is lost annually due to medical costs and lost productivity caused by major food pathogens (Buzby et al., 1996).

Table 1.2 Examples of food recalls due to pathogen contamination (USDA-FSIS, 2002)

Company	Product Recalled	Contaminant	Amount Recalled
Cargill Turkey, TX	Poultry Products	<i>L. Monocytogenes</i>	16.7 million pounds
Bar-S Foods, GA	Meat & Poultry	<i>L. Monocytogenes</i>	14.5 million pounds
Excel Corp, GA	Ground Beef/Pork	<i>E. coli O157:H7</i>	190,000 pounds
American Food, WI	Ground Beef	<i>E. coli O157:H7</i>	530,000 pounds
Savoie's, LA	Cajun Dressing	<i>Salmonella</i>	500,000 pounds
Zartic, GA	Chopped Beefsteak	<i>Salmonella</i>	2,700,000pounds

1.3 Market Analysis for Pathogen Detection

The broad market for pathogen detection extends across a range of industries including food processing companies, environmental monitoring agencies, healthcare industries and the military. Combined, the total market size for pathogen detecting biosensors is \$563 million dollars and is growing at a compounded annual growth rate (CAGR) of 4.5% (Radke and Alocilja, 2003). The food pathogen testing market alone is expected to grow to \$192 million and 34 million test units by 2005. The food processing industry can be further segmented into the type of food product (meat, dairy, fruit, vegetables, processed foods) and the target pathogen (bacteria, viruses, fungi and other biohazardous agents). The total number of microbial tests performed by food industry sectors is around 144 million tests per year and is shown in Table 1.3.

Table 1.3 US food industry microbial tests per sector. (Strategic Consulting, 1999)

Sector	Number of Plants	Total Tests	Average/Plant/week
Beef and Poultry	1,679	32,212,471	369
Dairy	1,388	45,887,576	636
Fruit/Vegetables	652	13,981,305	412
Processed foods	2,260	52,196,282	444
Total	5,979	144,277,634	464

Market data shows that a biosensor for the rapid detection of pathogens has an excellent chance of success in the marketplace. Also, pathogen detecting biosensors are a "disruptive" technology and tend to create their own markets. If a low cost and reliable product were to be introduced into the marketplace, it is possible that the net number of pathogen tests would increase simply because the technology would be available. Food companies would perform more frequent product testing and new segments would also open up as restaurants and consumers seek to verify the safety of the food they eat.

1.4 Biosecurity and Agroterrorism

The deliberate introduction of a biological pathogen into US livestock, poultry or crops would increase food prices, reduce food exports (costing billions of dollars in lost revenue) and potentially increasing the number of illnesses associated with foodborne pathogens. Indeed, biosecurity has become an increasingly important element in the battle against terrorist acts. Biosecurity threats include disease causing agents of high consequence, such as viruses, bacteria and toxins. Human exposure to pathogens may occur through inhalation, skin exposure or ingestion of contaminated food or water. Foodborne pathogens pose a risk to food safety and are a threat to the nation's food supply chain.

One such danger to the nation's food supply is the threat posed through agroterrorism. Agroterrorism encompasses many aspects, including the destruction of cropland, the intentional spread of livestock diseases, and the deliberate use of food pathogens to disrupt the safety of the nation's food supply (Kohnen, 2000). The World Health Organization (WHO) has indicated that terrorists may try to contaminate food supplies

and has urged countries to strengthen their surveillance. The WHO cites past examples of intentional food attacks, including a *Salmonella* Typhimurium outbreak in Oregon where more than 750 people became ill after members of a cult contaminated restaurant salad bars (WHO, 2002).

The National Institute of Allergy and Infectious Diseases (NIAID), an institute of The National Institutes of Health (NIH) and the Centers for Disease Control and Prevention (CDC) categorize biological pathogens as either Category A, B or C. Category A agents include organisms that pose a risk to national security because they can be easily disseminated or transmitted from person to person; result in high mortality rates and have the potential for major public health impact; might cause public panic and social disruption; and require special action for public health preparedness (NIAID, 2004). Category B agents include those that are moderately easy to disseminate; result in moderate morbidity rates and low mortality rates; and require specific enhancements of the nation's diagnostic capacity and enhanced disease surveillance. Category C agents include emerging pathogens that could be engineered for mass dissemination in the future because of availability; ease of production and dissemination; and potential for high morbidity and mortality rates and major health impact. NIAID and the CDC have identified foodborne pathogens such as *Salmonella spp.*, *L. Monocytogenes*, and *E. coli* O157:H7 as Category B bioterrorism agents (NIAID, 2004; CDC, 2004). In particular, *E. coli* O157:H7 poses a significant threat to the nation's food supply as it has emerged as one of the deadliest foodborne pathogens due to its combination of virulence and pathogenicity (CDC, 2001).

1.5 Routes of Infection

E. coli are bacteria that naturally occur in the intestinal tracts of humans and warm-blooded animals to help the body synthesize vitamins. A particularly dangerous type is the enterohemorrhagic *E. coli* O157:H7 or EHEC. In 2000, EHEC was the etiological agent in 69 confirmed outbreaks (twice the number in 1999) involving 1564 people in 26 states (CDC, 2001). Of known vehicles, 69% were attributed to food sources, 11% to animal contact, 11% to water exposures, and 8% to person-to-person transmission (CDC, 2001). Past outbreaks have also been traced to contaminated well water and improperly disinfected swimming pools (Keane et al., 1994).

E. coli O157:H7 produces toxins that damage the lining of the intestine, cause anemia, stomach cramps and bloody diarrhea, and a serious complication called hemolytic uremic syndrome (HUS) and thrombotic thrombocytopenic purpura (TTP) (Doyle et al., 1997). In North America, HUS is the most common cause of acute kidney failure in children, who are particularly susceptible to this complication. TTP has a mortality rate of as high as 50% among the elderly (FDA, 2004). Recent food safety data indicates that cases of *E. coli* O157:H7 are rising in both the US and other industrialized nations (WHO, 2002).

Human infections with *E. coli* O157:H7 have been traced back to individuals having direct contact with food in situations involving food handling or food preparation. In addition to human contamination, *E. coli* O157:H7 may be introduced into food through meat grinders, knives, cutting blocks and storage containers. Regardless of source, *E. coli* O157:H7 has been traced to a number of food products including meat and meat products, apple juice or cider, milk, alfalfa sprouts, unpasteurized fruit juices, dry-

cured salami, lettuce, game meat, and cheese curds (Doyle et al., 1997; FDA, 2001). Possible points of entry into the food supply chain include naturally occurring sources from wild animals and ecosystems, infected livestock, contaminated processing operations, and unsanitary food preparation practices, as illustrated in Figure 1.1.

The US government has significantly expanded its investment to ensure food safety. One example is the implementation of a food safety initiative to help detect and respond to outbreaks of foodborne illness (HHS, 2000). Key components of this initiative include construction of the national Early Warning System, development of new methods for monitoring the food supply, and improving awareness of safe food practices. Through this initiative, the Food and Drug Administration (FDA), the Environmental Protection Agency (EPA), the CDC, and the USDA are working to increase research in the development of devices used for assessing the risk of the food supply. An example of this research is the development of biosensors for quickly detecting bacterial contamination in food.

1.6 Use of Biosensors and Rapid Detection Methods

The detection and identification of foodborne pathogens and other contaminants in raw food materials, food products, processing and assembly lines, hospitals, ports of entry, and drinking water supplies continue to rely on conventional culturing techniques. Conventional methods involve enriching the sample and performing various media-based metabolic tests (agar plates or slants). These are elaborate and typically require 2–7 days to obtain results (FDA, 2000).

Food Supply Chain

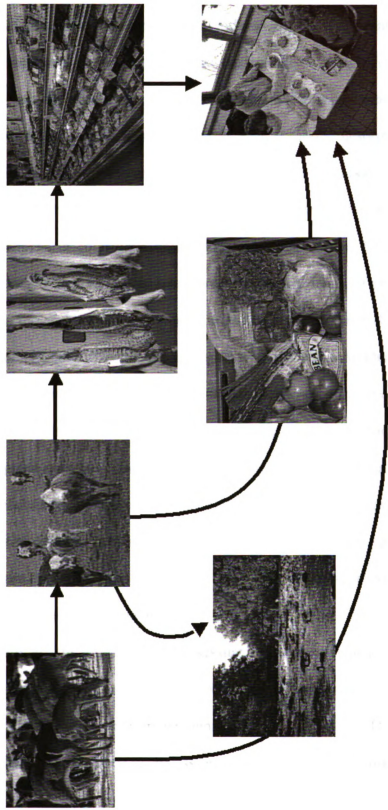


Figure 1.1 Schematic of food supply chain showing potential entry points for contamination of foodborne pathogens (ARG Brochure).

An increased demand for high-throughput screening, especially in the clinical and pharmaceutical industries, has produced several technological developments for detecting biomolecules. Some of these emerging technologies include enzyme linked immunosorbent assay (ELISA), polymerase chain reaction (PCR) and hybridization, flow cytometry, molecular cantilevers, matrix-assisted laser desorption/ionization, immunomagnetism, artificial membranes, and spectroscopy (Food Manufacturing Coalition, 1997). Pathogen detection utilizing ELISA methods for determining and quantifying pathogens in food have been well established (Cohn, 1998). The PCR method is extremely sensitive but requires pure samples and hours of processing along with expertise in molecular biology (Meng et al., 1996, Sperveslage et al., 1996). Flow cytometry is another highly effective means for rapid analysis of individual cells at rates up to 1000 cells/sec (McClelland and Pinder, 1994), however, it has been used almost exclusively for eukaryotic cells. These detection methods are relevant for laboratory use but cannot adequately serve the needs of health practitioners and monitoring agencies in the field. These systems are costly, require specialized training, have complicated processing steps in order to culture or extract the pathogen from food samples, and are time consuming. In comparison, a field-ready biosensor is inexpensive, easy to use, portable and provides results in minutes.

Biosensors are analytical instruments possessing a bio-molecule as a reactive surface in close proximity to a transducer, which converts the binding of an analyte to the capturing bio-molecule into a measurable signal (Turner et al., 1978; D' Souza, 2001). They often operate in a reagentless process enabling the creation of user friendly and

field ready devices. Biosensors are needed to quickly detect disease-causing agents in food and water in order to ensure continued safety of the nation's food supply.

At the moment, biosensors that have been developed for the detection of pathogenic bacteria in food and water may be classified into two groups: optical and electrochemical. An integrated optical interferometer was developed for detecting *S. Typhimurium* in 10 minutes (Seo et al., 1999). The sensor involved the use of a planar waveguide with antibody coated channels to make the channels immunochemically selective for antigen molecules. The presence of antigen was detected by measuring the phase shift generated by a change in the waveguide refractive index. The sensor was able to detect bacteria concentrations of 10^5 - 10^7 CFU/mL in a sample flow rate of 50 μ L/min. An optical biosensor utilizing a fiber optic light guide and luminometer was used to detect *E. coli* O157:H7 and *Salmonella* in inoculated samples of ground beef and fresh vegetables in a time of 1 hour (Liu et al., 2003; Mathew and Alocilja, 2004). The sensor was based on light (chemiluminescence) released by the reaction of HRP-labeled antibody-antigen complexes and chemiluminescent reagents. The sensor was able to detect concentrations of 10^2 to 10^5 CFU in a total sample size of 50 μ L. A surface plasmon resonance biosensor was reported to detect *E. coli* O157:H7 in meat and environmental samples (Meeusen et al., 2003; DeMarco and Lim, 2002). The SPR biosensor worked by detecting the change in refractive index of surfaces functionalized with antigen specific receptors. The SPR sensor was able to detect concentrations of 10^5 CFU/mL in a sample size of 1mL. A portable evanescent wave fiber-optic biosensor was used to detect *E. coli* O157:H7 in samples of ground beef in 25 minutes and a concentration as low as 10^2 CFU/mL (Bao et al., 1996).

Electrochemical biosensors, include amperometric, conductometric, impedimetric, (and in some cases resonant, surface acoustic wave (SAW) and capacitive sensors). These systems have the advantage of being highly sensitive, rapid, inexpensive and are highly amenable towards microfabrication (Gau et al., 2001; Rishpon and Ivnitski, 1997). They measure the change in electrical properties of electrode structures as cells become entrapped or immobilized on or near the electrode. A flow injection amperometric immunofiltration system was developed for the detection of *E. coli* and *Salmonella* in a time of 35 minutes (Abdel-Hamid et al., 1998). That biosensor involved the use of functionalized porous nylon membranes for antigen immobilization followed by measuring the change in current of a working electrode. The sensitivity of the device was 50 CFU/mL for a sample volume of 1mL. An enzyme linked amperometric immunosensor was developed for the detection of *Salmonella* in a time of 4 hours (Brooks et al., 1992). The biosensor measured the change in current of a platinum working electrode functionalized with polyclonal antibody. The sensitivity of the device was 10^4 CFU/mL in a sample size of 200 μ L. Using porous filter membranes, flow-through conductometric immuno-filtration biosensors were developed for the detection of *E. coli* O157:H7 in liquid media (Muhammad-Tahir and Alocilja 2003; Sergeyeva, 1996). An immunoelectrochemical biosensor utilizing immunomagnetic separation was developed for the detection of *S. Typhimurium* and *E. coli* O157:H7 in chicken carcass wash water in a time of 2.5 hours (Che et al., 2000). Sampling involved the separation of antigen via magnetic beads coated with polyclonal antibody. After incubation, the sample was processed through a flow injection analysis cell for amperometric detection. The sensitivity of the sample was 10^3 CFU/mL in a sample flow rate of 500 μ L/min. An

impedimetric biosensor was developed to detect *E. coli* O157:H7 in pure culture in a time of 5 minutes (Ruan et al., 2002). The biosensor utilized functionalized indium tin oxide electrodes and detected the impedance change caused by the immobilization of bacteria on the electrode surface. The sensitivity was 10^3 CFU/mL in a sample size of 100 μ L. Another impedimetric biosensor was developed for the detection of *Trypanosoma cruzi* (causative agent of Chaga's disease) in a time of 1 hour (Diniz et al., 2003). Impedance measurements were carried out in an electrochemical cell where the adsorption of antigens caused a change in impedance. The biosensor was able to differentiate between positive and negative in 20 μ L samples. A microfabricated amperometric biosensor was created for *E. coli* detection in a time of 40 minutes (Gau et al., 2001). The device used an array of independent square electrodes functionalized with a self assembled monolayer (SAM) of streptavidin to capture rRNA for the bacteria. The detection system was sensitive to 10^3 CFU (without PCR) in a sample size of 5 μ L. A microfabricated impedimetric biosensor was developed to detect *L. monocytogenes* in a time of 15 minutes (Gomez et al., 2001). The device involved antibodies bound to a pair of electrodes enclosed in a microfluidic chamber. The sensor was able to detect fewer than 10 cells in a 6nL volume (10^5 CFU/mL). The use of wireless electrochemical sensors was reported for the detection of *Bacillus subtilis*, *E. coli* JM109, *Pseudomonas putil* and *Sachromyces cerevisiae* (Ong et al., 2002). The resonant device involved the use of a printed inductor-capacitor circuit placed in a liquid sample containing bacteria. The concentration of bacteria present in the sample could be monitored by measuring the system resonant frequency. The biosensor was not selective of bacteria species. SAW devices and magnetoelastic thin film sensors were also been used to detect target analytes

remotely (Dutra et al., 2000; Grimes et al., 1999). These sensors involved detecting the change in system resonant frequency in response to the presence of the analyte. Interdigitated electrodes were used to detect the presence and measure the concentration of a target analyte in fluids (Sergeyeva et al., 1996). Another impedimetric biosensor was used successfully to detect the presence of glucose oxidase binding to interdigitated electrodes deposited on silicon oxide (SiO₂) surfaces (Van Gerwen et al., 1998). It was demonstrated the possibility to detect urea concentrations as low as 50 μM on interdigitated electrodes immobilized with urease (Sheppard et al., 1995).

Sensors developed for detecting bacteria and enzymes with interdigital electrode arrays have had electrode widths and spacing ranging from 15 μm to 80 μm (Gomez et al., 2001; Sergeyeva et al., 1996; Sheppard et al., 1995). This has the effect of detecting not only the impedance change at the sensor surface, but also the environmental events taking place significantly above the surface binding events. By using a novel electrode width and spacing of 3 μm by 4 μm, respectively, the sensor should be able to detect only the event of bacteria binding to the surface, thus minimizing other events occurring at 10 μm or greater above the surface.

In general, biosensors experience difficulties detecting low levels of bacteria due partly to the sample size. Interference of the food matrix represents a major challenge when developing sensor systems. A novel biosensor is needed that is able to detect bacteria in a liquid-food sample that requires no enrichment, minimal sample processing and low environmental interference from food particulates.

1.7 Novelty of Research

The biosensor to be presented in this dissertation is novel both in design and application. The novelty of the design is that it is the first biosensor to incorporate a high density, interdigitated microelectrode array to detect bacteria in solution by measuring the impedance of cells bound to the sensor surface through antibody-antigen interaction. Table 4 demonstrates the novelty of the biosensor versus similar existing biosensors, which have not detected whole cell bacteria on interdigitated electrodes in a large sample size. Furthermore, the electrode width and spacing (3 μ m and 4 μ m, respectively) is unique only to this design and was selected specifically to detect for micron-sized bacteria. The application is also novel in that the biosensor is tested in solutions containing mixed particulates of ground beef, romaine lettuce or bovine feces.

Table 1.4 Novelty of this research compared to existing electrochemical biosensors

Biosensor Reference	Biosensor Description	Speed	Sample Size	Target Analyte	Novelty of Research
(Radke, 2004)	High Density Microelectrode Array	<10min	20mL	Whole Cell Bacteria	
(Gomez, 2001)	MEMS Microfluidic Device	15 min	6nL	Whole Cell Bacteria	Larger Sample Size
(Gau, 2001)	MEMS Square Electrodes	40 min	5 μ L	RRNA	Detects Whole Cell Bacteria, Larger Sample
(Van Gerwen, 1998)	Interdigitated Electrode Array	----	----	Enzyme	Detects Whole Cell Bacteria
(Abdel-Hamid, 1998)	Single Electrode with Porous Nylon Membrane	35 min	1mL	Whole Cell Bacteria	Multiple Electrodes
(Sergeyeva, 1996)	Electrode Array	1 hour	1mL	Whole Cell Bacteria	Electrodes, Sample, Time
(Brooks, 1992)	Single Platinum Electrode	----	200 μ L	Whole Cell Bacteria	Multiple Electrodes

1.8 Hypothesis and Specific Aims

Hypothesis: In this dissertation it is hypothesized that a biosensor incorporating an interdigital microelectrode array and functionalized for recognition of pathogenic bacteria in solution can be designed and fabricated.

To demonstrate proof of concept, the following specific aims are identified:

Specific Aim 1: To design and fabricate a biosensor that incorporates an interdigital microelectrode array and functionalized surface for biological recognition.

Specific Aim 2: To employ the biosensor for detecting the presence of serially diluted *E. coli* O157:H7 bacteria in pure culture in a sample size of 20mL.

Specific Aim 3: To employ the biosensor for distinguishing the target bacteria in a liquid sample size of 20mL containing mixed microflora.

Specific Aim 4: To provide initial research for employing the biosensor to detect *E. coli* O157:H7 bacteria extracted from artificially contaminated samples of ground beef, bovine feces and romaine lettuce.

Chapter 2. Literature Review

2.1 Overview of the Impedimetric Biosensor

This research aims to detail the design, fabrication and testing of an impedimetric biosensor with MEMS technology integrated with biosensing methods to detect *E. coli* O157:H7 cells. MEMS is an enabling technology allowing for micron-sized transducers. MEMS technology makes it possible for the transducer to be integrated with electronics and undergo batch fabrication in large quantities. The general objective is to develop a biosensor to detect for whole bacteria cells in food and water.

A high density interdigital electrode array biosensor chip is used in the experiments to detect different concentrations of *E. coli* O157:H7 in solution. Figure 2.1 is a schematic depicting the operating principles of the biosensor. First, a microelectrode array is fabricated on a silicon substrate to serve as the electrical transducer (Figure 2.1a). Second, the biosensor surface is functionalized by attaching analyte specific antibodies via crosslinkers to form a biological transducer (Figure 2.1b). Finally, when the biosensor is tested in solution, target analyte becomes bound to the antibodies immobilized to the surface (Figure 2.1c). The presence of bacteria on the surface causes the impedance measured across the electrodes to change. The impedance change can be

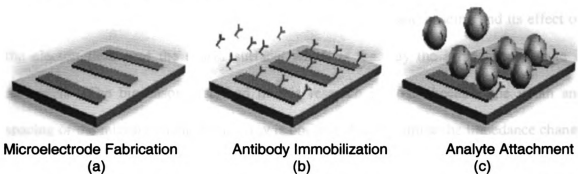


Figure 2.1 Schematic of detection theory (adapted from Gorschlüter et al., 2002).

measured and correlated to find the analyte concentration.

The biosensor chip is a thin silicon substrate with interdigitated electrodes and immobilized antibodies patterned onto the surface. Because the electrodes are interdigitated, opposing electrodes are connected to voltage sources of different polarity creating a strong electric field (Figure 2.2a). When the interdigital array is immersed in a sample solution, the active area is exposed to the bacteria. Surface antibodies immobilized between the electrodes via heterobifunctional crosslinkers act as tethers, which serve the purpose of holding the bacteria in place between the electrodes (Figure 2.2b). When bacteria bind to antibodies, a region of 2-4 μm (size of bacteria) above the sensor surface becomes modified and the impedance created by the pathogenic bacteria provides the sensing mechanism (Figure 2.2c). Different cellular concentrations of bacteria bound to the sensor surface yield different changes in electrical impedance between the electrodes. During testing, only minimal dissociation occurs between the covalently bound amine crosslinkers and the silanized glass surface since the testing solution has a neutral pH (Jung, 2001).

As outlined in chapter 1, there have been many sensors developed that detect the change in impedance when bacteria are tethered in the vicinity of micro and nano-sized interdigitated electrodes. Large electrode array (>10 μm) and small electrode arrays (<1000nm) sensors have not optimized the electrode width and spacing and its effect on the electric field near the sensor surface, which is the way the impedance change is measured. The biosensor described in this research is novel because the width and spacing of the interdigital electrode array is optimized to maximize the impedance change at the surface of the electrode array and not throughout the test sample. This allows for

the biosensor to detect bacteria in a large, bulk solution with minimal environmental effects, which is a novel testing method in comparison to some other interdigitated electrode devices. Detecting for whole cell bacteria offers advantages over PCR, ELISA and DNA based biosensors because these methods report positive results for samples with dead or non-viable cells. A whole cell biosensor reports results based on detecting live, viable bacteria.

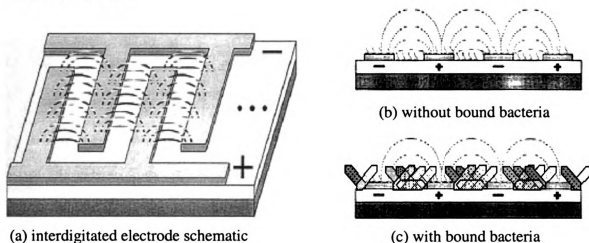


Figure 2.2 Electric field between: (a) interdigital electrode array; (b) cross-section of interdigital array, (c) cross-section of interdigital array with immobilized bacteria on the surface (adapted from Van Gerwen et al., 1998).

2.2 Lipid Bilayer Membrane Theory

Cells consist of a lipid bilayer membrane surrounding an intracellular fluid containing numerous organelles (mitochondrion, nucleus, lysosomes, etc.). The membrane is the most significant portion of the cell in this research. Biological membranes are constructed mainly from phospholipids. Phospholipids are molecules containing long, hydrophobic fatty chains (tails) with a charged, hydrophilic phosphate group (head) to make one end to be water soluble. The molecules spontaneously orient themselves creating a self assembled double layer with the hydrophobic tails joining

together. As shown in Figure 2.3, this results in a layer with a hydrophobic fatty interior and a hydrophilic charged exterior. The phospholipid bilayer membrane is about 10 nm thick and folds around to enclose the entire cell, keeping cellular material on the inside and the aqueous environment on the outside.

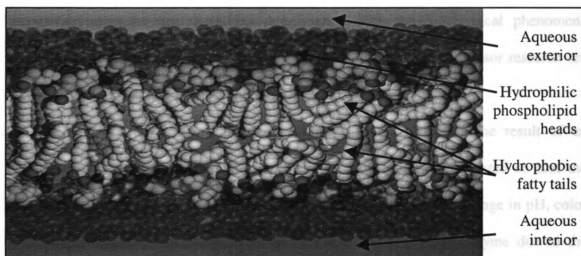


Figure 2.3 Cross-section of lipid bilayer membrane showing charged hydrophilic phospholipid head groups and hydrophobic fatty acid tail groups aligned to form a cell membrane (Venable et al., 2000).

The phospholipid bilayer serves as the outer membrane of the bacterial cell and is the basic structural building block of the cellular membrane. It is constructed so that the cell may survive in an aqueous environment while maintaining the independent cellular cytoplasm. While the fatty acid double layer serves well as a boundary layer, it does not provide much physical strength. Cellular stability is achieved through a network of proteins (along with cholesterol molecules) both inside and outside the cell membrane. It is this network of proteins that constitutes the framework, giving the cell its shape and ability to control motion, transport molecules, and adhere to surfaces.

2.3 Biological Recognition

Perhaps the biggest single difference between chemical and biological sensors is the use of biological substances in biosensor devices. Biosensors incorporate a biological recognition element to provide selective targeting for analyte(s) of interest. Biological recognition elements are molecules that interact with the biochemical phenomena occurring at the cellular level. The major biomolecules used in biosensor research are enzymes, antibodies, DNA/RNA, and biomimetic polymers.

Enzymes for use in biosensor applications involve measuring the result of an enzyme-catalyzed reaction involving the analyte. The enzyme is selected so that the product of the reaction involves a measurable characteristic, such as change in pH, color or electrochemical conductivity. Glucose oxidase is one popular enzyme due to the commercial success of glucose biosensors for measuring glucose in blood, fermentations, and food processing. One major limitation of the use of enzymes as a biological recognition element is the long-term stability of the enzyme activity and sensitivity to changes in pH and temperature.

Oligonucleotide strands are the most specific biological recognition molecules known. The use of DNA probes for isolating and identifying gene sequences through hybridization is common in biosensor research. One disadvantage of the use of DNA biosensors is the long time required for hybridization and the slow binding step of target oligonucleotides. The primary benefit to DNA/RNA is their high specificity.

Biomimetic molecules are molecular recognition elements engineered to have synthetic receptors that mimic the receptors found on enzymes or antibodies. They are typically synthesized from similar chemical molecules or are formed by molecular

imprinting. Using polymerization, a synthetic matrix with receptor-like recognition characteristics can be created to mimic the selectivity of antibodies. Biomimetics is a relatively new, but promising, field in biosensor research. The subject of this research, however, is antibody-based biosensors.

Antibodies come in different classes including, IgA, IgD, IgE, IgG and IgM. Of these, IgG is used almost exclusively in biosensors research and will be the subject of this study. The IgG antibody is a protein with a molecular weight of about 150,000 Daltons. A schematic of the IgG antibody showing the structural features is shown in Figure 2.4.

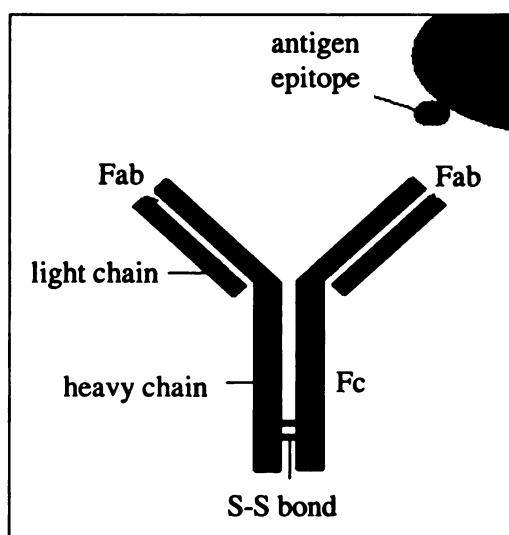


Figure 2.4 Antibody schematic.

The antibody structure is represented as a "Y" shaped structure with a base and two branches. It is considered a bifunctional receptor since it has twin-binding sites at the branches (Fab) of the molecule. The base of the molecule is particularly important for biosensor research because it allows the antibody to attach to other molecules or directly on surfaces (Shriver-Lake et al., 1997). This can be accomplished either chemically or through the use of a crosslinker and is discussed in detail in Section 2.4.

The recognition of the analyte and the receptor occurs when the binding site of the antibody meets with a specific site in the cellular membrane called an antigenic determinant, or epitope. Epitopes may be found on the cell membrane, the soma or the flagella of bacteria and are denoted by O, H and F, respectively. For this work, however, it is mainly important to understand that antibody attachment forms a bridge between the cellular membrane and the substrate upon which the antibodies are immobilized. The adhesion mechanism occurs when a cell comes into contact with a surface coated with antibodies. The antibodies bind to specific epitopes on the cellular membrane and flagella.

2.4 Membrane Impedance Theory

For any given homogenous conducting material, a bulk property called the resistivity, ρ , can be defined as having the dimensions of Ω -cm. Given this intrinsic property of the material, the resistance, R , of any arbitrary shape may be determined (Nilsson and Riedel, 1996):

$$R = \frac{\rho L}{A}$$

where A is the cross-sectional area in cm^2 and L is the length of the material in cm. Thus, if we consider the cells to be a cylinder of known length and cross-sectional area, it is possible to estimate the resistance due to the cytoplasm inside the cell membrane. The value of resistance for the entire cell will have to be adjusted to include such factors as the membrane resistance, the availability of ions to pass through the cell membrane, the action potential across the membrane, and the ionic content of the surrounding solution

(Borkholder, 1998). The overall membrane resistivity is large with estimates ranging from $1\text{M}\Omega\text{-m}$ to $100\text{G}\Omega\text{-m}$.

The lipid bilayer membrane also acts as spherical capacitor since it serves as an insulating layer separating two conducting solutions. The capacitance, C , is determined by the permittivity of the material, ϵ_R , the area of the capacitor, A , and the thickness, d :

$$C = \frac{\epsilon_R \epsilon_0 A}{d}$$

where ϵ_0 is the permittivity of free space ($8.85 \times 10^{-12} \text{ C-V}^{-1}\text{-m}^{-1}$) (Nilsson and Riedel, 1996). For most biological membranes, the total thickness, d , of the lipid bilayer is about 10nm and results in a membrane capacitance of $0.01\text{pF}/\mu\text{m}^2$ (Tien and Ottova, 2000).

When measuring the complex impedance characteristics (determination of both the resistance and the capacitance), it is important to understand the dispersive behavior of the cellular membrane. When an electric field is applied to a material, energy in the field is either lost through heat (resistance) or stored by polarization of the material's molecules. Polarization refers to the charge accumulation at the surfaces between materials with different electrical properties within the electric field. The response of a material to an applied electric field is described by its resistivity and permittivity. As described above, the resistivity gives a measure of a material's ability to conduct (allow charge to pass through it), whereas permittivity gives a measure of the polarizability of the material (to store charge).

For most materials (including biological cells), the permittivity is only constant over a limited frequency range. Permittivity decreases as the signal frequency increases. The step changes in permittivity are called dispersions and reflect the reduction of

polarization at increasing frequencies. Biological materials show large dispersions at low frequencies, mainly due to interfacial polarization at the cell membrane (Ciureanu et al., 1997). At higher frequencies, the dispersion (and thus the polarization effect) is minimized (Figure 2.5).

Cells in solution exhibit three different types of dispersions centered in the audio-, radio-, and ultra-high frequency (UHF) ranges and are referred to as the α , β , γ dispersions, respectively (Figure 2.6). The α -dispersion, centered in the audio frequency range (10 - 10^4 Hz) is mainly due to the polarization of the measuring electrodes and ions (pH dependent) of the liquid medium. The γ -dispersion occurs at ultra-high frequencies (GHz) and is mainly due to the polarization of small dipolar species, such as water molecules. As a result, the γ -dispersion range is not selective for cells in solution. The β -dispersion range (10^4 - 10^7 Hz), on the other hand, is caused by the polarization of the bilayer lipid membrane (which also causes membrane capacitance) of the whole bacteria (Marks and Davey, 1999). Thus, impedance measurements for estimating the amount of cells in solution is carried out in the 1kHz-10MHz range.

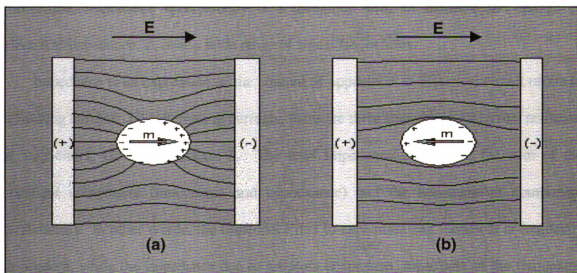


Figure 2.5 Schematic of dispersion in a cell at low (a) and high (b) frequencies.

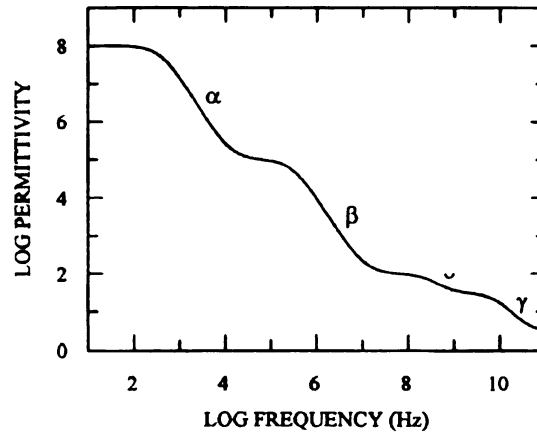


Figure 2.6 Spectrum of the dielectric properties of cell suspensions.

2.5 Impedance Measurements

The sensing mechanism for the impedimetric biosensor is based on detecting the change in impedance due to the presence of *E. coli* O157:H7 cells bound to the sensor surface. The antibodies bound to the surface between electrodes act to capture and immobilize the cells on the surface of the biochip. The impedimetric biosensor utilizes electrochemical methods and impedance spectroscopy to detect the target analyte. Simplified, impedance spectroscopy is a technique used to measure the change in electrical impedance, Z , over a wide range of signal frequencies.

Impedance is an expression of the amount of opposition an electrical circuit offers to a flowing current. For alternating currents, there are three impedance elements: resistors, R , capacitors, C , and inductors, L . The total impedance consists of the sum of the transient component (inductance and capacitance) and the non-transient component (resistance). In other words, the impedance due to capacitors and inductors is frequency dependent, while the impedance due to resistors is constant, regardless of the frequency. The impedance of a circuit due to capacitors and inductors is referred to as the reactance,

X. Inductance, however, is negligible in biological materials, since it is a measure of energy storage in magnetic fields. For the purposes of this research, the inductance will not be considered in making impedance measurements.

The impedance caused by the resistance in a circuit is also known simply as resistance and the impedance caused by the capacitance is known as the reactance. The magnitude of the impedance, then, can be expressed as the sum of the resistance and reactance and is equal to:

$$|Z| = \sqrt{R^2 + X^2}$$

and,

$$X = X_C = \frac{1}{\omega C}$$

where ω is the angular frequency ($\omega=2\pi f$) of the circuit.

As described in the Section 2.4 above, cell suspensions exhibit dispersion (polarization) due to cell membrane and cytoplasm biomass in the audio (α -dispersion) and radio (β -dispersion) frequency range of 10 - 10^7 Hz. Impedance analysis techniques can detect small changes in electrical current, on the order of 10^{-9} A, which can be translated into impedance, conductance, resistance, and capacitance.

The simplest model of a cell is an RC circuit in series where the capacitor and resistor represent the cell membrane and cytoplasm. The equivalent impedance of the system can be expressed as:

$$|Z| = \sqrt{R_{CYT}^2 + \frac{1}{\omega^2 C_{BLM}^2}}$$

and the idealized impedance spectrum is shown in Figure 2.7.

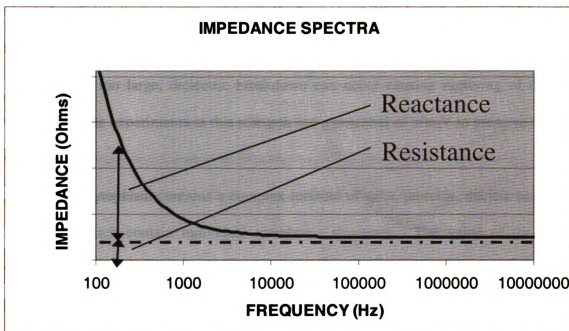


Figure 2.7 Ideal impedance spectrum of RC circuit with reactive and resistive components.

As the signal frequency increases, the transient impedance decreases because of decreased dispersion of the cell membrane. The dominant impedance element of cells in solution is the dielectric capacitance and resistance at high frequencies. At low frequencies, the reactance is the dominant portion of the impedance.

2.6 Circuit Elements

Simulation of the electric field was performed on different electrode widths and spacing to determine the electric field strength near the sensor surface. The electrical properties of the bacteria cell structures and testing media are incorporated into the simulation to determine the optimum electrode width and spacing.

The membrane surrounding the cell has a lipid bilayer structure and is about 4-10nm thick. The effect of proteins and water on the membrane dielectric constant is unclear but

reported permittivity values range typically between 2-10. Low-frequency alternating current (AC) electric fields induce a large potential drop across the plasma membrane. If the voltage is too large, dielectric breakdown can occur causing rupturing of the cell membrane. The experiments in this research use a potential of 50mV to preserve the cell membrane.

Cellular cytoplasm contains a complex mixture of salts, proteins, nucleic acids and organelles, which contain individual membrane structures. The value of the inside permittivity typically has a range of 50-100 (Gimsa et al., 1996). In most cases, however, the cytoplasm can be approximated as a highly conducting salt solution with a large concentration of organic material (Markx and Davey, 1999).

When measuring electrical properties in solution, chemical reactions result in the formation of a space charge layer (layer of ions) near the electrode. Figure 2.8 shows an illustration of the space charge layer near an electrode and depicts the resulting capacitance caused by the ion layer. Looking at the negatively charged metal electrode, the positive ends of the water molecule become aligned in a plane (inner Helmholtz plane, IHP), forming the hydration sheath. Positively charged hydrated ions then align in another plane (outer Helmholtz plane, OHP), creating what is referred to as a double-layer. Under an alternating current, the voltage drop between the metal electrode and the OHP act as a parallel plate capacitor with a gap of about 1 nm (Kovacs, 1998).

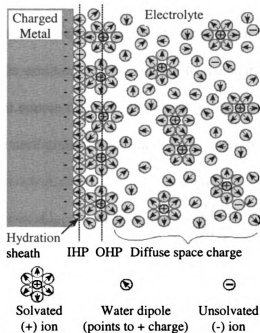


Figure 2.8 Schematic of the electrode-solution interface showing the inner and outer Helmholtz planes (Bockris and Reddy, 1970).

The Helmholtz capacitance, often referred to as the double-layer capacitance, C_{DL} , serves as a constant source of noise in measuring the impedance. The theoretical capacitance of the double-layer capacitance is given by the equation,

$$C_{DL} = \frac{\epsilon_0 \epsilon_R A}{x}$$

where ϵ_R is the relative dielectric permittivity of the medium between the two planes (phosphate buffered saline in this case), A is the surface area of the metal electrode array and x is the distance to the outer Helmholtz plane (a distance of about 10 Å). The actual value of the double layer capacitance is a function of ion concentration, temperature, surface roughness of the metal electrode among other factors (McAdams et al., 1995).

Another source of noise in the system occurs on the backside of the electrodes and is referred to as the parasitic capacitance. The gold electrodes are separated from the

silicon substrate by a layer of silicon oxide. While the silicon oxide serves as a dielectric to insulate the electrodes, it also causes a capacitance to occur between the electrodes and the silicon substrate. In addition to the Helmholtz capacitance, the oxide separation capacitance is a constant source of noise when measuring the impedance. The parasitic capacitance for a set of interdigitated electrodes, C_{PAR} , is given by the equation,

$$C_{PAR} = nl\epsilon_0\epsilon_R \frac{\cos\left(\frac{\pi w_{SP}}{2L}\right)}{2\sin\left(\frac{\pi w_{SP}}{2L}\right)}$$

where n is the number of electrodes, l is the electrode length, L is the sum of the electrode width and spacing and w_{SP} is the length of the spacing between electrodes (Van Gerwen et al., 1998). The relative dielectric permittivity, ϵ_R , is for the oxide layer in between the metal electrode and the silicon substrate.

The circuit diagram used for measuring the impedance of electrodes in solution is given in Figure 2.9 where C_{DL} is the double layer capacitance between the electrode and the electrolyte, C_{DI} is the dielectric capacitance of the electrolyte, and R_{SOL} is the solution resistance (Ehret et al., 1997).

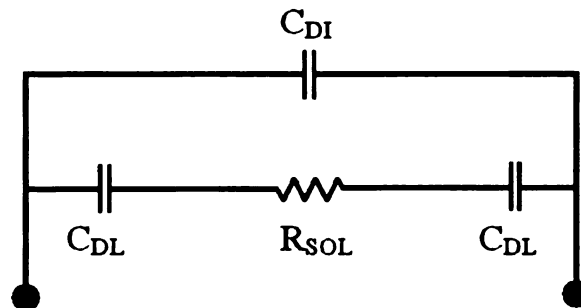


Figure 2.9 Equivalent circuit of the impedance measurement system with electrodes in solution (adapted from Ehret et al., 1997).

The circuit model can be interpreted as having two parallel branches, the dielectric capacitance branch (C_{DI}) and the impedance branch ($C_{DL} + R_{SOL} + C_{DL}$). In cases where the frequency is sufficiently high ($>1\text{MHz}$), the current will tend to run through the dielectric capacitance of the medium instead of the medium resistance. Therefore, the dielectric capacitance of the medium dominates the total impedance, and the contribution of the double layer capacitance and medium resistance to the total impedance is minimal. At lower frequencies ($<1\text{MHz}$), the current does not flow through the dielectric capacitor and the effects of the electrode double layer capacitance and the solution resistance dominate the total impedance.

Cells bound to antibodies immobilized to the biosensor surface add different impedance elements in series to the impedance branch and a new model is needed. For the new model, the electric field simulation uses a relative permittivity of 60, 10 and 80 for the cell cytoplasm, cell membrane and testing solution, respectively (Wiegand et al., 2002; Suehiro et al., 2003). The mean length and diameter of *E. coli* is $2.57\mu\text{m}$ and $0.49\mu\text{m}$, respectively, and has a semi-log normal distribution (Koppes et al., 1978). The resistivity of the bacterial cell membrane ($10^6 \Omega\text{-cm}^2$), the resistivity of the bacteria cytoplasm ($200\Omega\text{-cm}$) and the capacitance of the lipid bilayer membrane ($1\mu\text{F}\text{-cm}^2$) cause a change in impedance between interdigitated electrodes (Tien and Ottova, 2000). It should be noted that the units for the resistivity are different for the cytoplasm and cell membrane; this is because notation in the field of electrochemistry refers to membrane resistance in terms of cell surface area, while the cytoplasmic resistance is in the standard term of a cylinder.

Figure 2.10 is a modified circuit diagram for bacteria bound to antibodies immobilized to the sensor surface. It includes the impedance of bacteria, which consists of R_{CYT} , the resistance of the cytoplasm, R_{BLM} , the resistance of the cell membrane and C_{BLM} , the capacitance of the cell membrane. The impedance elements also include C_{DL} , C_{DI} , and R_{SOL} from the original model. Additionally, C_{PAR} , the parasitic capacitance, represents the capacitance created from the oxide separation of the gold electrodes and the silicon.

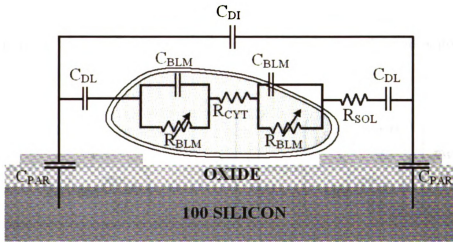


Figure 2.10 Circuit model for the impedance of bacteria immobilized between two interdigitated electrodes.

The equivalent impedance for the circuit in Figure 2.10 is given by the equation,

$$Z = \frac{(\beta\omega C_{DL} + R_{SOL}\omega C_{DL} + 1)}{\omega C_{DI}(\beta\omega C_{DL} + R_{SOL}\omega C_{DL} + 1) + \omega C_{DL}} + \frac{1}{\omega C_{PAR}}$$

where β is a term used to simplify the expression as is equal to:

$$\beta = \frac{R_{BLM}}{\sqrt{1 + (\omega R_{BLM} C_{BLM})^2}} + R_{CYT}$$

2.7 Electrode Spacing Model

The spacing of the interdigital array is determined by calculating the electric field near the surface of an interdigitated electrode array. The electric field strength between electrodes is geometrically dependent on both the width of the spacing between the electrodes (w_{SP}) and the electrode width (w_{EL}). The shorter the spacing between the electrodes, the stronger the electric field will be between electrodes; the larger the electrodes, the stronger the electric field will extend above the electrode surface. The effect has been theoretically analyzed (Binns and Lawrenson, 1973; Jacobs et al., 1995) by calculating the electric field between the interdigitated electrodes and is given by the equation,

$$\varphi(x, y) = \frac{V}{2K\left(\sin\frac{\pi w_{SP}}{2L}\right)} \operatorname{Re} \left[F \left(\alpha \sin \left(\frac{\sin\left(\pi \frac{x+iy}{L}\right)}{\sin\left(\frac{\pi w_{SP}}{2L}\right)} \right), \frac{\pi w_{SP}}{2L} \right) \right]$$

where the electric potential φ changes along the x-y axis, the characteristic length L is the sum of both, $L=w_{SP}+ w_{EL}$ and V is the applied voltage differential between electrodes of different polarity ($+V/2$ is applied to the positive electrodes and $-V/2$ to the negative electrode). The electric field geometry is governed by the first order ellipse $F(\alpha,\beta)$ where α is the amplitude, β is the modular angle and $K(k)$ is the modulus. The theoretical solution is calculated in Figure 2.11, which shows the curves under which a certain amount of current is flowing.

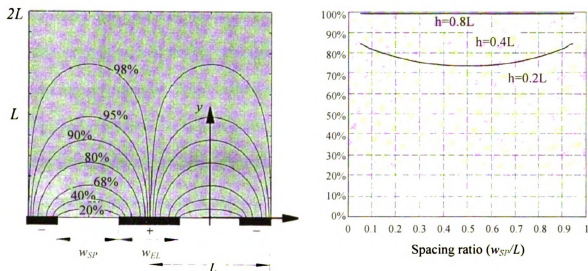


Figure 2.11 Calculated electric field lines (a) above interdigital electrodes; (b) as a function of electrode spacing ratio w_{sp}/L (Van Gerwen et al. 1998; used with permission).

For example, electrode width and spacing of $5\mu\text{m}$ ($L=10\mu\text{m}$) results in 80% of the total electric field flowing in a layer not higher than $5\mu\text{m}$ above the biosensor surface. Figure 2.11b shows the amount of current flowing in a layer of particular thickness. For a spacing ratio of 0.5, the layer with a thickness of $0.4L$ carries 92% of the current. It is shown here that if the spacing is too small (with respect to the electrode width) there are very high electric fields at the corners of the electrode. This has the effect of a reduced current in the middle of the electrode, minimizing the influence of the center electrode area on overall impedance.

This model points to the advantage of using micron sized electrodes when detecting for whole cell bacteria. It is expected that this will translate into better sensor sensitivity as well. It allows for selection of the optimal electrode geometry based on maximizing the percentage of electric field through a specified layer of thickness. In other words, the thickness of the analyte (*E. coli* O157:H7 bacteria in our case) will determine the optimal electrode width and spacing of the interdigitated array. This system, however, is more

complicated than electrode geometry in space. The effect of the lipid bilayer membrane, cellular cytoplasm, and testing solution all must be factored into the model. For this, Finite Element Analysis (FEA) is used to incorporate the permittivities of all elements in the system, including the silicon substrate, the silicon dioxide, the gold electrodes, the testing solution, the lipid bilayer membrane, and the cell cytoplasm. The results of the model are used to design the electrode structure of the biosensor and can be found in the Results and Discussion section with further detail in Appendix C.

2.8 Immobilization Methods

As mentioned in Section 2.3 (Biological Recognition), the key feature that distinguishes biosensors from other types of sensors is the use of a biomolecule on the surface layer of the sensor. The surface layer may be as simple as a biomolecule bound directly to the surface or, in more complex situations, the biomolecule is attached through multiple layers of chemical and biological interactions. The transducer must be chemically modified in order to immobilize the active molecules (active molecules refer to both chemical and biomolecules) to the surface.

There are five major immobilization methods in biosensor research: covalent binding, entrapment, cross-linking, adsorption and biological binding. Briefly, covalent binding refers to the attachment of the active molecule to the transducer surface using a chemical reaction such as silanization, peptide bond formation, or linkage to activated surface groups (thiol, epoxy, amino, etc). Entrapment refers to physical trapping of the active molecule into a thin film or coating, such as a polymer or sol gel (Taylor and Schultz, 1996). Cross-linking is similar to entrapment but only a crosslinker (such as

gluteraldehyde) is used to provide a chemical linkage to the active molecule and the transducer's activated surface, film or coating. Adsorption involves the association of the active molecule with the transducer's activated surface, film or coating through hydrophobic, hydrophilic, and/or ionic interactions. Biological binding is the direct attachment of the active biomolecule to the transducer's activated surface, film or coating via biochemical binding. Other methods, such as proteins immobilized by adsorption tend to suffer partial denaturation and leaching off the surface while in solution. Similarly, capture molecules immobilized through entrapment of surface polymers tend to attract residues and form multiprotein complexes, the effects of which are likely to interfere with the antibody function.

For this research, a combination of covalent binding and cross-linking methods are used to attach the antibody to the biosensor. (An argument can be made that biological binding also occurs as the bacteria bind to the immobilized antibody, but this section serves only to review immobilization methods of biomolecules and not the analyte attachment itself.) For this research, the general method used to attach the antibody is to first activate the oxide surface of the sensor through silanization. The activated surface allows for hydroxyl groups on the silica surface to serve as binding sites for the covalent

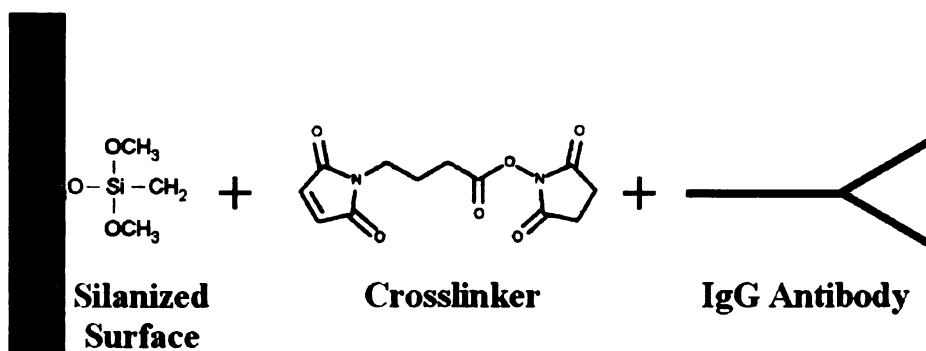


Figure 2.12 Antibody immobilization method.

attachment of organic molecules. One end of the crosslinker is covalently bound to the hydroxyl group of the silanized surface while the other end is reactive with the antibody (Figure 2.12). When selecting crosslinkers for use in biosensor applications, it is important to note that the crosslinker is reactive with the base (Fc region) of the antibody and that the antibody binding sites (Fab regions) are facing outward, enhancing the binding capability of the antibody. This is the preferred method of antibody immobilization when the substrate is subjected to fluid flow or extended times in solution. The antibody immobilization procedure used in this research is outlined in detail in the Methods and Materials section.

2.9 Microfabrication

Electrochemical biosensors involving microfabricated electrodes are an integral part of biosensor research. Microfabrication is based on electronic integrated circuit (IC) and thin-film manufacturing methods. The processes used in microfabricated devices include photolithography, wet and dry etching, wet and dry oxidation, doping, physical vapor deposition, chemical vapor deposition, evaporation and sputtering among others. There are too many processes to discuss here but comprehensive reviews can be found in reference textbooks (Kovacs, 1998; Madou, 2002; Van Zant, 2000) used to teach graduate and undergraduate microfabrication classes. The main processes utilized in this research are photolithography and evaporation and are discussed below. Figure 2.13 shows the lift-off fabrication sequence used in this study.

Microelectronic fabrication begins with photolithography, the technique used to transfer copies of a master pattern onto the surface of a solid material, usually a

semiconductor such as silicon. The photolithography process involves the use of a photomask to block ultraviolet radiation directed at a substrate coated with photoresist. The photomask is a glass or quartz plate with a master pattern made from a 0.1 μ m thick layer of chromium, which serves to absorb the UV radiation while the glass or quartz is transparent. The photomask is placed in direct contact (hard contact) with a photoresist coated surface and then exposed to UV radiation for a prescribed time. This results in a 1:1 image transfer of the entire mask onto the photoresist.

The first step in photolithography, when using Si as a substrate, is to grow a thin layer of oxide on the surface. This can be accomplished by either dry or wet oxidation of the wafer at temperatures in the range of 900-1150°C. After oxide growth, a thin layer of organic polymer, sensitive to ultraviolet radiation, is deposited on the surface. Before the coated wafers are exposed to the UV radiation they undergo a mild bake (soft bake) in order to remove the solvent of the resist and to anneal, reducing surface stress. Once they are soft baked, they then are transferred to a mask aligner where they are exposed to UV radiation. Resist exposure is controlled by using the proper intensity, direction, exposure time and wavelength, which is typically in the near UV range of 350-500nm. The mask serves to both block UV light and to pass UV light where desired onto the resist coated wafers. Resist that is exposed to the UV light undergoes a chemical reaction making it susceptible to development in an organic solvent.

Development transforms the pattern of the mask onto the resist, where it serves to mask further downstream processes. Development occurs by immersing the wafer in a solvent selective for chemically modified (by the UV) resist. This is also known as wet resist stripping and results in a wafer with a pattern of bare and photoresist (PR) covered

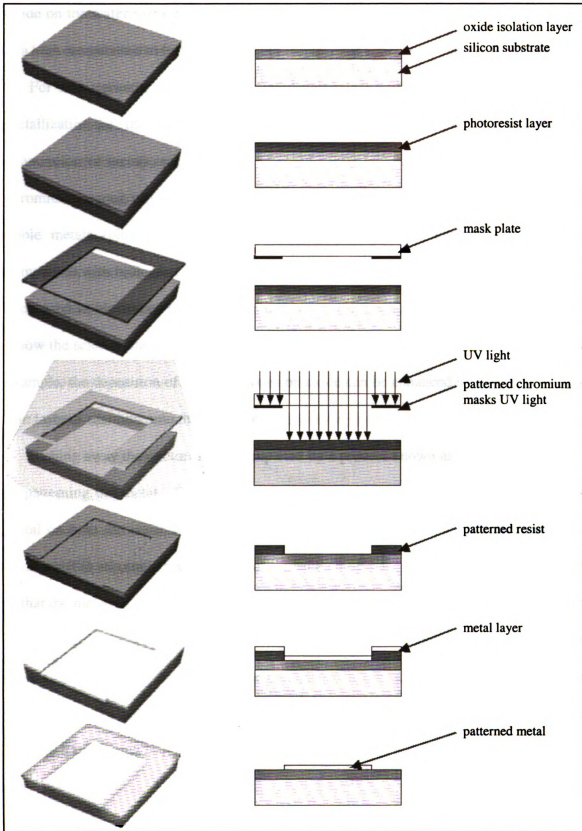


Figure 2.13 The sequence of the typical lift-off process.

oxide on the wafer surface. After PR development, the wafer is baked again (hard bake) at a high temperature to harden the PR and increase the adhesion of the PR to the wafer.

For this research, the next step after development and hard bake is the thin film metallization of the wafer surface. Deposition is accomplished by the thermal evaporation of metals, such as platinum, gold, silver, aluminum, copper, titanium, and chromium, among others. Electrochemical biosensor electrodes are generally made of noble metals (platinum, silver, gold) because their catalytic properties make them compatible with biological materials. Indium tin oxide, palladium and iridium have also been used as electrodes in electrochemical biosensors. Depositing a thin film of metal below the selected metallic film can enhance the adhesion of metals to the substrate. For example, the deposition of gold electrodes on oxide can be enhanced by first depositing a thin layer of titanium onto the substrate.

Etching away the photoresist is completed by a process known as 'lift-off' and results in patterning the metal. Because the metal is deposited over the entire wafer, there is metal on both the resist and the exposed substrate. The removal of the metal covered photoresist is accomplished with wet chemical etching selective to the resist. The result is that the metal on top of the photoresist is dissolved away while the metal pattern on the oxide is left intact. After lift-off, the wafer is inspected and subjected to a variety of post fabrication processing including wafer dicing, packaging, and surface functionalization for further modification. A detailed procedure of the microfabrication process is included in the Bill of Process in Appendix B.

Chapter 3. Methods and Materials

The following steps and experiments were conducted for this research:

1. Biosensor Fabrication (*Specific Aim 1*)
 - a. Microfabrication of Biosensor Device
 - b. Functionalization of Biosensor Device
3. Validation Testing (*Specific Aim 2*)
 - a. Pure culture of non-pathogenic generic *E. coli*
 - b. Pure culture of pathogenic *E. coli* O157:H7
4. Specificity Testing (*Specific Aim 3*)
 - a. Pure culture of *S. infantis*
 - b. Mixed culture of *E. coli* O157:H7 and *S. infantis*

3.1 Microfabrication of the Biosensor

The biosensor was fabricated from 4" (100) p-type silicon wafers, thickness 500-550 μm . The wafers were supplied with a 2 μm thick layer of thermal oxide grown over the silicon to serve as an insulator between the electrodes and the substrate. Prior to fabrication, the wafer was polished to create a smooth surface. The polished wafers were cleaned in isopropyl alcohol (Spectrum Chemical; New Brunswick, NJ) and dried under a stream of nitrogen gas inside a glove box.

Photolithography was used to pattern S1805 photoresist (PR), which was purchased from Shipley (Marlboro, MA). Photolithographic patterning was accomplished by first placing the clean wafer onto the resist spinner and pipetting 800 μL of PR onto the center of the wafer. The resist spinner was then engaged to spin at 4000rpm for 30 seconds resulting in a PR coating thickness of about 500nm. After spinning, the wafer was visually examined to ensure that uniform coverage of PR over the wafer surface was achieved. Uniform coverage is important because missing PR will result in the absence of the electrode pattern in the final device. After inspection of PR coverage, the wafer was placed in an oven at 90°C for 45 minutes to soft bake the PR to ensure dryness, a requirement prior to UV exposure.

After the soft bake was completed, the wafer was taken to a mask aligner (AB-M, San Jose, CA). The photomask (Adtek Photomask, Montreal, QC) was placed into the mask aligner and centered over the wafer. The mask aligner was then engaged to expose the wafer to 2.2 seconds of UV light at 440nm. The exposure time of 2.2 seconds was based on the time required for the UV radiation to penetrate and react with a 500nm thick coating of PR. Different photoresist materials and thickness may require different

exposure times. After exposure, the wafer was placed in a PR developer solution for 1 minute to dissolve away exposed areas and then dried under a stream of nitrogen gas. Next, the PR mask was inspected by a metallurgical microscope to ensure the pattern was developed properly. After inspection, the wafer was placed in an oven at 135°C for 1 hour to hard bake the PR mask.

After the hard bake, metal deposition occurred in an Edwards Auto306 thermal evaporator (BOC Edwards, West Sussex, UK). The wafer, along with titanium and gold pellets, were loaded into the evaporator. The evaporator was pumped down to a pressure of 4×10^{-6} Pa and a current (2.2A for titanium and 1.6A for gold) was applied to evaporate the metal in the chamber. First, a 3-5nm layer of titanium was deposited to ensure strong adhesion of the metal to the silicon oxide surface. This was followed by the deposition of a 50nm layer of gold. The metallization process deposited metal over the entire wafer, which had a PR mask on the surface.

After metal deposition, a lift-off process was used to form the MEMS electrode arrays. The wafer was immersed into a crystallizing dish filled with acetone (J.T. Baker; Phillipsburg, NJ). The dish was sonicated for 2 minutes to dissolve the PR mask. Metal was removed with the PR resulting in the lift-off of patterned metal areas. After sonication, the wafer was cleaned in isopropyl alcohol and distilled water and dried under a stream of nitrogen. After lift-off, the wafer was inspected with a metallurgical microscope, an atomic force microscope, and a surface profilometer to inspect the quality of the electrode array.

After lift-off, the wafer was diced into 68 individual 12mm x 8mm dies for use as biosensors. First, a coating of PR was applied to protect the surface from the harsh

environments of the wafer dicing band saw. (The protective PR coating was applied using the resist spinner in the same process described above.) The dicing band saw was engaged to dice the wafer dies to a depth of 450 μ m allowing for individual dies to be broken apart by hand. At this stage, microfabrication of the sensor chips was completed. The complete bill of process for microfabrication can be found in Appendix B.

3.2 Functionalizing the Sensor Surface

After microfabrication of the electrode array in the cleanroom, the chip surface was functionalized for the attachment of the antibody. First, the chips were immersed in acetone in a crystallizing dish to dissolve away the protective PR layer. The chips were then cleaned in a mixture of methanol (Sigma; St. Louis, MS) and hydrochloric acid (CCI; Columbus, WI) for 30 minutes followed by immersion in boiling distilled water for 30 minutes. The chip surfaces were allowed to air dry completely. The cleaning and drying of the chips allowed for a fresh, activated surface for silanization.

Silanization of the clean chip surfaces occurred in an anaerobic glove box (Coy; Lansing, MI). Inside the glove box, the chips were immersed in a crystallizing dish containing a solution of [3-Mercaptopropyl] trimethyloxysilane (MTS) for 2 hours (Sigma; St. Louis, MS). The MTS solution was diluted in toluene to a concentration of 2%. The silanizing agent MTS is shown in Figure 3.1. The chips were then rinsed in toluene and allowed to dry completely in a glove box under anaerobic conditions. The chips were removed from the glove box.

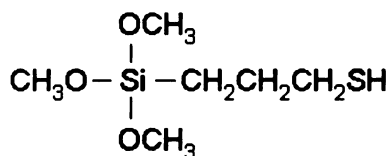


Figure 3.1 (3-Mercaptopropyl) trimethyloxysilane (MTS) used for silanization (courtesy of Sigma-Aldrich).

After silanization, crosslinkers were added to the sensor surface. The crosslinker used was *N*-γ-maleimidobutyryloxy succinimide ester (GMBS) (Sigma; St. Louis, MA) dissolved in dimethylformamide (DMF) (Spectrum; New Brunswick, NJ). The solution was made from 25mg of GMBS dissolved in a minimum amount of DMF and diluted to 2mM in ethanol (Pharmco; Brookfield, CT). The chemical structure of the crosslinker GMBS is shown in Figure 3.2. Enough crosslinker solution was pipetted to cover the electrode array of each individual die and left for 1 hour. After crosslinking, the biosensor was rinsed in phosphate buffered saline (PBS, pH 7.4).

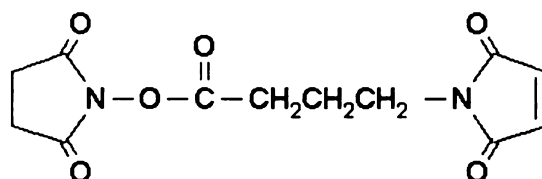


Figure 3.2 *N*-γ-maleimidobutyryloxy succinimide ester (GMBS) used for crosslinking (courtesy of Sigma-Aldrich).

After application of the crosslinker, polyclonal antibody was immobilized to the sensor surface. Purified polyclonal antibodies specific to generic *E. coli* and *E. coli* O157:H7 were used in this research. The purified goat IgG for *E. coli* O157:H7 (Kirkegaard & Perry Laboratories; Gaithersburg, MA) has low cross-reactivity to other *E.*

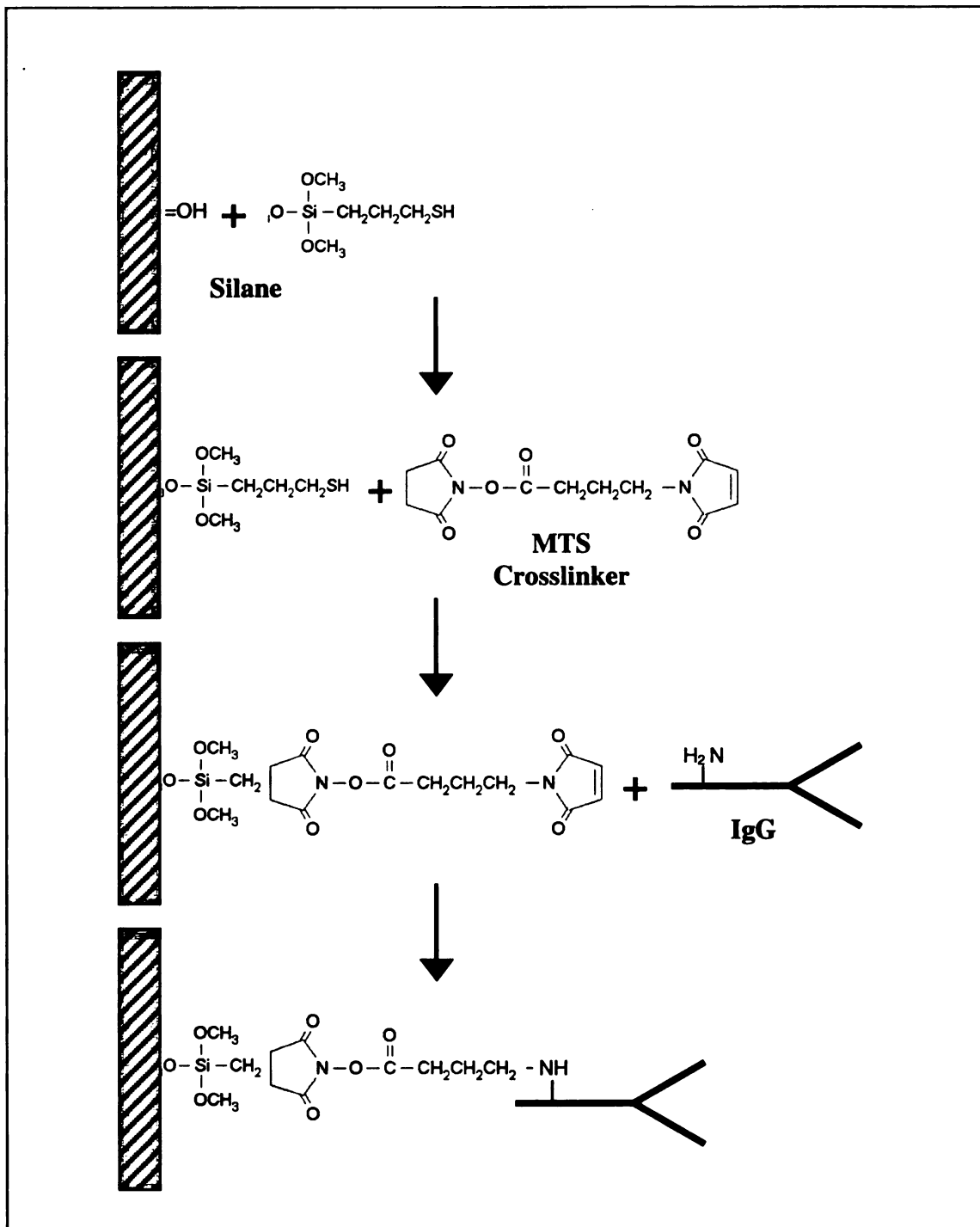


Figure 3.3 Process of antibody attachment to the silicon oxide (adapted from Bhatia et al., 1989).

coli. The polyclonal antibody was rehydrated and diluted with PBS to a concentration of 150µg/mL and 250µL of it was placed on each individual crosslinker coated sensor chip. The chips were placed in a petri dish, sealed with parafilm (Pechiney, Chicago, IL) and allowed to incubate at 37°C for 1 hour. An antibody concentration of 150µg/mL was used based on the results reported in the antibody immobilization procedure (Bhatia et al., 1989). After incubation, the surface was rinsed with PBS (pH 7.4) and allowed to air dry. At this stage, the biosensor (or chip) preparation was completed. The biosensors were then refrigerated at 4°C until needed for sample testing. The antibody immobilization process (Shriver-Lake et al., 1997) is outlined in Figure 3.3. A complete bill of process for surface functionalization and formulations for the reagents used can be found in Appendix B.

3.3 Validation of the Biosensor

Specific Aim 2 reads: To employ the biosensor for detecting the presence of serially diluted bacteria in pure culture in a sample size of 20mL.

To validate the biosensor against pure culture, separate experiments were conducted using non-pathogenic *E. coli* (ATCC#25922) and pathogenic *E. coli* O157:H7 (ATCC#43895) obtained from the Biosystems Engineering collection, Michigan State University.

Nutrient broth (Difco; Detroit, MI) was used for bacterial enrichment. A 10µL loop of each bacteria isolate was cultured in 10mL of Nutrient Broth and incubated for 24 hours at 37°C to make a stock culture. The stock culture was serially diluted in 0.1% of peptone water (Sigma; St. Louis, MS) to obtain logarithmic concentrations of the

organism from 10^0 CFU/mL to 10^7 CFU/mL. The different concentrations were added to PBS (pH 7.4) creating test samples of 20mL with concentrations ranging from 10^0 CFU/mL to 10^7 CFU/mL. The sample concentrations were then determined by the standard plating method according to the FDA Bacteriological Analytical Manual (FDA, 1998). For generic *E. coli* confirmation, MacConkey agar (Difco, Detroit, MI) was used to plate 100 μ L of each serial dilution. The colonies were counted after 24 hours of incubation at 37°C. For *E. coli* O157:H7 confirmation, Sorbitol MacConkey agar (Difco, Detroit, MI) was used to plate 100 μ L of each serial dilution. (*E. coli* O157:H7 can be distinguished by its inability to ferment sorbitol.) The colonies were counted after 24 hours of incubation at 37°C.

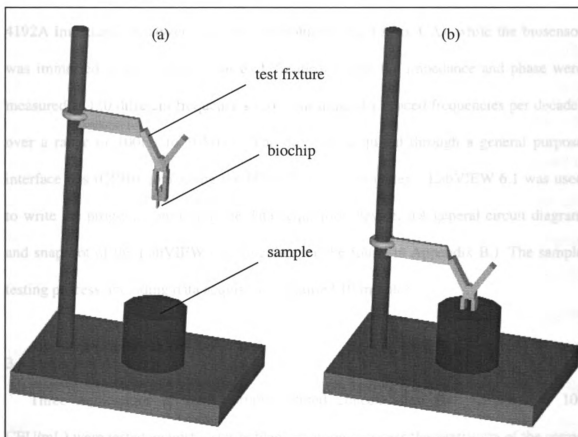


Figure 3.4 Biosensor test apparatus in (a) raised and (b) lowered position.

After sample preparation, a biosensor was obtained from refrigerated storage and inserted into the apparatus test fixture. The biosensor was then lowered into the sample so that the electrode array was immersed into solution. Figure 3.4 shows the biosensor test apparatus and fixture in raised and lowered position (Appendix B contains detailed drawings of the biosensor apparatus and test fixture.) After being lowered into solution, the biosensor was left for 5 minutes to allow antigen to bind to the biosensor. The impedance signal was then measured.

3.4 Signal Measurement

A potential of 50mV was applied across the electrodes with a 0V bias and the impedance magnitude of the biosensor was measured from 100Hz-10MHz with an HP 4192A Impedance Analyzer (Agilent Technologies, Palo Alto, CA), while the biosensor was immersed in the sample. For each frequency step, the impedance and phase were measured at 120 different frequencies (20 logarithmically spaced frequencies per decade) over a range of 100Hz to 10MHz. The data was acquired through a general purpose interface bus (GPIB) connecting the HP 4192A to a computer. LabVIEW 6.1 was used to write the program controlling the data acquisition device. (A general circuit diagram and snapshot of the LabVIEW user interface can be found in Appendix B.) The sample testing process, including data acquisition, required 10 minutes.

3.5 Statistical Analysis

Three replications of each serially diluted concentration (10^0 CFU/mL to 10^7 CFU/mL) were tested against a sterile blank solution to assess the sensitivity of the assay. The randomized trials were performed for several consecutive days to nullify the effect of

daily variation in bacterial counts. All biosensors were assumed to have the same physical properties. The means and standard deviations of the impedance magnitude and phase angle were calculated for frequencies between 100Hz-10MHz. The significance of the differences between means was determined and analyzed based on a one-way ANOVA followed by a Tukey's W test to a significance of 95% ($p < 0.05$). The lower detection limit of the biosensor (sensitivity) was determined as the lowest bacteria concentration with a mean impedance value significantly different from the blank.

3.6 Specificity Study

Specific Aim 3 reads: To employ the biosensor for distinguishing the target bacteria in a liquid sample of mixed microflora.

For the specificity testing, characterized strains of pathogenic *E. coli* O157:H7 (ATCC #43895) and *S. infantis* (ATCC #51741) were obtained from the Biosystems Engineering collection, Michigan State University. Nutrient broth (Difco; Detroit, MI) was used for bacterial enrichment. A 10 μ L loop of each bacteria isolate was cultured in 10mL of nutrient broth and incubated for 24 hours at 37°C to make stock cultures of each bacteria strain. The stock cultures were serially diluted in 0.1% of peptone water (Sigma; St. Louis, MS) to obtain logarithmic concentrations of the organisms from 10⁰ CFU/mL to 10⁷ CFU/mL. The different concentrations were added to PBS (pH 7.4) creating test samples of 20mL with both *E. coli* O157:H7 and *S. infantis* concentrations ranging from 10⁰ CFU/mL to 10⁷ CFU/mL. The sample concentrations were then determined by the standard plating method according to the FDA Bacteriological Analytical Manual (FDA, 1998). For *E. coli* O157:H7, Sorbitol MacConkey agar (Difco, Detroit, MI) was used to

plate 100 μ L of each serial dilution. The colonies were counted after 24 hours of incubation at 37°C. For *S. infantis*, Bismuth Sulfite agar (Difco; Detroit, MI) was used to plate 100 μ L of each serial dilution.

After sample preparation, a biosensor was obtained from refrigerated storage and inserted into the apparatus test fixture. The biosensor was then lowered into the sample so that the electrode array was immersed into the solution, as shown previously in Figure 3.4. The biosensor was left for 5 minutes to allow antigen to bind to the biosensor surface. The impedance signal was then measured as described in Section 3.4.

In the specificity study, the sample testing sequence is shown in Table 3.1. Assays of pure culture of the target bacteria were first conducted to determine the overall specificity

Table 3.1 Specificity testing matrix

Test	Sample Species	Target Antigen	Non-Target Antigen
I	<i>E. coli</i> O157:H7 (Pure Culture)	<i>E.coli</i> O157:H7	-----
II	<i>S. infantis</i> (Pure Culture)	-----	<i>S. infantis</i>
III	<i>E. coli</i> O157:H7 and <i>S. infantis</i> (Mixed Culture)	<i>E.coli</i> O157:H7	<i>S. infantis</i>

of the biosensor as described in Section 3.1. Test I was on pure culture of the target antigen *E. coli* O157:H7. Test II was on pure culture of *S. infantis* with no target antigen. Test III was on a mixture of *E. coli* O157:H7 and *S. infantis* to determine the effects of *S. infantis* on the ability of the biosensor to detect for *E. coli* O157:H7, the target antigen. The biosensor was functionalized with *E. coli* O157:H7 specific antibodies for all three tests. Assays on dilution series of target and non-target bacteria in the same sample were conducted to assess the specificity of the biosensor in mixed cultures. All microbial

analysis, signal measurement and statistical analysis were conducted as described in Section 3.4 and 3.5.

3.7 Testing in Complex Media

Experiments were conducted on complex food matrices to explore the performance of the biosensor in these substrates. The Methods and Materials and Results and Discussion for the complex media study are included in Appendix D.

3.8 Facilities and Equipment

Fabrication of the biosensor chip was completed in the WM Keck Microfabrication Facility. The WM Keck Microfabrication Facility, MSU, is a full service clean room for electronic device fabrication. The clean room has capability for deep UV photolithography, wafer dicing and bonding, and metal evaporation. All biosensor testing was conducted in the Biosensors Laboratory. The laboratory is equipped to handle Biosafety Level 2 organisms according to the MSU biosafety standard procedures (MSU, 1998). All microbial analysis was conducted in the Biosensors Laboratory. All laboratory and biohazard wastes were labeled, handled, and disposed of according to the MSU standard procedures for handling bio-hazardous waste (MSU, 1998). The laboratory is under supervision by the Office of Radiation, Chemical, and Biological Safety (ORCBS) of MSU.

Chapter 4. Results and Discussion

4.1 Simulation Results

Simulation of the electric field was performed for different interdigitated electrode widths and spacing. The simulations were performed using Maxwell 2D and Maxwell 3D Finite Element Method (FEM) software (Ansoft Corporation; Pittsburgh, PA) over a variety of width and spacing combinations. The results for $1\mu\text{m} \times 1\mu\text{m}$, $6\mu\text{m} \times 6\mu\text{m}$, $5\mu\text{m} \times 10\mu\text{m}$ and $10\mu\text{m} \times 5\mu\text{m}$ arrays are shown in Figure 4.1. These simulation values are representative of electrode size ranges found in the literature and have been used to optimize the electrode width and spacing (Gomez et al., 2001; Sergeyeva et al., 1996; Sheppard et al., 1995; Van Gerwen et al., 1998).

The results show that evenly spaced electrodes cause an evenly distributed electric field resulting in uniform coverage across the sensor surface. When the electrode width is larger than the electrode spacing, the electric field tends to favor the area near the middle of the electrode. When the electrode width is smaller than the electrode spacing, the electric field is disproportionately larger in the spaces and at the edges of the electrodes. Furthermore, the electric field is not uniform when width and spacing are different.

Figure 4.1a shows the simulation results for a $1\mu\text{m} \times 1\mu\text{m}$ electrode array. The electric field distribution is quite uniform across the surface of the sensor. The small width and spacing of the array results in the electric field being concentrated within $2\mu\text{m}$ of the sensor surface. This distance is closer than needed for applications involving bacteria in the $2\mu\text{m}$ - $4\mu\text{m}$ range. The $6\mu\text{m} \times 6\mu\text{m}$ (Figure 4.1b) also shows uniform

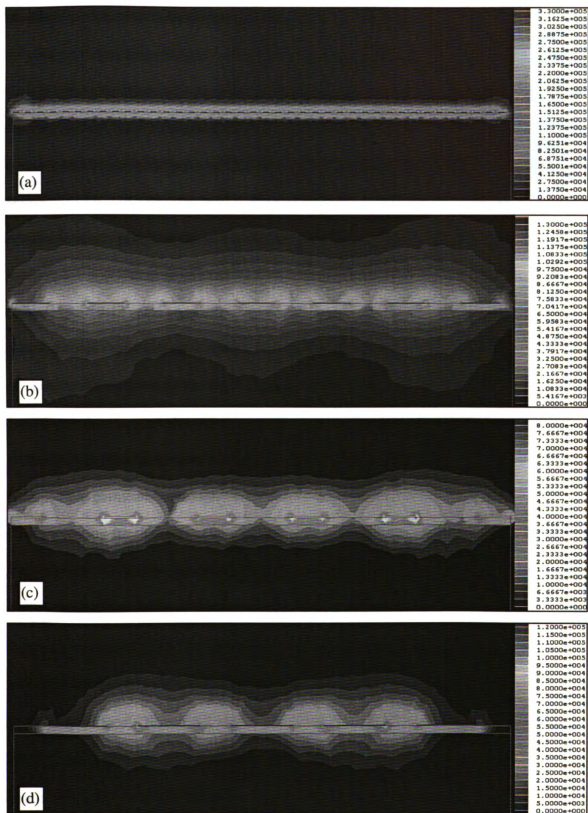


Figure 4.1 Simulation results for different electrode widths and spacing: (a) $1\mu\text{m} \times 1\mu\text{m}$ array; (b) $6\mu\text{m} \times 6\mu\text{m}$ array; (c) $5\mu\text{m} \times 10\mu\text{m}$ array and (d) $10\mu\text{m} \times 5\mu\text{m}$ array.

distribution across the surface. The large size of the array, however, allows for the electric field to permeate deep into the sample, about 15 μm above the surface. Contrary to the 1 μm x 1 μm array, this distance is larger than needed for applications involving bacteria. The 5 μm x 10 μm array (Figure 4.1c) shows the effects of having larger spacing with respect to the electrode width. The result is that the field is not uniform across the sensor surface. In fact, the field is disproportionately strong around the electrode and weaker in the spacing. This is a problem since bacteria bound on or near the electrode will impact impedance more than bacteria bound to the oxide spacing. The 10 μm x 5 μm array (Figure 4.1d) also results in a non-uniform distribution but differs from the 5 μm x 10 μm array in that the field is disproportionately concentrated near the spacing. Because of this, bacteria bound to the oxide spacing will have a larger impact on the measured impedance than bacteria bound on or near the electrode. The 5 μm x 10 μm and 10 μm x 5 μm arrays both contribute to a large characteristic length ($L=w_{SP}+w_{EL}$) resulting in the electric field permeating through the solution farther away from the sensor surface.

In selecting for the optimum electrode width and spacing, the goal was for a uniform electric field with a characteristic length resulting in most of the electric field being within 5 μm of the surface. Based on the simulation, the optimum electrode width and spacing was determined to be 3 μm and 4 μm , respectively, based on a mean *E. coli* length of 2.5 μm and a target of 90% of total electric field strength below a distance of 5 μm from the sensor surface. Figure 4.2 shows the simulation results for an applied potential of 100mV and interdigitated electrodes with a width of 3 μm and spacing of 4 μm . The resulting electric field distribution is nearly as uniform for configurations with electrodes

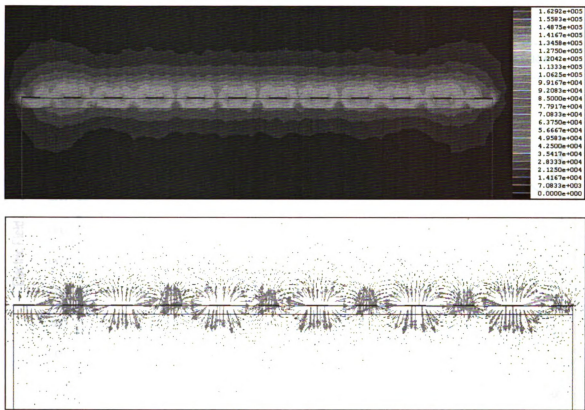


Figure 4.2 Electric field simulation of $4\mu\text{m} \times 3\mu\text{m}$ electrode array: (top) electric field magnitude; (bottom) vector representation of electric field.

that are evenly spaced. The electric field uniformity is demonstrated by the nearly horizontal line shown surface field plot of Figure 4.3. The $3\mu\text{m} \times 4\mu\text{m}$ configuration is also optimal since the electric field is concentrated within $5\mu\text{m}$ above the sensor surface as shown in Figure 4.4. For example, if there is a large particle floating at a distance of $10\mu\text{m}$ above the sensor surface the effect on sensor impedance will be minimal since 98% of the electric field is below $10\mu\text{m}$. Because the application of the sensor is to test for bacteria in a complex food matrix (such as ground beef), the change in impedance due to foreign particles near the sensor surface will need to be minimized.

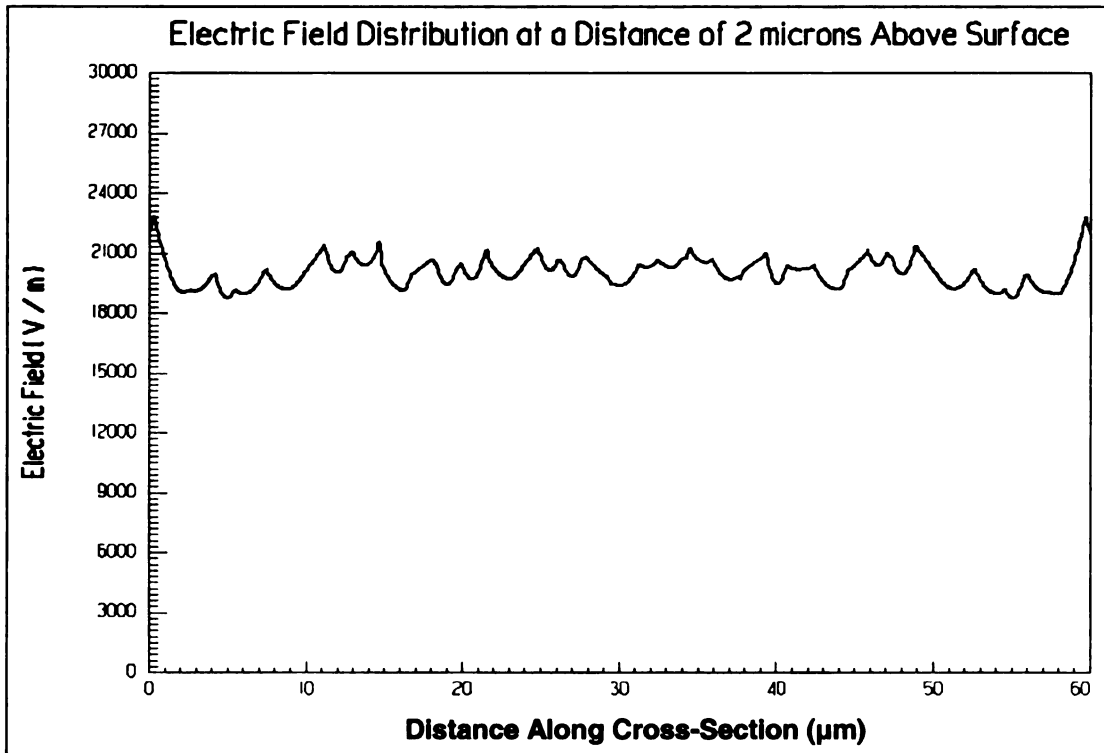


Figure 4.3 Surface plot of the electric field distribution at 2 μm from the electrode array.

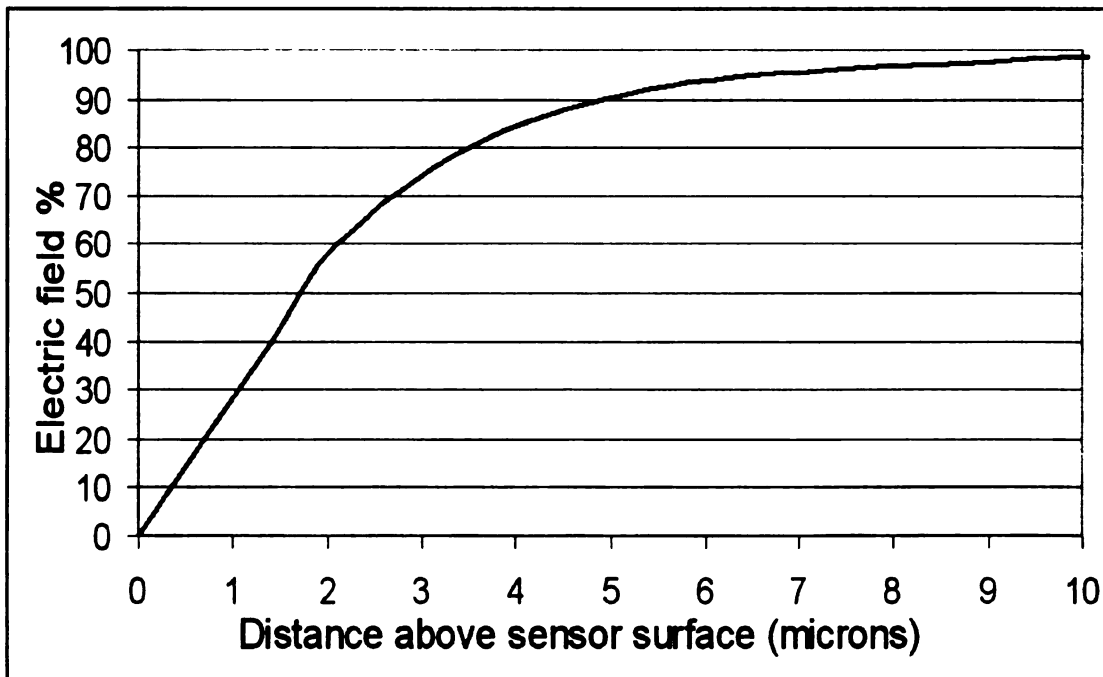


Figure 4.4 Percentage of electric field above sensor surface.

Table 4.1 summarizes the electric field uniformity, bias, and penetration depth for all the simulated array sizes.

Table 4.1 Comparison matrix of simulation sizes

Array Size	1µm x 1µm	6µm x 6µm	5µm x 10µm	10µm x 5µm	3µm x 4µm
Field Uniformity	Uniform	Uniform	Non Uniform	Non Uniform	Near Uniform
Field Bias	None	None	Electrode	Spacing	None
Field Depth	2µm	12µm	12-15µm	12-15µm	5-7µm

The simulation also included immobilized bacteria of different diameters to evaluate how the electric field distribution will change in the presence of target analyte. Figure 4.5 displays a cross-section of the biosensor suspended in solution with simulated bacteria immobilized on the surface and shows that most of the electric field is relatively uniform across the sensor surface. The simulation also shows that the electric field on the surface permeates through the bacteria. The presence of the immobilized bacteria results in an increase in the impedance measured across the two electrodes. This simulation validates the choice for using a 3µm x 4µm array since the bacteria is well within the range of the electric field, yet the field does not permeate deeper than necessary into the solution above the biosensor surface.

After selecting the optimum electrode width and spacing, the next goal was to select an appropriate active area. The active area was determined based on an estimate of the surface area required to accommodate as many as 10^7 CFU of immobilized *E. coli* cells on the sensor surface. Assuming the bacteria is 1µm or smaller in diameter, the minimum surface area needed is $10^7 \mu\text{m}^2$ (10mm^2) to capture all the bacteria in a 1mL sample. There is no existing data to support how large the active area of the device needs to be.

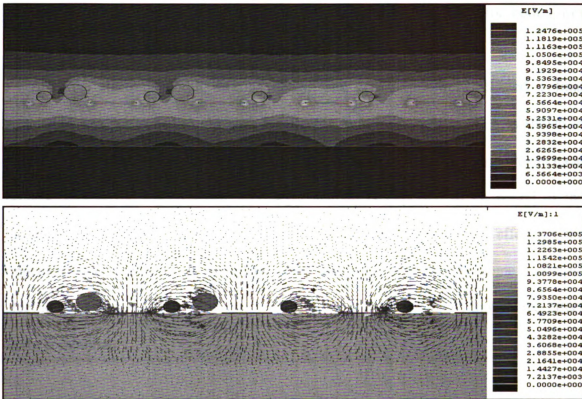


Figure 4.5 Simulation of $3\mu\text{m} \times 4\mu\text{m}$ array with immobilized bacteria: (top) electric field magnitude; (bottom) vector representation of electric field.

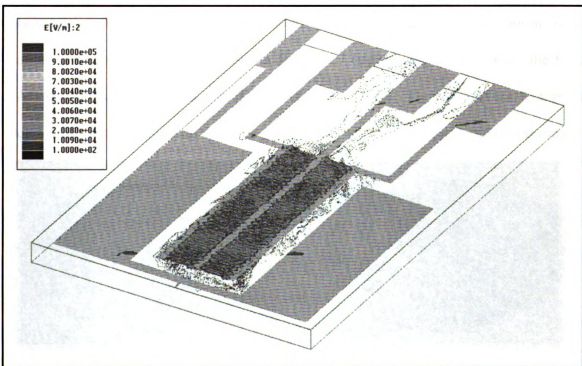


Figure 4.6 Maxwell 3D simulation of the electric field on sensor surface.

An area of 10mm^2 was selected to allow for adequate binding sites for both lower concentrations and high concentrations of bacteria.

After the electrode width, spacing, length and active area were selected, a final simulation was performed to visualize the electric field magnitude in 3D. As shown in Figure 4.6, the electric field is densely concentrated in the electrode array. This is ideal because this is the region where the target analyte is expected to be bound to the biosensor. Furthermore, areas outside of the array will have minimal effect on the impedance measurement. It should be noted also that there may be some undesired electric field presence caused by the circuit traces and contact pads, though the effect again is minimal.

4.2 Fabrication Results

In fabricating the biosensor, the first step needed was to design the pattern needed to fabricate the photomask for use in photolithography. The photo mask pattern looks similar to the patterned silicon wafer in Figure 4.7 (right). Figure 4.8 shows the final CAD layout drawing used to manufacture the photo mask. The final device features 4 rectangular contact pads, with the three pads leading to electrode arrays each measuring

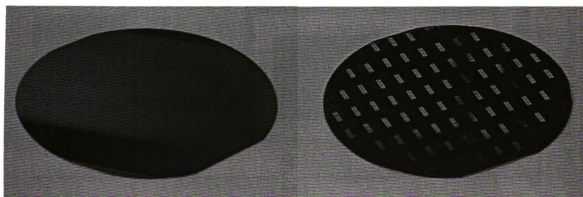


Figure 4.7 A 4" Silicon wafer before (left) and after (right) processing.

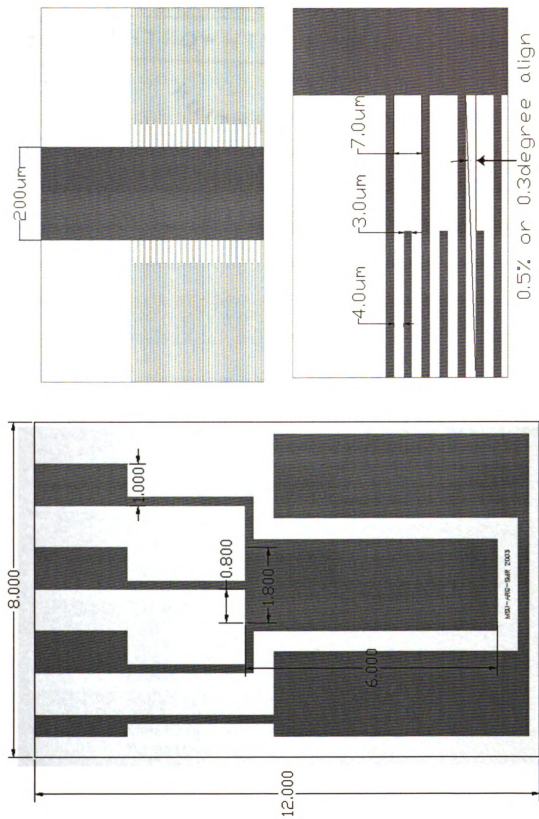


Figure 4.8 CAD Drawing of Biosensor: (left) layout; (top-right) closeup of electrode arrays; (bottom-right) detail of electrode arrays.

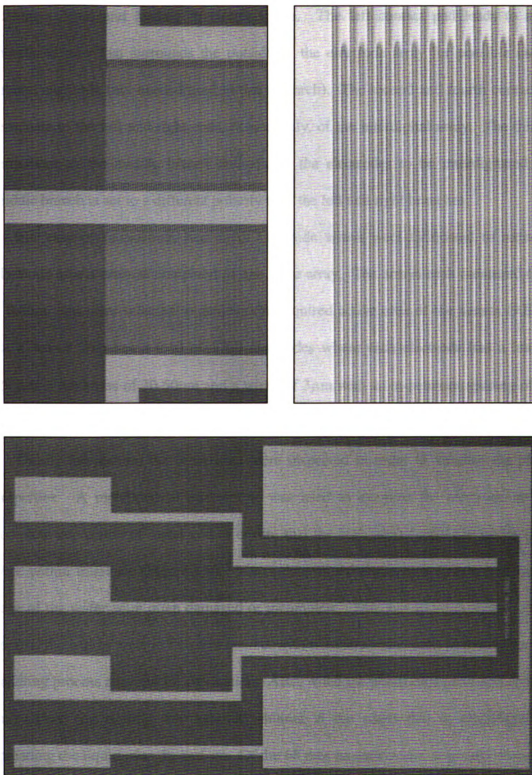


Figure 4.9 (left) die shot of biosensor; (upper-right) high density electrode arrays; (lower-right) close up of electrodes.

2.5mm x 1mm and leading to circuit traces. The left contact pad leads to a large metallized area that surrounds the outside of the electrode array for possible use as a ground electrode (not needed/used in this research). The second and fourth contact pads terminate to the left and right ends, respectively, of the interdigital array. The third pad terminates to the middle branch and allows the electrodes to be interdigitated. The middle branch is set to a different polarity than the left and right branches.

For ease of fabrication, two small electrode arrays were fabricated to reduce the electrode aspect ratio as compared to one large array. The arrays each measured 6.0mm x 0.8mm and were selected to achieve the required active area of the sensor (9.6mm²). Each sensor chip has a total of 1700 electrodes where each electrode had a length of 750μm, a thickness of 30-50nm and a width of 3μm with an in-between spacing of 4μm. After fabrication, each sensor was diced to a dimension of 12mm x 8mm.

During fabrication, the biosensors were inspected in order to validate the physical properties. A metallurgical microscope was used to examine the electrode array for complete deposition of metal and to ensure that the high aspect ratio electrodes (250:1) were within tolerance (Figure 4.9). It was determined that sensors located at the outer edge of the wafer were often damaged or incomplete. This was to be expected since the edge of the wafers were in frequent contact with tweezers and chucks as part of the wafer handling process required for fabrication. Also, when the photoresist (PR) was spun onto the wafers, the coating was naturally thinner at the edges due to centrifugal force spreading the liquid over the surface. Of the 68 dies on each wafer, anywhere from 12-16 dies (all at the edges) were not usable. This was expected and quite normal for a non-automated fabrication facility. The dies in the middle of the wafer were consistently

uniform and of high quality. Figure 4.10 is a quality diagram showing where damaged dies are often located.

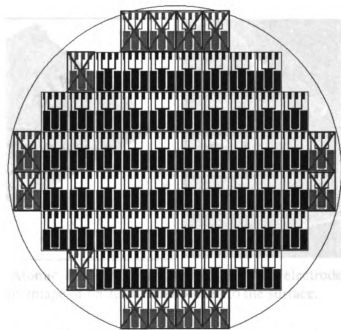


Figure 4.10 Quality control diagram showing likely locations for damaged dies.

Atomic force microscopy (AFM), scanning electron microscopy (SEM) and confocal scanning laser microscopy (CLSM) were used to validate the fabrication of the biosensor. AFM was used to measure the length, thickness, width and spacing of the electrode on a clean sensor surface. AFM images show that the sensor is within tolerance having an electrode width of $3\mu\text{m}$, spacing of $4\mu\text{m}$ and a thickness of 35nm (Figure 4.11). The CLSM was used to validate antibody immobilization and determine where it occurred (Figure 4.12). CLSM images show that the antibody immobilization is occurring on both the oxide area between the electrodes and the electrodes themselves. The antibodies have a natural affinity to the thiol group of the gold electrodes, thus it can be concluded that the antibody covers the entire electrode array. Actual antibody concentration on the

surface was not determined, though a concentration of 150 μ g/mL was used in the immobilization procedure.

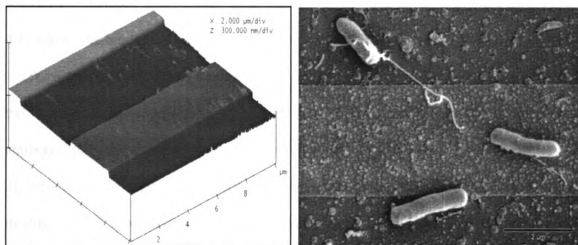


Figure 4.11 (left) Atomic Force Microscopy image of the electrodes; (right) Scanning Electron Microscopy image of bacteria immobilized to the surface.

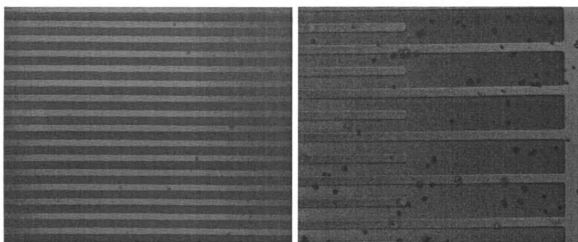


Figure 4.12 Confocal Laser Scanning Microscopy image of electrodes showing antibody immobilized to electrode and oxide surfaces.

SEM was used to measure the physical properties (length and width) of clean biosensors, to verify binding of bacteria to antibodies immobilized on the sensor surface and to observe the surface properties of functionalized biosensors. When measuring for the electrode length and width, the clean sensors were not silanized, and thus were

without a biological sensing surface, and showed the state of the sensor immediately after the microfabrication process. The biosensors exposed to bacteria were immersed in solutions containing non-pathogenic *E. coli* followed by a gentle rinse in PBS. Figure 4.11 shows the binding of non-pathogenic *E. coli* to the surface of the biosensor.

A comparison was made between clean and functionalized biosensors. In observing the functionalized biosensors, it was found that modification of the sensor surface with antibodies caused an irreversible thin film of silanes to build up on the sensor surface. Though attempts were made to clean the sensor surface after each use, the repeated treatment of the oxide surface with oxysilanes resulted in a permanent change to the sensor surface between trials. Figure 4.13 shows the difference between a clean sensor and a surface modified with crosslinkers and antibodies via silanization. As a result of this finding, a new biosensor was used for each trial and then was sterilized and discarded after testing.

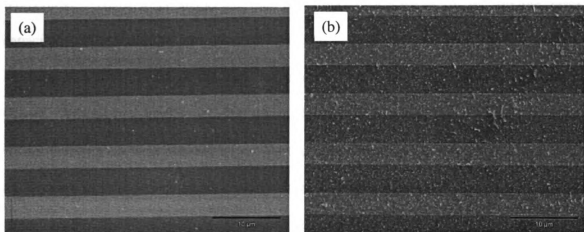


Figure 4.13 The effects of surface modification: (left) clean biosensor surface; (right) silanized biosensor surface.

4.3 Results and Discussion of Pure Culture Testing

4.3.1 Frequency Dependence

The change in impedance of the biosensor is directly proportional to the number of bacteria immobilized on the sensor surface. The impedance spectra for different concentrations of non-pathogenic *E. coli* and pathogenic *E. coli* O157:H7 bacteria in pure culture are shown in Figures 4.14 and 4.15. The measured impedance for all concentrations of bacteria from 10^0 to 10^7 CFU/mL and the blank for non-pathogenic *E. coli* and *E. coli* O157:H7 are plotted over a frequency range of 10Hz-10MHz.

The impedance is dependent on both frequency and bacteria concentration. At high frequencies (>1 MHz) there is little change in impedance with respect to bacteria concentration because the impedance is largely dominated by dielectric capacitance of the sample media. At these high frequencies, the effect of bacteria bound to the biosensor surface is minimized due to the relaxation of small dipole species (water molecules). Also, it is suspected that the impedance caused by the double layer capacitance (C_{DL}) and the parasitic capacitance (C_{PAR}) is minimized at high frequencies resulting in a convergence of the impedance toward the resistance of the testing solution (R_{SOL}). At low frequencies (<1 kHz), the difference in impedance is shown to increase with increasing bacteria concentration. At these low frequencies, the impedance caused by bacteria is found to increase linearly with the number of cells present in solution. However, this linear increase in impedance does not register for low cell concentrations and only begins to take effect at 10^3 CFU/mL and greater. This is because a solution with low bacteria concentration ($<10^4$ CFU/mL) results in fewer bacteria being immobilized on the biosensor surface while solutions with high cell concentrations result in bacteria

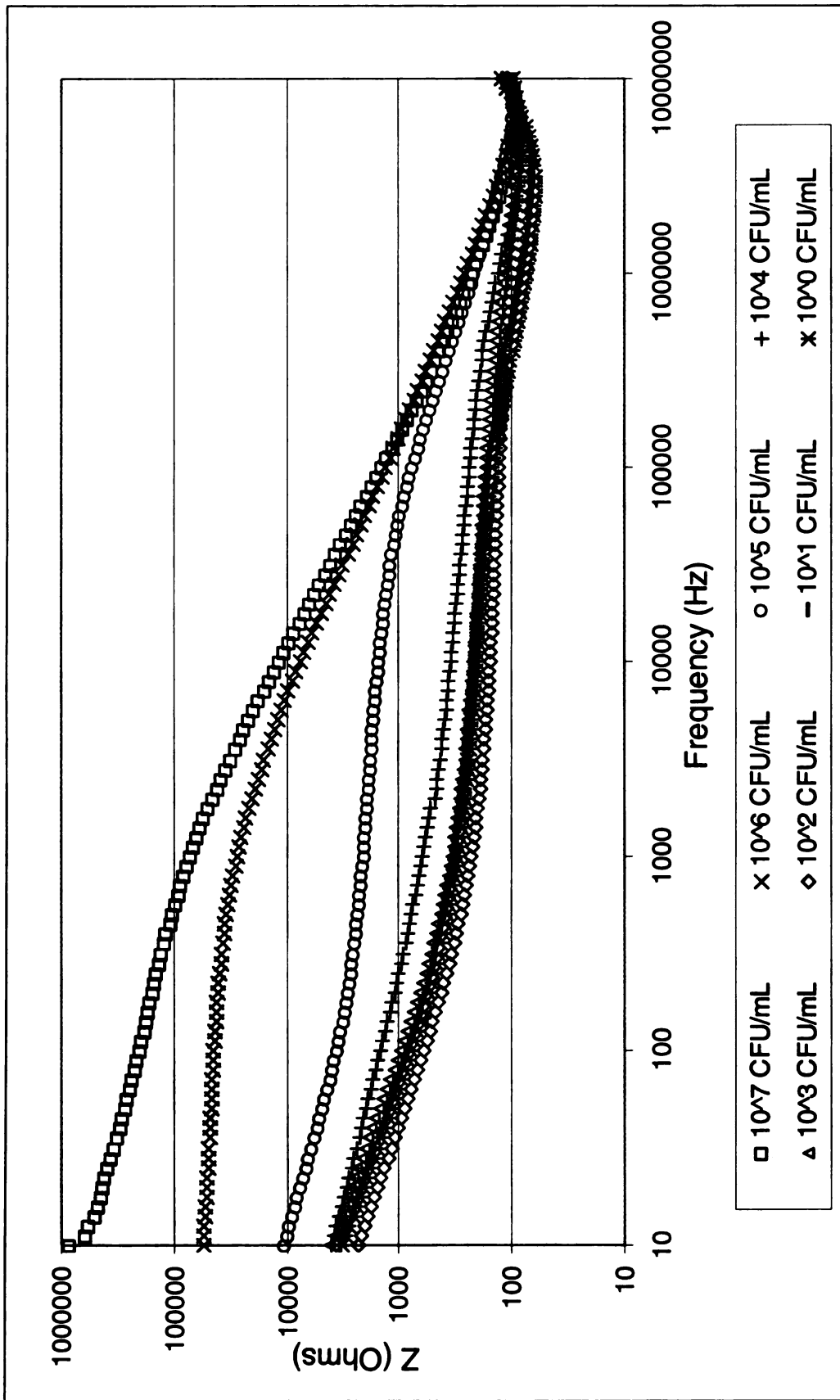


Figure 4.14 Impedance for a frequency distribution from 10Hz to 10MHz for non-pathogenic *E. coli*.

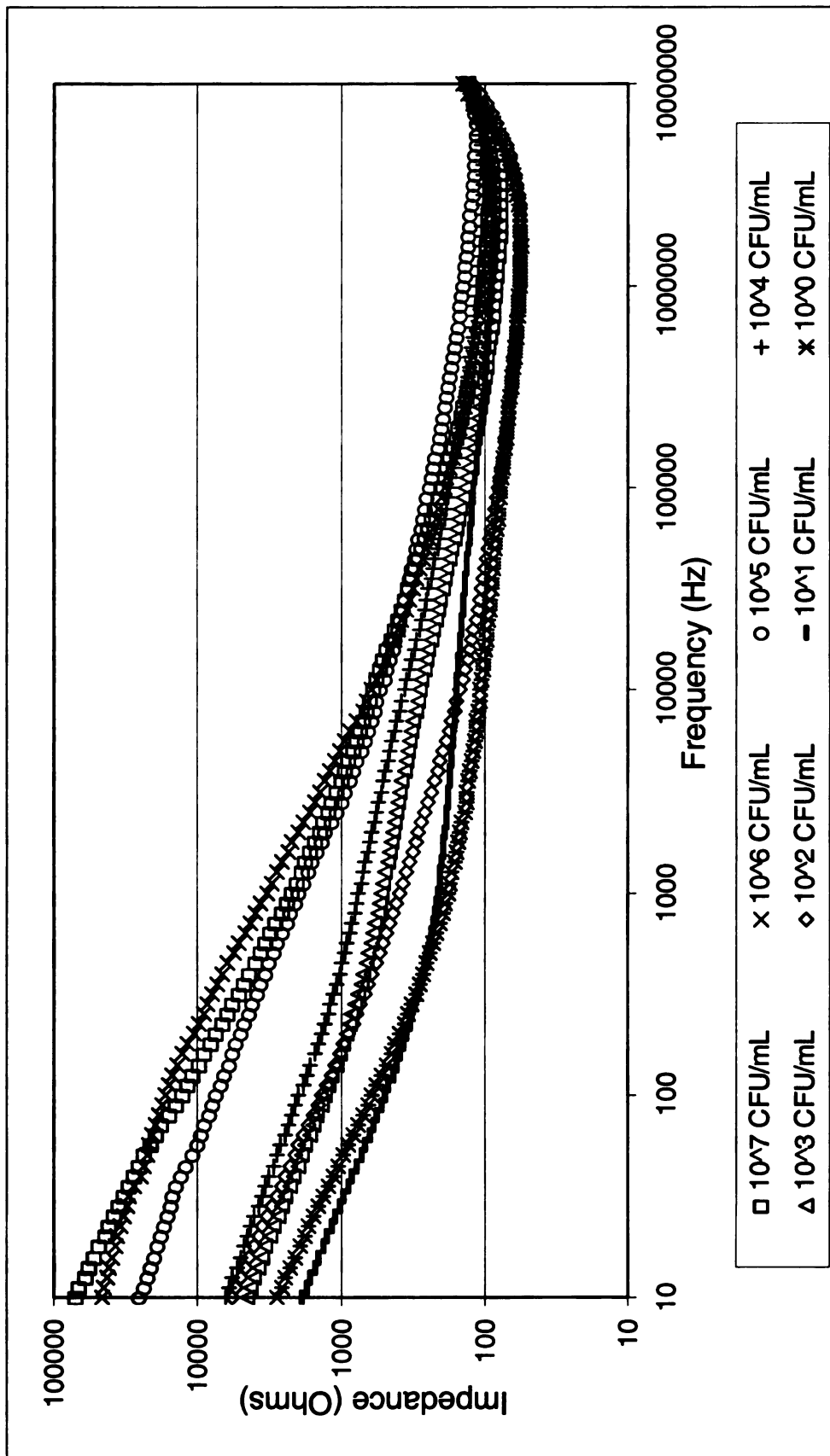


Figure 4.15 Impedance for a frequency distribution from 10Hz to 10MHz for *E. coli* O157:H7.

covering the sensor surface. In fact, there is no statistically significant detectable difference in impedance between bacteria concentrations from 10^0 to 10^3 CFU/mL at a frequency of 1kHz. It is suspected that the polarization effect of the bacteria on the biosensor surface only begins to change the impedance at concentrations greater than 10^3 CFU/mL because of the sufficient number of bacteria required to change the impedance above the base impedance of the biosensor. The inability of the biosensor to detect impedance changes for low bacteria concentrations may be due to the effect of double layer capacitance and parasitic capacitance found in the biosensor, which act independently of whether bacteria are present in solution.

For high frequencies, the current passes through the dielectric capacitance instead of the cellular impedance and medium resistance (Ehret et al., 1997; Van Gerwen et al., 1998). Therefore, the dielectric capacitance of the medium dominated the total impedance, and the cellular impedance, double layer capacitance and medium resistance can be largely ignored. Since the dielectric capacitance is the only contribution to the impedance at high frequencies, the impedance value is inversely proportional to the frequency.

At low frequencies, the effect of cellular impedance is dominant (Yang et al., 2004). The total impedance has contributions from the double layer capacitance, the cellular impedance, and the solution resistance. There is a frequency region (1kHz-1MHz), however, where the impedance is controlled by a combination of all the impedance elements. The change in double layer capacitance and cellular impedance is more significant compared to the change in medium resistance, implying that the decrease in

impedance value due to the bacterial growth is dominated by the increase in cellular impedance and double layer capacitance.

Surface chemistry issues related to the silanization process allowed antibodies to bind to the gold electrodes. While having antibodies on the gold electrodes increases that amount of bacteria immobilized on the biosensor surface it also increased the base level of noise in the system, particularly for samples with low bacteria concentrations. At high bacteria concentrations, increased antibody immobilization to the gold electrodes actually increases biosensor performance since the high number of bacteria present in the sample will allow for more binding, translating into a higher impedance measurement. At lower frequencies, however, the increased antibody immobilization to the gold electrodes provides more background noise to the system reducing the effect of bacteria on impedance change at low concentrations.

4.3.2 Effect of Non-pathogenic and Pathogenic Bacteria

For both non-pathogenic and pathogenic species, there is no statistically significant detectable difference in impedance between the blank and bacteria concentrations from 10^0 to 10^3 CFU/mL at a frequency of 1kHz. This demonstrates that for both generic *E. coli* and *E. coli* O157:H7, the impedance measured by the biosensor is heavily influenced by the double layer capacitance and parasitic capacitance at low frequencies. In the case of Helmholtz capacitance, it is interesting to note that as crosslinkers and antibodies adsorb to the surface, the effective area available for ion exchange is reduced. And even more so as the electrodes become covered with bacteria. With increasing frequency, the presence of bacteria has a decreasing effect on overall biosensor impedance resulting in a

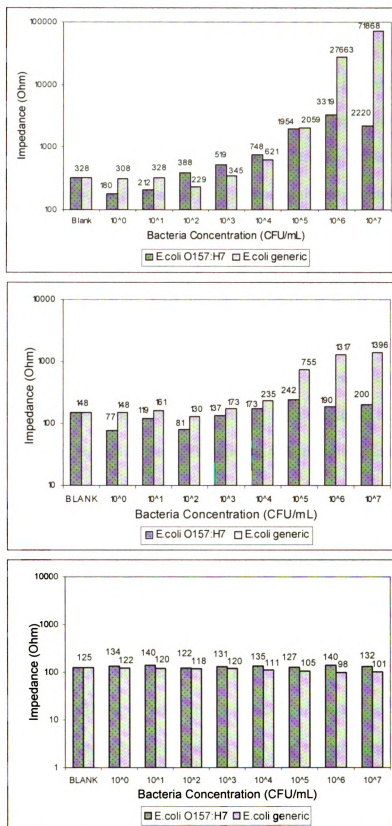


Figure 4.16 Comparison of *E. coli* and *E. coli* O157:H7 at selected frequencies: (top) 1kHz; (middle) 100kHz; (bottom) 10MHz.

convergence of the impedance. This could be due to the impedance being dominated by the dielectric behavior of the medium at high frequencies.

Comparing pathogenic bacteria and nonpathogenic bacteria, it is shown that *E. coli* O157:H7 yields lower impedance than *E. coli*. This effect is most pronounced at low frequencies. Figure 4.16 shows the biosensor responses at 1kHz, 100kHz, and 10MHz. Note that the impedance difference at 1kHz is pronounced as the impedance is largely due to the number of bound bacteria. At 10MHz, there is little difference between generic *E. coli* and *E. coli* O157:H7 since the impedance is due to the dielectric capacitance of the testing medium. High frequency measurements yield little measurable difference between bacteria concentrations for either species.

It is suspected that the pathogenic bacteria do not bind as well as the nonpathogenic strain as observed from the impedance measurements. The specificity of their respective antibodies are different, though non-specific binding of interferant bacteria species with specific antibodies is not a problem for this study because the samples were artificially inoculated only with the target organisms and nothing more. Another possible reason for the difference in impedance between pathogenic and non-pathogenic species is that the physical properties of the cells are different. For this study (including the electric field simulation), the properties of the lipid bilayer membrane and cellular cytoplasm were assumed to be the same for both generic *E. coli* and *E. coli* O157:H7. It may be that the physical properties of different *E. coli* species are different and have an effect of the measured impedance. Currently, there has not been any research regarding the actual values of the membrane and cellular impedance of different *E. coli* species. Experiments to determine specificity will focus on the effects of multiple species present in the testing

solution as described in the specificity testing.

After measuring the impedance data against time at low frequencies, it was found that the impedance increased the longer the biosensor remained in solution. Figure 4.17 shows Cole-Cole plots of the impedance for 0, 15, 30 and 60 minutes after insertion in the test solution. The increase in impedance could be due to an increased number of bacteria cells binding to the sensor surface over time. Based on the data, the increased impedance is most pronounced within the first 20 minutes after insertion into solution. The Cole-Cole plots show that after 35 minutes, the rate at which new cells bind to the surface slows down considerably. Also, it is intuitive that given enough elapsed time, dense packing of bacteria may eventually occur on the surface. By taking impedance measurements at specific time intervals, the effect of bacteria concentration is shown. At high frequencies, the effect of cells bound to the biosensor surface have little effect on impedance thus there is no change in impedance with an increase in time. The attached bacterial cells acted as impedance elements in series with medium resistance.

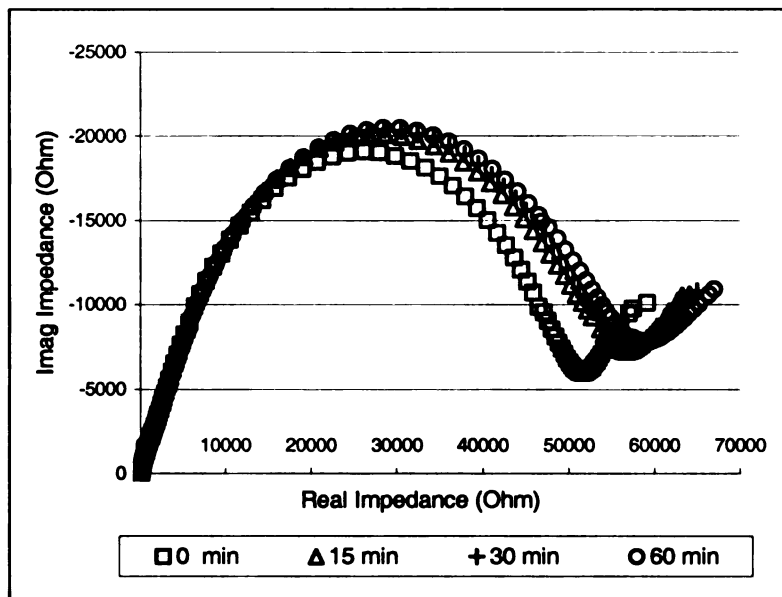


Figure 4.17 Cole-Cole plot showing the real and imaginary impedance with time.

The impedance caused by bacteria was found to increase linearly with the number of cells present in solution. Figure 4.18 shows SEM (1600X) micrographs of a solution with a concentration of 10^2 CFU/mL resulting in few bacteria being immobilized on the sensor surface and a solution with a concentration of 10^6 CFU/mL resulting in bacteria completely covering the sensor surface. The difference in the number of immobilized bacteria for high and low concentrations supports the impedance results that a high number of bacteria is required to change the measured impedance above the base impedance of the biosensor. The membrane resistance of attached bacterial cells affect the biosensor impedance. These attached cells act as elements connected in series and block the current flow from the electrodes in a passive way causing the impedance to increase. The larger the number of attached cells, the larger the magnitude of the resulting increase in impedance.

For nonpathogenic *E. coli* in pure culture, the statistical analysis shows that the biosensor has a lower detection limit of 10^5 CFU/mL with respect to the blank when using a log transformation of impedance data at a frequency of 1kHz (Figure 4.19). For pathogenic *E. coli* O157:H7 in pure culture, a lower detection limit of 10^4 CFU/mL is obtained with respect to the blank.

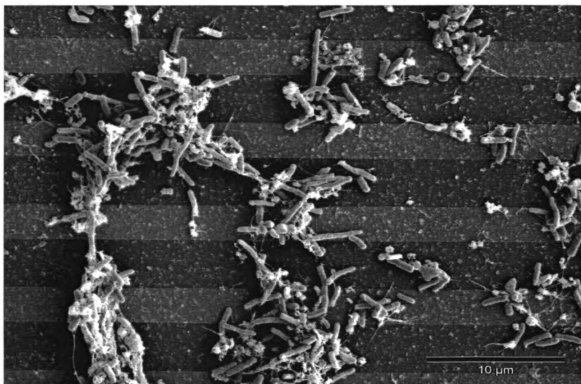
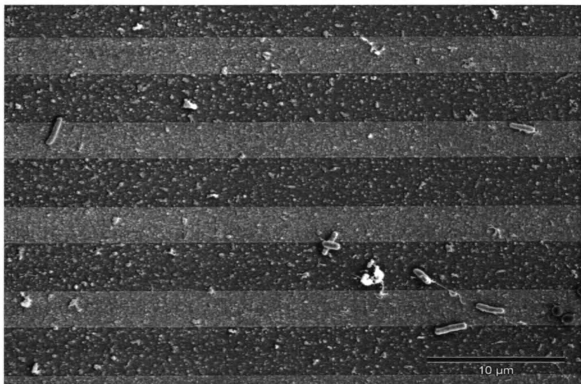


Figure 4.18 Scanning Electron Microscopy images of bacteria bound to the biosensor surface: (top) sample containing 10^2 CFU/mL; (bottom) sample containing 10^6 CFU/mL.

Concentration (CFU/mL)	Mean \pm SD and Significance ¹	
	<i>E. coli</i> Impedance (log Ω) ²	<i>E. coli</i> O157:H7 Impedance (log Ω) ³
BLANK	2.42 \pm 0.13 a	2.29 \pm 0.32 a
2 x 10 ⁰	2.45 \pm 0.04 a	2.25 \pm 0.05 a
2 x 10 ¹	2.51 \pm 0.32 a	2.32 \pm 0.10 a
2 x 10 ²	2.32 \pm 0.04 a	2.50 \pm 0.33 a
5 x 10 ³	2.52 \pm 0.03 a	2.70 \pm 0.16 a,b
1 x 10 ⁴	2.73 \pm 0.07 a,b	2.87 \pm 0.02 b,c
1 x 10 ⁵	3.20 \pm 0.16 b	3.28 \pm 0.09 c,d
1 x 10 ⁶	4.40 \pm 0.16 c	3.50 \pm 0.16 d
1 x 10 ⁷	4.67 \pm 0.31 c	3.34 \pm 0.09 c,d

[1] Means with same letter are not significantly different ($p > 0.05$)

[2] Log transform of *E. coli* impedance data from a frequency of 1kHz

[3] Log transform of *E. coli* O157:H7 impedance data from a frequency of 1kHz

Figure 4.19 Statistical significance of mean differences between concentrations in pure culture.

4.4 Results and Discussion of Specificity Study

In this study, the biosensor was functionalized for *E. coli* O157:H7 but was tested for the presence of *S. infantis* in pure culture. The impedance spectra for different concentrations of *S. infantis* in pure culture is shown in Figure 4.20. As expected, there was no significant difference in impedance with respect to different concentrations of *S. infantis* bacteria, as shown in the data where the impedance spectra are close together. Further, the polyclonal antibody has low cross-reactivity with *Salmonella spp.* (Kirkegaard and Perry, 1992) and any non-specific binding that did occur was not large enough to significantly increase the impedance with respect to the blank. This suggests that *S. infantis* did not attach to the *E. coli* O157:H7 specific antibodies immobilized on the biosensor surface, demonstrating specificity of the biosensor in the presence of non-target organisms.

The impedance spectra for a mixed culture of *E. coli* O157:H7 and *S. infantis* is shown in Figure 4.21. For the mixed culture, the increase in impedance is less

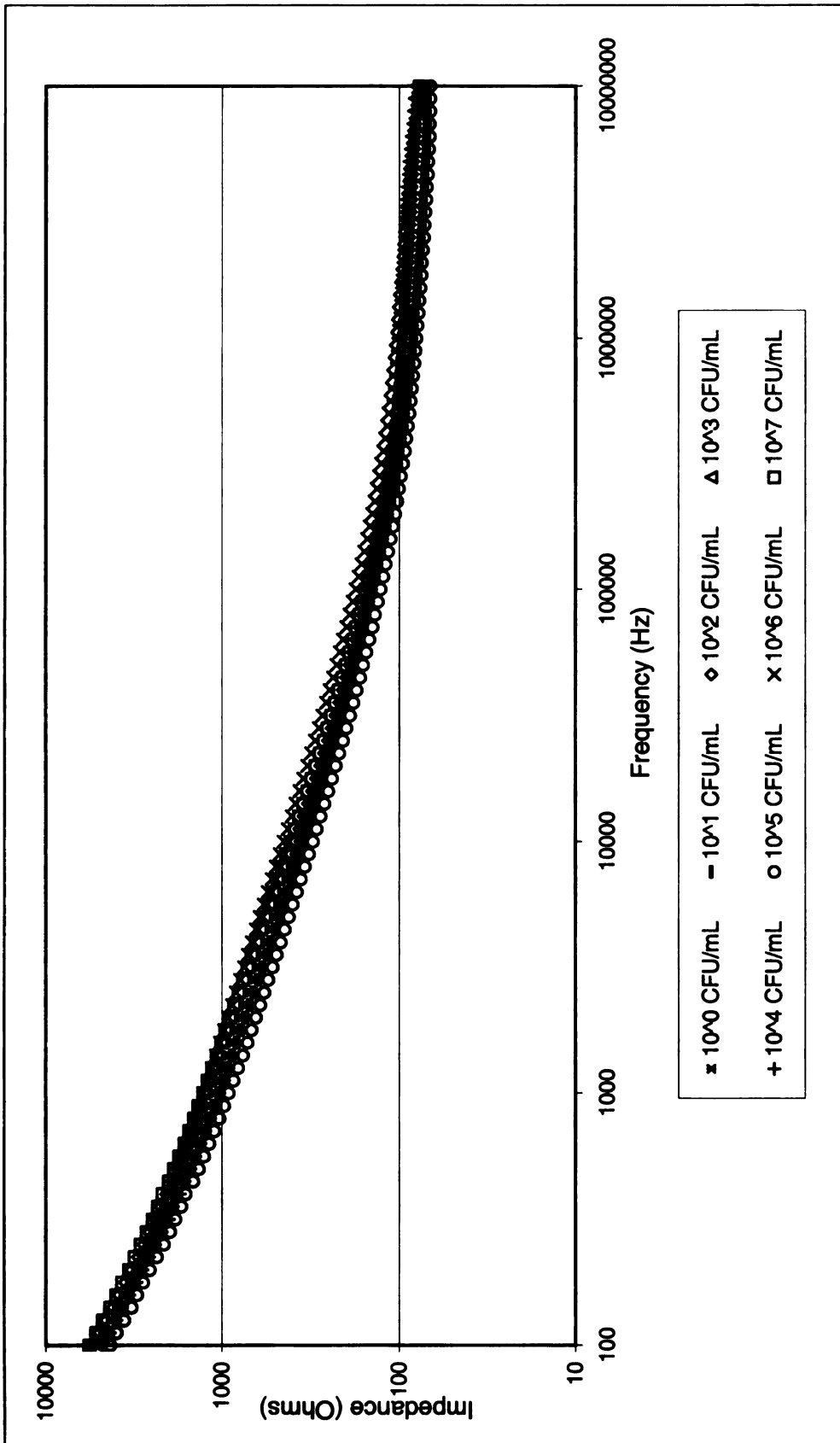


Figure 4.20 Impedance for a frequency distribution from 100Hz - 10MHz for a pure culture of *S. infantis*.

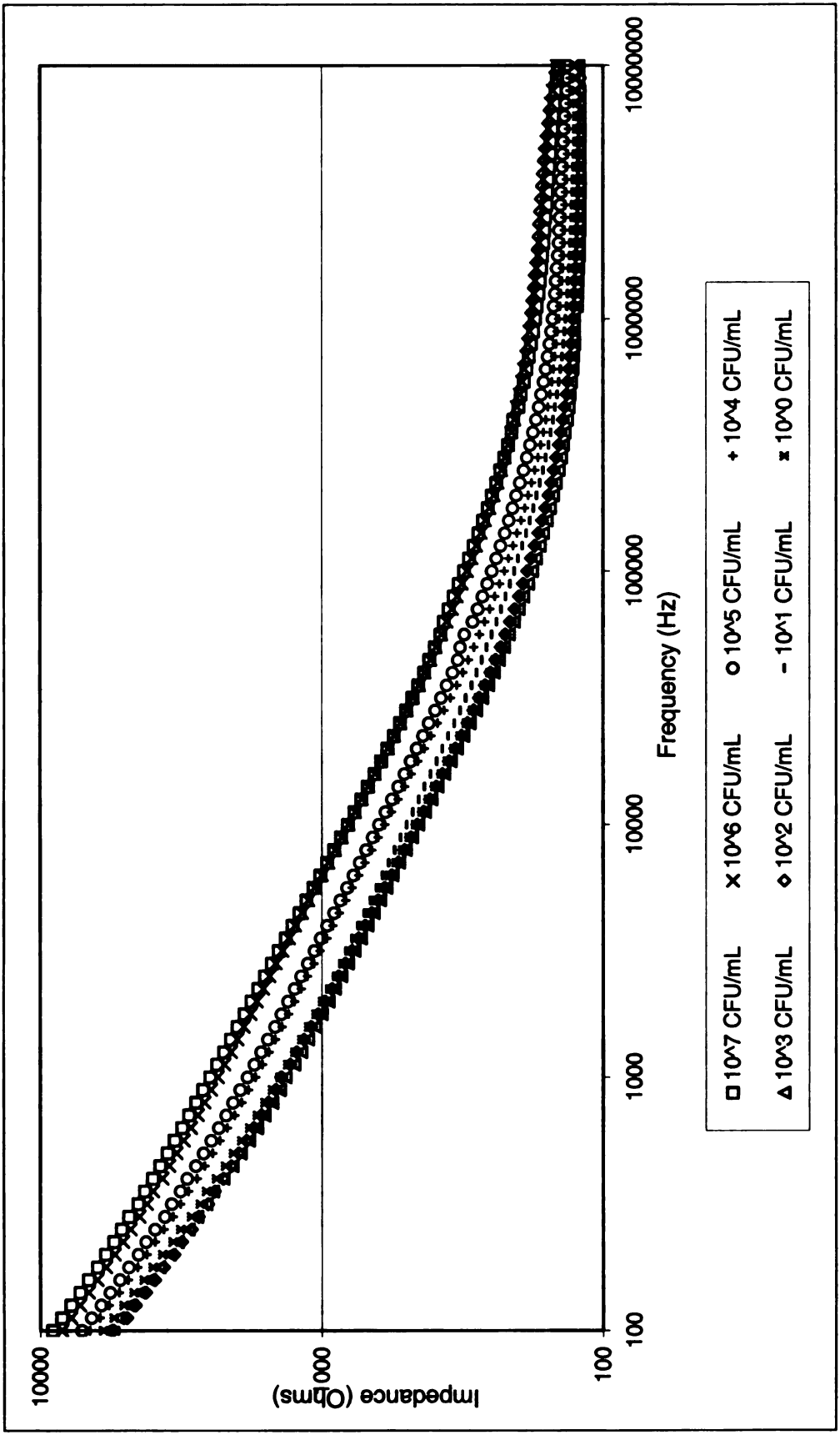


Figure 4.21 Impedance for a frequency distribution from 100Hz - 10MHz for a mixed culture of *S. infantis* and *E. coli* O157:H7.

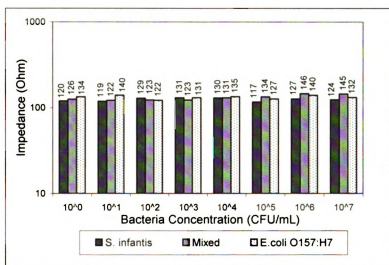
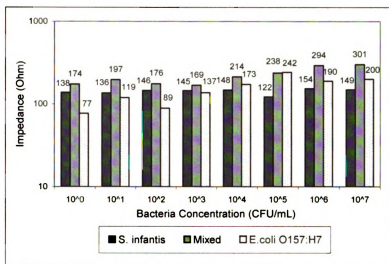
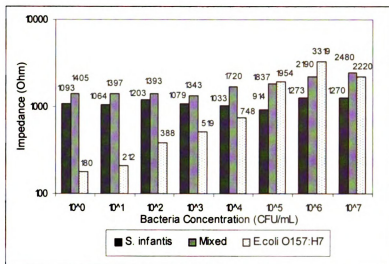


Figure 4.22 Comparison of *E. coli* O157:H7, *S. infantis*, and mixed culture at selected frequencies: (top) 1kHz; (middle) 100kHz; (bottom) 10MHz.

pronounced than in pure culture, but the impedance spectra are much more spread out when compared to the *S. infantis* pure culture. In examining frequency dependence, the impedance difference between concentrations become significant at 10^6 CFU/mL for low frequencies (Figure 4.22). The mixed culture impedance is greater than the *S. infantis* impedance whether at low or high frequencies or at low or high bacteria concentrations. This suggests that in mixed culture samples, target *E. coli* O157:H7 are bound by the antibodies on the surface. At low frequencies, the mixed culture impedance is higher than both *S. infantis* and *E. coli* O157:H7. It is suspected that the impedance is higher than *S. infantis* due to the presence of *E. coli* O157:H7 bound on the surface of the biosensor. The *E. coli* O157:H7 impedance value is less than the value for both mixed culture and pure culture of *S. infantis*. This may potentially be due to *S. infantis* having different conductive properties than *E. coli* O157:H7. While large numbers of *S. infantis* did not bind to the biosensor surface, the presence of the bacteria in the solution potentially changes the value of the solution resistance and the double layer capacitance of the solution. This would explain the resulting higher impedance values (at low frequencies) when *S. infantis* is in solution, both in the presence and absence of *E. coli* O157:H7.

At low concentrations of mixed culture, the impedance measurement is significantly higher than the single species culture of *S. infantis*. It should be noted that the serially diluted mixed culture contains twice the number of bacteria than either of the single species cultures, suggesting non-specific binding in the presence of large amounts of bacteria.

For the specificity study, the statistical analysis shows that the biosensor has a lower detection limit of 10^4 CFU/mL when using a log transformation of impedance data at a frequency of 1kHz (Figure 4.23). For mixed culture, a lower detection limit of 10^6 CFU/mL is obtained.

Concentration (CFU/mL)	Mean \pm SD and Significance ¹		
	<i>E. coli</i> O157:H7 Impedance (log Ω) ²	Mixed Culture Impedance (log Ω) ³	<i>S. infantis</i> Impedance (log Ω) ⁴
2×10^0	2.25 \pm 0.05 a	3.14 \pm 0.09 a	3.04 \pm 0.05 a
2×10^1	2.32 \pm 0.10 a	3.14 \pm 0.03 a	3.03 \pm 0.03 a
2×10^2	2.50 \pm 0.33 a,b	3.14 \pm 0.04 a	3.06 \pm 0.05 a
5×10^3	2.70 \pm 0.16 b,c	3.12 \pm 0.11 a	3.03 \pm 0.01 a
1×10^4	2.87 \pm 0.02 c	3.23 \pm 0.05 a,b	3.01 \pm 0.02 a
1×10^5	3.28 \pm 0.09 d	3.25 \pm 0.12 a,b	2.95 \pm 0.10 a
1×10^6	3.50 \pm 0.16 d	3.36 \pm 0.08 b	3.10 \pm 0.04 a
1×10^7	3.34 \pm 0.09 d	3.38 \pm 0.16 b	3.10 \pm 0.08 a

[1] Means with same letter are not significantly different ($p > 0.05$)

[2] Log transform of *E. coli* O157:H7 impedance data from a frequency of 1kHz

[3] Log transform of mixed culture impedance data from a frequency of 1kHz

[4] Log transform of *S. infantis* impedance data from a frequency of 1kHz

Figure 4.23 Statistical significance of mean differences between concentrations for the specificity study.

Experiments were conducted on complex food matrices to explore the performance of the biosensor in these substrates. Results are preliminary and are included in Appendix D for reference.

4.5 Summary and Conclusions

4.5.1 Summary of Lower Detection Limits

In testing the biosensor, the best results occurred under pure culture conditions. The lower detection limit for detecting *E. coli* O157:H7 in pure culture was 10^4 CFU/mL. In terms of specificity, the biosensor was specific to *E. coli* O157:H7 when functionalized with *E. coli* O157:H7 polyclonal antibodies. When testing for *S. infantis* with sensors

functionalized for *E. coli* O157:H7, the biosensor yielded no response between different *S. infantis* concentrations suggesting that surface binding of non-specific bacteria did not occur. In the presence of mixed culture between *S. infantis* and *E. coli* O157:H7, the biosensor had a lower detection limit of 10^6 CFU/mL, largely because of the interferant effects of *S. infantis* bacteria on the target organism.

4.5.2 Limitations and Future Possibilities

The goal was to develop a portable device to enable health care professionals, bioterrorism rapid-response teams, and food safety monitoring personnel to quantify results in less than 10 minutes for both clinical detection and point-of-care use. Innovation of the biosensor comes in the form of targeting pathogenic bacteria in a large sample volume whilst requiring only a 10 minute detection time.

The biosensor utilized an antibody concentration of $150\mu\text{g/mL}$ based on the procedure used to immobilize antibodies to the biosensor surface (Bhatia et al., 1989; Shriver-Lake et al., 1997). Increasing the antibody concentration would allow for a greater number of target organisms to bind to the biosensor at a given concentration. Increasing the biosensor active area would have the same effect. It may also be possible to bind different antibody species onto the same biosensor making it into a multi-analyte detector.

The price of microfabricated devices, as in the semiconductor industry, diminishes to pennies per biosensor when produced in sufficient numbers. The biosensor platform would fare well in the market place if commercialized to address the growing need for food pathogen testing (Alocilja and Radke, 2003).

APPENDIX A

Table A.1 Reported and estimated cases of foodborne illness by agent type in the US (Mead, 1998).

Disease or Agent	Illnesses		Hospitalizations		Deaths	
	Total	Foodborne	Total	Foodborne	Total	Foodborne
Bacterial						
<i>Bacillus cereus</i>	27,360	27,360	8	8	0	0
<i>Botulism</i> , foodborne	58	58	46	46	4	4
<i>Brucella spp.</i>	1,554	777	122	61	11	6
<i>Campylobacter spp.</i>	2,453,926	1,963,141	13,174	10,539	124	99
<i>Clostridium perfringens</i>	248,520	248,520	41	41	7	7
<i>Escherichia coli</i>	73,480	62,458	2,168	1,843	61	52
<i>E. coli</i> , non-O15	36,740	31,229	1,084	921	30	26
<i>E. coli</i> , enterotoigenic	79,420	55,594	21	15	0	0
<i>E. coli</i> , other diarrheogenic	79,420	23,826	21	6	0	0
<i>Listeria monocytogenes</i>	2,518	2,493	2,322	2,298	504	499
<i>Salmonella</i> Typhi	824	659	618	494	3	3
<i>Salmonella</i> , nontyphoidal	1,412,498	1,341,873	16,430	15,608	582	553
<i>Shigella spp.</i>	448,240	89,648	6,231	1,246	70	14
Staphylococcus food	185,060	185,060	1,753	1,753	2	2
Streptococcus, foodborne	50,920	50,920	358	358	0	0
<i>Vibrio cholerae</i> , toxigenic	54	49	18	17	0	0
<i>V. vulnificus</i>	94	47	86	43	37	18
<i>Vibrio</i> , other	7,880	5,122	99	65	20	13
<i>Yersinia enterocolitica</i>	96,368	86,731	1,228	1,105	3	2
Subtotal	5,204,934	4,175,565	45,826	36,466	1,458	1,297
Parasitic						
<i>Cryptosporidium parvum</i>	300,000	30,000	1,989	199	66	7
<i>Cyclospora cayetanensis</i>	16,264	14,638	17	15	0	0
<i>Giardia lamblia</i>	2,000,000	200,000	5,000	500	10	1
<i>Toxoplasma gondii</i>	225,000	112,500	5,000	2,500	750	375
<i>Trichinella spiralis</i>	52	52	4	4	0	0
Subtotal	2,541,316	357,190	12,010	3,219	827	383
Viral						
Norwalk-like virus	23,000,000	9,200,000	50,000	20,000	310	124
Rotavirus	3,900,000	39,000	50,000	500	30	0
Astrovirus	3,900,000	39,000	12,500	125	10	0
Hepatitis A	83,391	4,170	10,841	90	83	4
Subtotal	30,883,391	9,282,170	123,341	21,167	433	129
Grand Total	38,629,641	13,814,924	181,177	60,854	2,718	1,809

Table A.2 Reported and estimated cases of foodborne illness by surveillance type in the US (Mead, 1998).

Disease or Agent	Estimated Total Cases	Reported Cases By Surveillance Type			% Foodborne Origins	Hospitalization Rate	Case Fatality Rate
		Active	Passive	Outbreak			
Bacterial							
<i>Bacillus cereus</i>	27,360		720	72	100	0.006	0.0000
<i>Botulism, foodborne</i>	58		29		100	0.800	0.0769
<i>Brucella spp.</i>	1,554		111		50	0.550	0.0500
<i>Campylobacter spp.</i>	2,453,926	64,577	37,496	146	80	0.102	0.0010
<i>Clostridium perfringens</i>	248,520		6,540	654	100	0.003	0.0005
<i>Escherichia coli</i>	73,480	3,674	2,725	500	85	0.295	0.0083
<i>E. coli, non-O15</i>	36,740	1,837			85	0.295	0.0083
<i>E. coli, enterotoigenic</i>	79,420		2,090	209	70	0.005	0.0001
<i>E. coli, diarrheogenic</i>	79,420			2,090	30	0.005	0.0001
<i>Listeria monocytogenes</i>	2,518	1,259	373		99	0.922	0.2000
<i>Salmonella Typhi</i>	824		412		80	0.750	0.0040
<i>Salmonella, nontyphoidal</i>	1,412,498	37,171	37,842	3,640	95	0.221	0.0078
<i>Shigella spp.</i>	448,240	22,412	17,324	1,476	20	0.139	0.0016
Staphylococcus food	185,060		4,870	487	100	0.180	0.0002
Streptococcus, foodborne	50,920		1,340	134	100	0.133	0.0000
<i>Vibrio cholerae, toxigenic</i>	54		27		90	0.340	0.006
<i>V. vulnificus</i>	94		47		50	0.910	0.3900
<i>Vibrio, other</i>	7,880	393	112		65	0.126	0.0250
<i>Yersinia enterocolitica</i>	96,368	2,536			90	0.242	0.0005
Subtotal	5,204,934						
Parasitic							
<i>Cryptosporidium parvum</i>	300,000	6,630	2,788		10	0.150	0.005
<i>Cyclospora cayetanensis</i>	16,264	428	98		90	0.020	0.001
<i>Giardia lamblia</i>	2,000,000	107,000	22,907		10	n/a	n/a
<i>Toxoplasma gondii</i>	225,000		15,000		50	n/a	n/a
<i>Trichinella spiralis</i>	52		26		100	0.081	0.003
Subtotal	2,541,316						
Viral							
Norwalk-like virus	23,000,000				40	n/a	n/a
Rotavirus	3,900,000				1	n/a	n/a
Astrovirus	3,900,000				1	n/a	n/a
Hepatitis A	83,391		27,797		5	0.130	0.003
Subtotal	30,883,391						
Grand Total	38,629,641						

APPENDIX B

Table B.1 Bill of process for microfabrication of the biochip.

Bill Of Process-(Microfabrication)	
Step #	Process Description
1	Obtain 4" (100) silicon wafers from supplier. Wafers should contain a 2 μ m thick layer of thermally grown silicon oxide. The wafer surface should be polished.
2	Wafer cleaned in isopropyl alcohol solution followed by distilled water
3	Wafer dried with nitrogen stream
4	Wafer placed on chuck of photoresist (PR) spinner
5	A volume of 800 μ L of S1805 PR is pipetted onto the center of the wafer
6	PR spinner is actuated to spin wafer at 4000rpm for 30 seconds
7	After spin, wafer is visually examined to ensure complete PR coverage over entire wafer
8	Wafer transferred to oven for soft bake @ 90°C for 45 minutes
9	Wafer removed from oven
10	Wafer placed in photomask aligner
11	Photomask is aligned over the center of the wafer in the photomask aligner
12	Photomask aligner is actuated and wafer is exposed to 2.2 seconds of UV light. The UV light was set to emit at a wavelength of 440nm
13	Wafer is removed from photomask aligner
14	Wafer immersed in PR developer solution for a time of 1-2 minutes
15	Wafer removed from PR developer solution and dried under nitrogen stream
16	Wafer inspected with a metallurgical microscope to examine quality of PR mask
17	Wafer is transferred to oven for hard bake @ 135°C for 1 hour
18	Wafer removed from oven
19	Wafer loaded into metal evaporation chamber. Evaporation chamber includes titanium and gold pellets for use in the evaporation procedure
20	Vacuum unit pumped down to 4x10 ⁻⁶ Pa and current is applied to evaporate metal
21	A 3-5nm thick layer of Titanium is evaporated over entire surface of the wafer
22	A 50nm thick layer of Gold is evaporated over entire surface of the wafer
23	Vacuum unit is disengaged and wafer is removed
24	Wafer is immersed into crystallizing dish filled with acetone
25	The crystallizing dish (with wafer and acetone) is sonicated for 60 seconds for lift-off
26	Wafer is cleaned with distilled wafer followed by isopropyl solution
27	Wafer is dried under a stream of nitrogen
28	Wafer surface is inspected by metallurgical microscope, atomic force microscope and a surface profilometer to ensure proper lift-off was achieved
29	If satisfied with wafer, a protective layer of PR is applied as described in process 4-6
30	Wafer loaded onto dicing band saw
31	Dicing band saw set to dice wafer into 68 separate 8 x 12mm dies to a depth of 450 μ m
32	After dicing, wafer has been microfabricated and clean room work is complete

Table B.2 Bill of process for surface functionalization of the biochip.

Bill Of Process-(Functionalization)	
Step #	Process Description
1	Diced wafer is obtained after microfabrication in the clean room
2	Wafer is immersed in acetone to remove protective PR coating
3	Wafer is cleaned by immersing in a 50:50 mixture of HCl and methanol for 30 minutes
4	Wafer is immersed into boiling distilled water for 30 minutes
5	Wafer is allowed to air dry completely
6	Wafer is placed in an anaerobic chamber (glove box under inert conditions)
7	Inside the glove box, the wafer is immersed in a 2% MDS solution for 2 hours
8	Inside the glove box, the wafer is rinsed with dry toluene
9	The wafer is removed from glove box
10	Wafer is immersed in GMBS crosslinking solution for 1 hour
11	The wafer is washed with PBS
12	Antibody is carefully pipetted onto each electrode array region
13	Wafer with antibody is sealed with parafilm and incubated for 1 hour at 37°C
14	Wafer is removed from incubator and rinsed with PBS
15	Wafer is placed under refrigerated conditions of 4°C until use
16	Surface functionalization process is complete

Table B.3 Bill of process for testing in ground beef samples.

Bill Of Process-(Ground Beef Testing)	
Step #	Process Description
1	Grow bacteria (such as <i>E. coli</i> O157:H7) overnight in nutrient broth (NB) at 37°C
2	Weigh and separate 25g samples of ground beef
3	Place ground beef samples in sterile stomacher bag
4	Inoculate ground beef with 2mL of pure culture
5	Let sit at 4C under refrigerated conditions for 1 hour
6	Add 225ml of 0.1% peptone water
7	Stomach the sample for 2 minutes
8	Serially dilute the stomached sample to make 20mL volumes of sample
9	Insert fresh biochip into the apparatus test fixture
10	Lower fixture into the sample so the biochip array is in the solution
11	Wait 5 minutes for bacteria to bind to sensor surface
12	Begin taking impedance measurements with HP 4192A Impedance Analyzer
13	Impedance measurements take about 4 minutes to record from 100Hz - 13MHz
14	Remove sensor from sample and discard biochip
15	Sterilize sample and biochip using an autoclave

Table B.4 Bill of process for testing in romaine lettuce samples.

Bill Of Process-(Romaine Lettuce Testing)	
Step #	Process Description
1	Grow bacteria (such as <i>E. coli</i> O157:H7) overnight in nutrient broth (NB) at 37°C
2	Perform serial dilution on pure culture
3	Weigh and separate 3g samples of romaine lettuce
4	Place lettuce samples in sterile stomacher bag
5	Inoculate samples with 1mL of corresponding serially diluted bacteria concentration
5	Let sit at room temperature for 1 hour
6	Add 30ml of 0.1% peptone water
7	Stomach the sample for 30 seconds
8	Use the liquid portion to make 20mL volumes of samples
9	Insert fresh biochip into the apparatus test fixture
10	Lower fixture into the sample so the biochip array is in the solution
11	Wait 5 minutes for bacteria to bind to sensor surface
12	Begin taking impedance measurements with HP 4192A Impedance Analyzer
13	Impedance measurements take about 4 minutes to record from 100Hz - 13MHz
14	Remove sensor from sample and discard biochip
15	Sterilize sample and biochip using an autoclave

Table B.5 Bill of process for testing in samples of bovine feces.

Bill Of Process-(Bovine Feces Testing)	
Step #	Process Description
1	Grow <i>E. coli</i> O157:H7 overnight in nutrient broth (NB) at 37°C
2	Perform serial dilution on pure culture
3	Weigh and separate 20g samples of bovine feces
4	Place manure samples in sterile stomacher bag
5	Inoculate samples with 1mL of corresponding serially diluted bacteria concentration
5	Let sit at room temperature for 1 hour
6	Add 50ml of 0.1% peptone water
7	Stomach the sample for 30 seconds
8	Use the liquid portion to make 20mL volumes of samples
9	Insert fresh biochip into the apparatus test fixture
10	Lower fixture into the sample so the biochip array is in the solution
11	Wait 5 minutes for bacteria to bind to sensor surface
12	Begin taking impedance measurements with HP 4192A Impedance Analyzer
13	Impedance measurements take about 4 minutes to record from 100Hz - 13MHz
14	Remove sensor from sample and discard biochip
15	Sterilize sample and biochip using an autoclave

Table B.6 Bill of process for reagents used in fabrication and surface functionalization.

Bill Of Process-(Reagents)	
Reagent Name	Process Description
Nutrient Broth	Nutrient Broth (NB) was obtained from Difco Labs (Detroit, MI). The solution was prepared from 8g of NB mixed with 1000mL of distilled water and autoclaved at 121F for 20 minutes.
Phosphate Buffered Saline	Phosphate Buffered Saline (PBS) was made from 7.65g of NaCl, 0.724g of Na ₂ HPO ₄ , 0.21g of KH ₂ PO ₄ and 1000mL distilled water. After preparation the solution pH was adjusted to 7.4 with NaOH.
0.1% Peptone Water	Peptone Water (PW) was purchased from Sigma Labs (St. Louis, MS). The solution was prepared from 1g of PW added to 1L of distilled water. The solution was autoclaved at 121F for 20 minutes.
Polyclonal IgG Antibody	<i>E.coli</i> generic and O157:H7 specific polyclonal antibody were purchased from KPL Labs (Rockville, MA). The IgG was rehydrated in 1mL of PBS and diluted to a concentration of 150ug/mL in PBS.
Methanol:HCl	The 50:50 mixture contains equal parts of methanol purchased from CCI (Columbus, WI) and 1.0M HCl purchased from Sigma (St. Louis, MS).
2% MTS (Silane)	(3-Mercaptopropyl) trimethyloxysilane (MTS) purchased from Sigma (St. Louis, MS) was diluted in toluene purchased from J.T. Baker (Phillipsburg, NJ).
GMBS (Crosslinker)	4-maleimidobutyric acid N-hydroxysuccinimide (GMBS) was purchased from Sigma (St. Louis, MS) and diluted in N,N-Dimethylformamide purchased from Spectrum (New Brunswick, NJ). The solution was diluted to 2mM in ethanol purchased from Pharmco (Brookfield, CT).
Acetone	Acetone was purchased from J.T. Baker (Phillipsburg, NJ).
Toluene	Toluene was purchased from J.T. Baker (Phillipsburg, NJ).
Isopropyl Alcohol	Isopropyl Alcohol was purchased from Spectrum (New Brunswick, NJ).
Sorbitol MacConkey Agar	Sorbitol Mac Conkey Agar (SMAC) was purchased from Difco Labs (Detroit, MI). The solution was prepared from 50g of SMAC and 1000mL of distilled water followed by autoclaving at 121F for 20 minutes.
Bismuth Sulfite Agar	Bismuth Sulfite Agar (BS) was purchased from Difco Labs (Detroit, MI). The solution was prepared from 52g of BS and 1000mL of distilled water and heated to boiling.

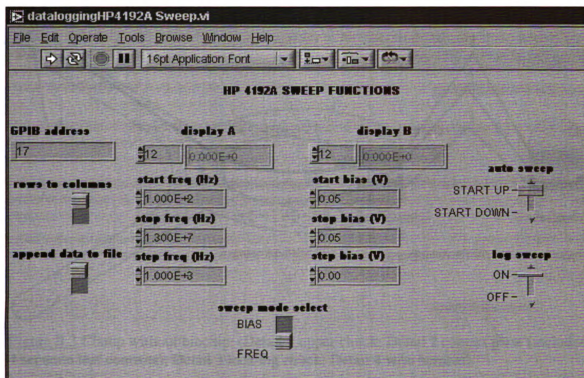


Figure B.1 Screen capture of user interface for LabVIEW 6.1 data acquisition software.

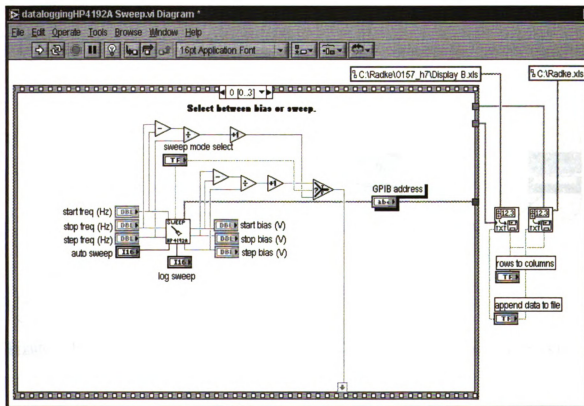


Figure B.2 Screen capture of circuit diagram for LabVIEW 6.1 data acquisition software.

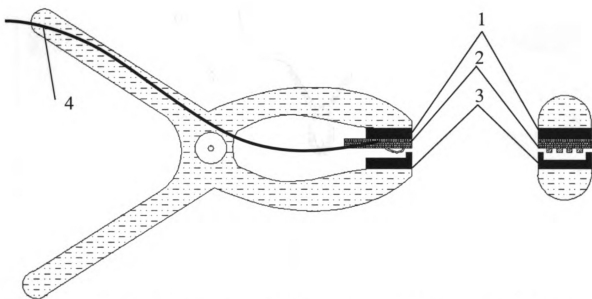


Figure B.3 Clamp without biochip. (Detail 1 upper chuck; Detail 2 contact plate (includes 4 separate leaf contacts); Detail 3 locating chuck; Detail 4 wire harness).

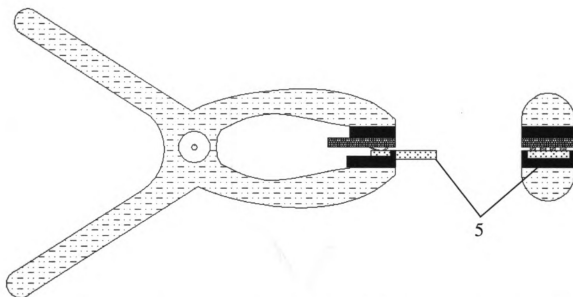


Figure B.4 Clamp with biochip in locating chuck. (Detail 5 biochip in locating chuck).

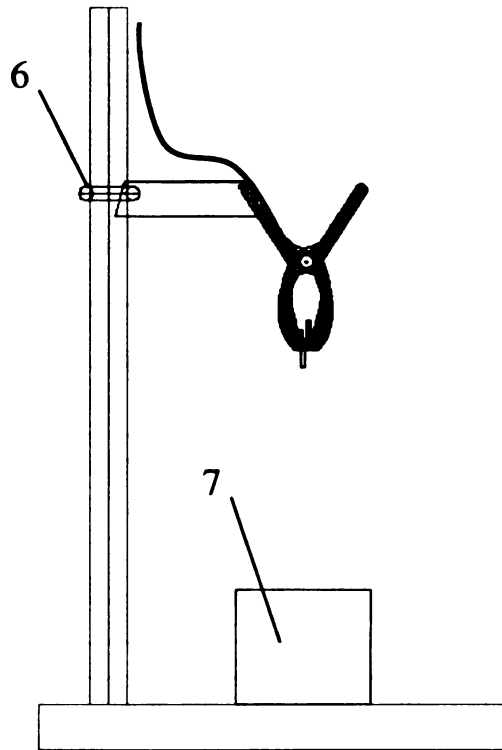


Figure B.5 Apparatus setup. (Detail 6 slide assembly; Detail 7 specimen sample).

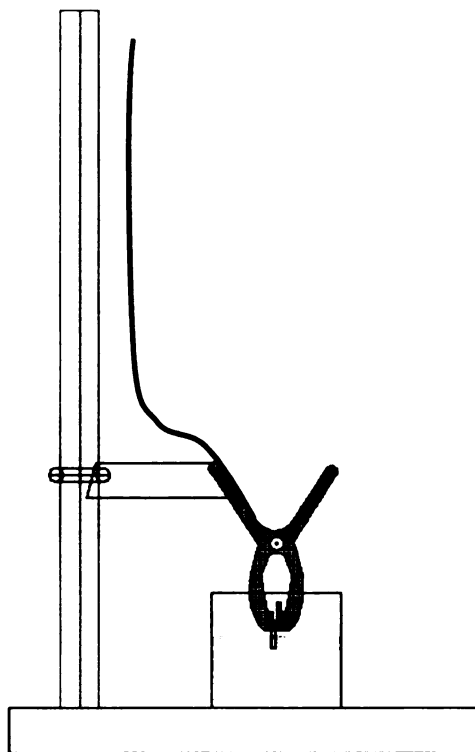


Figure B.6 Apparatus setup engaged in specimen testing.

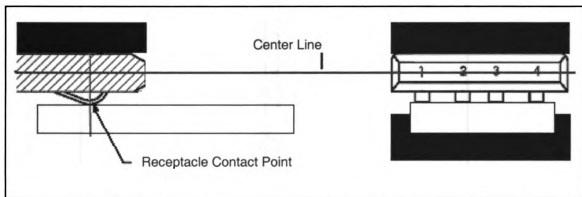


Figure B.7 Detail of contact mating to biosensor (4 separate leaf contacts for each pad).

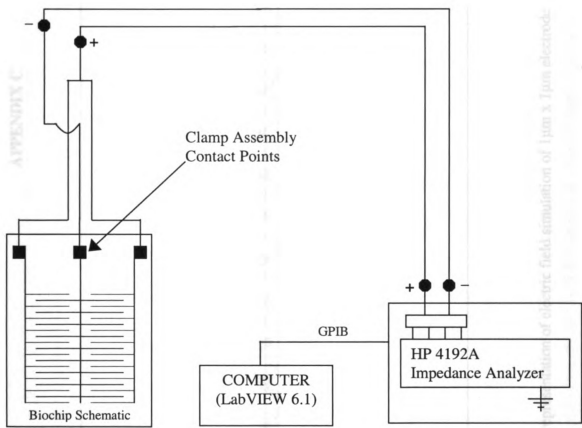


Figure B.8 Wiring schematic showing HP 4192A impedance analyzer connected to biochip.

APPENDIX C

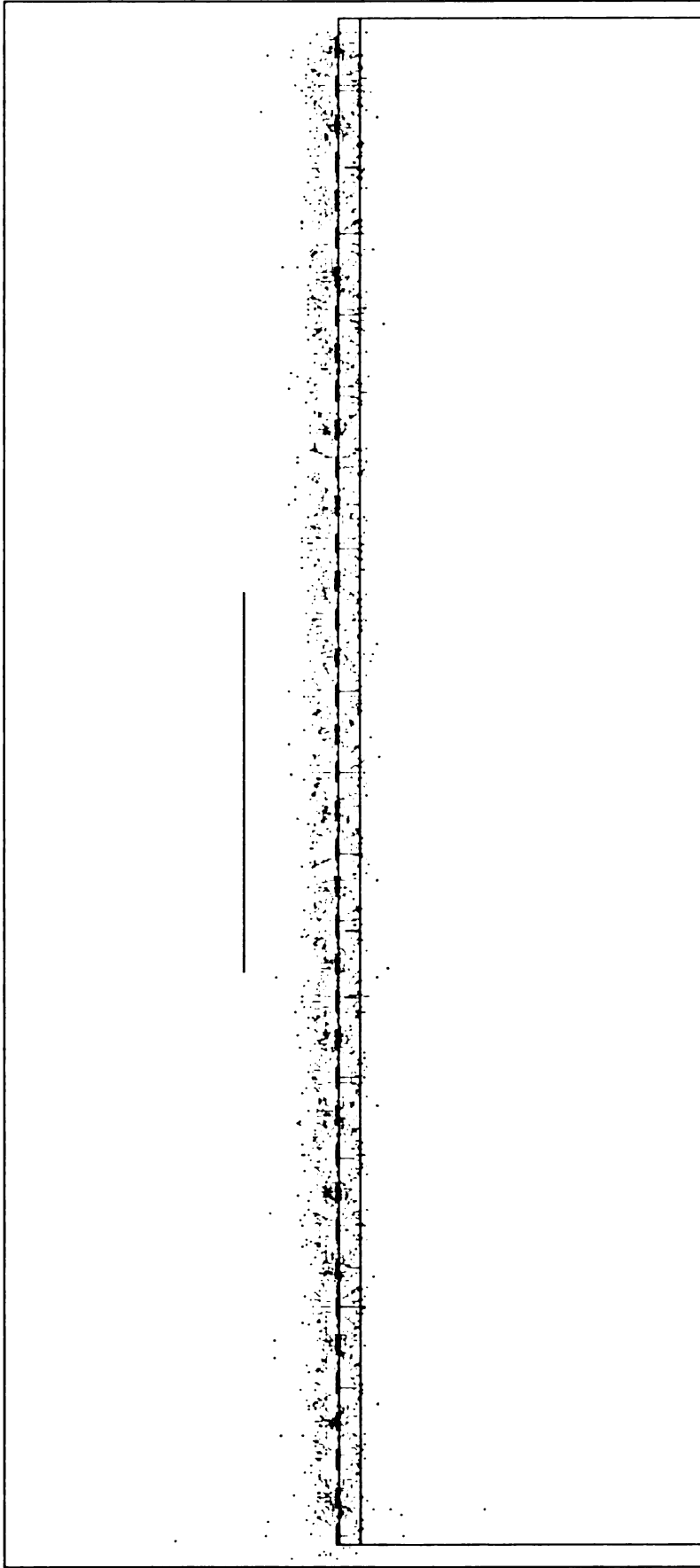


Figure C.1 Vector representation of electric field simulation of $1\mu\text{m} \times 1\mu\text{m}$ electrode array.

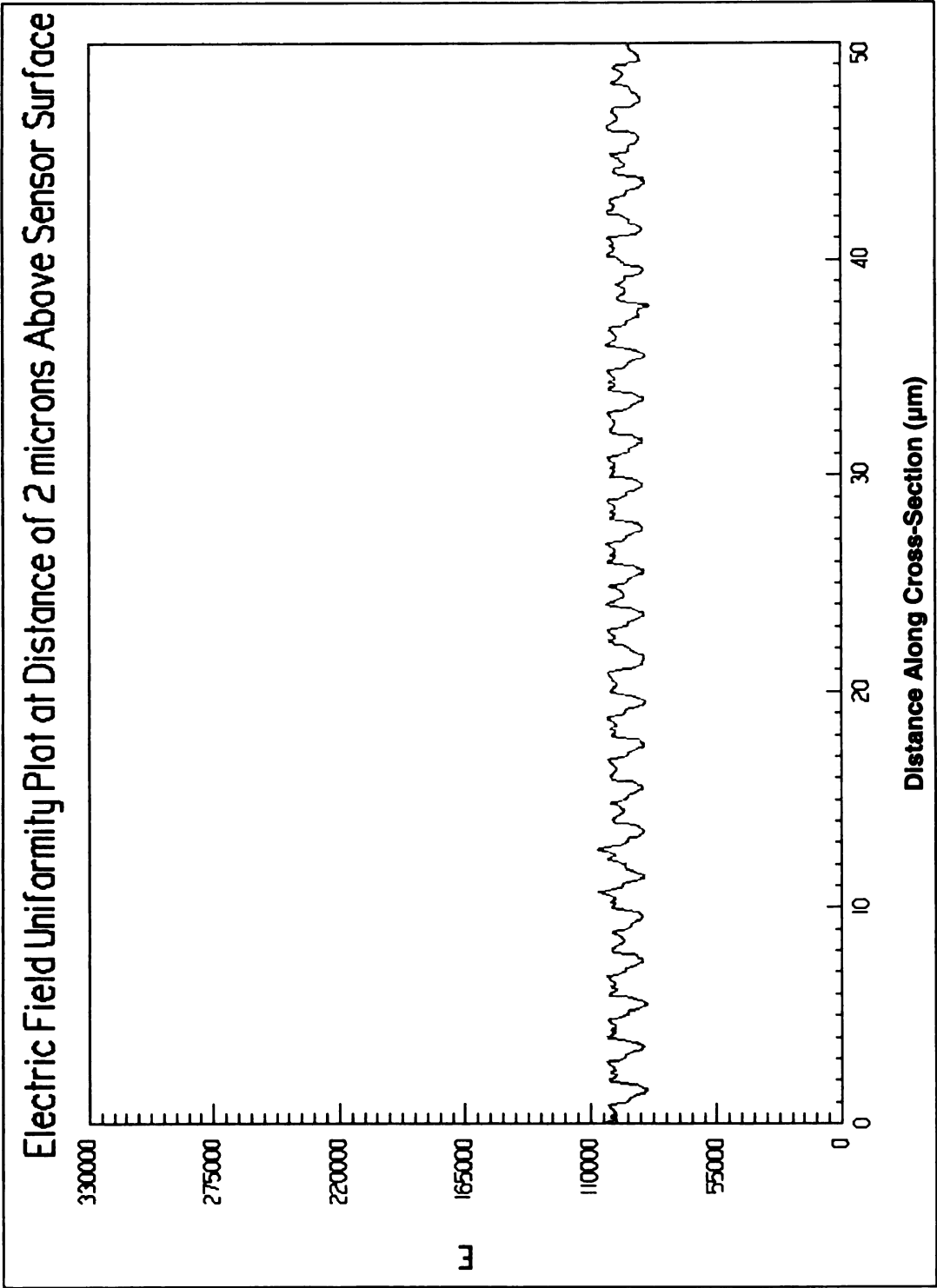


Figure C.2 Surface plot of the electric field distribution at a 2 μm distance from a 1 μm x 1 μm electrode array.

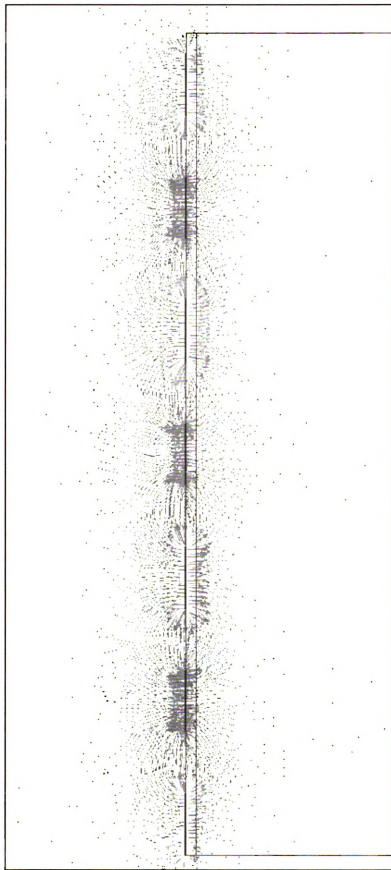


Figure C.3 Vector representation of electric field simulation of $10\mu\text{m} \times 5\mu\text{m}$ electrode array.

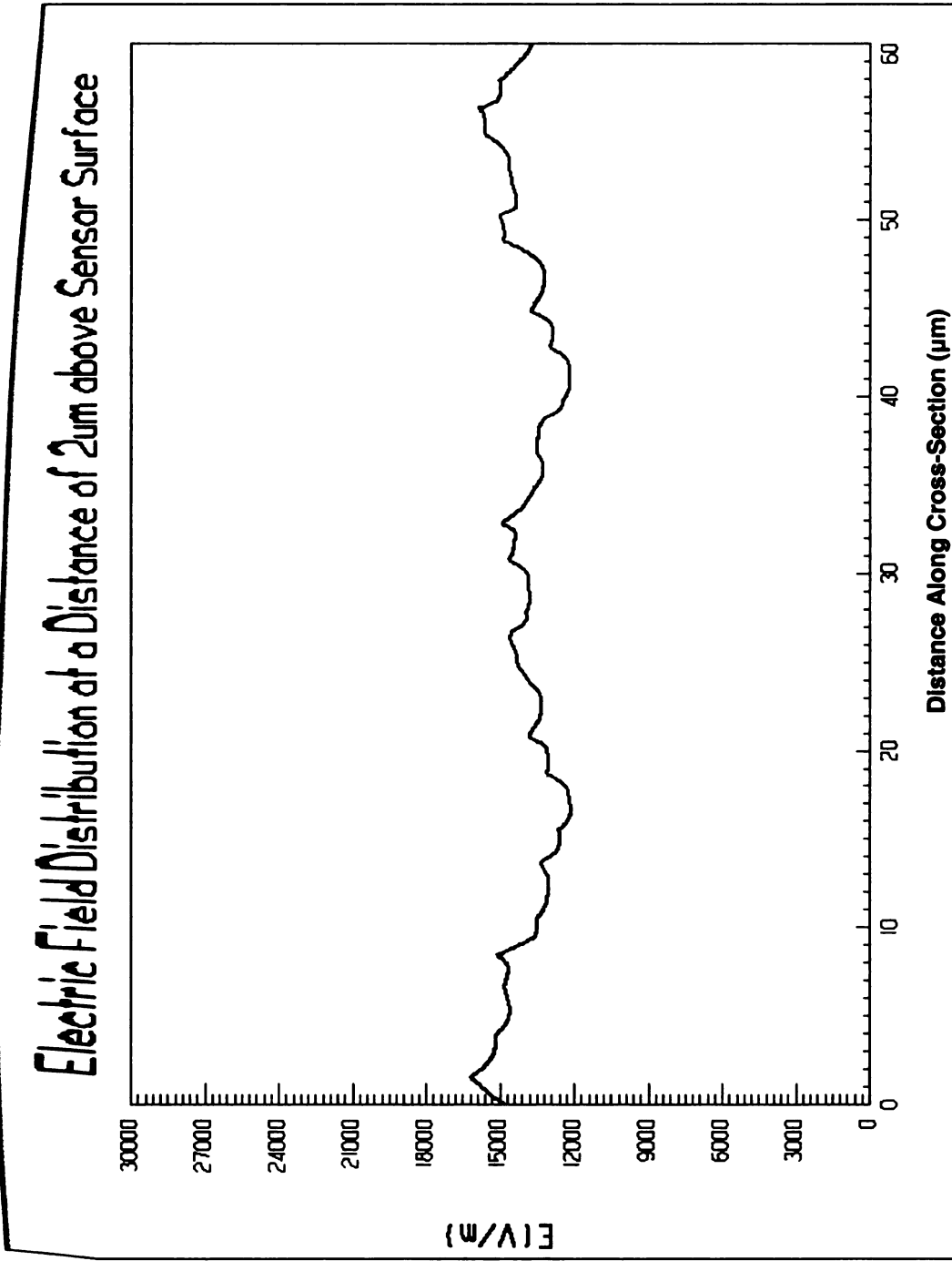


Figure C.4 Surface plot of the electric field distribution at a 2 μ m distance from a 10 μ m x 5 μ m electrode array.

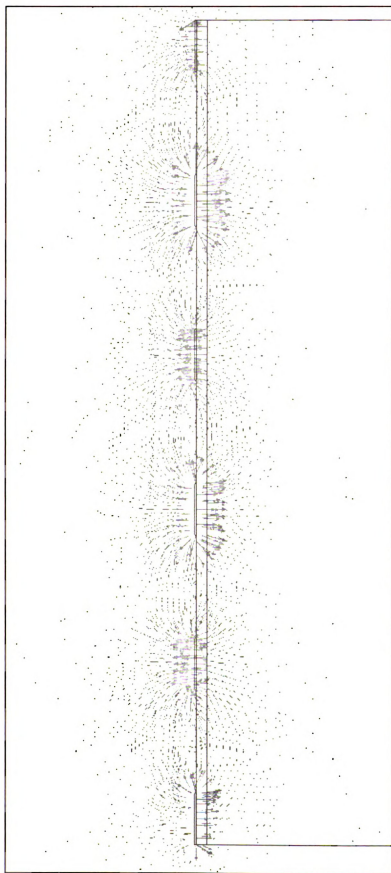


Figure C.5 Vector representation of electric field simulation of $5\mu\text{m} \times 10\mu\text{m}$ electrode array.

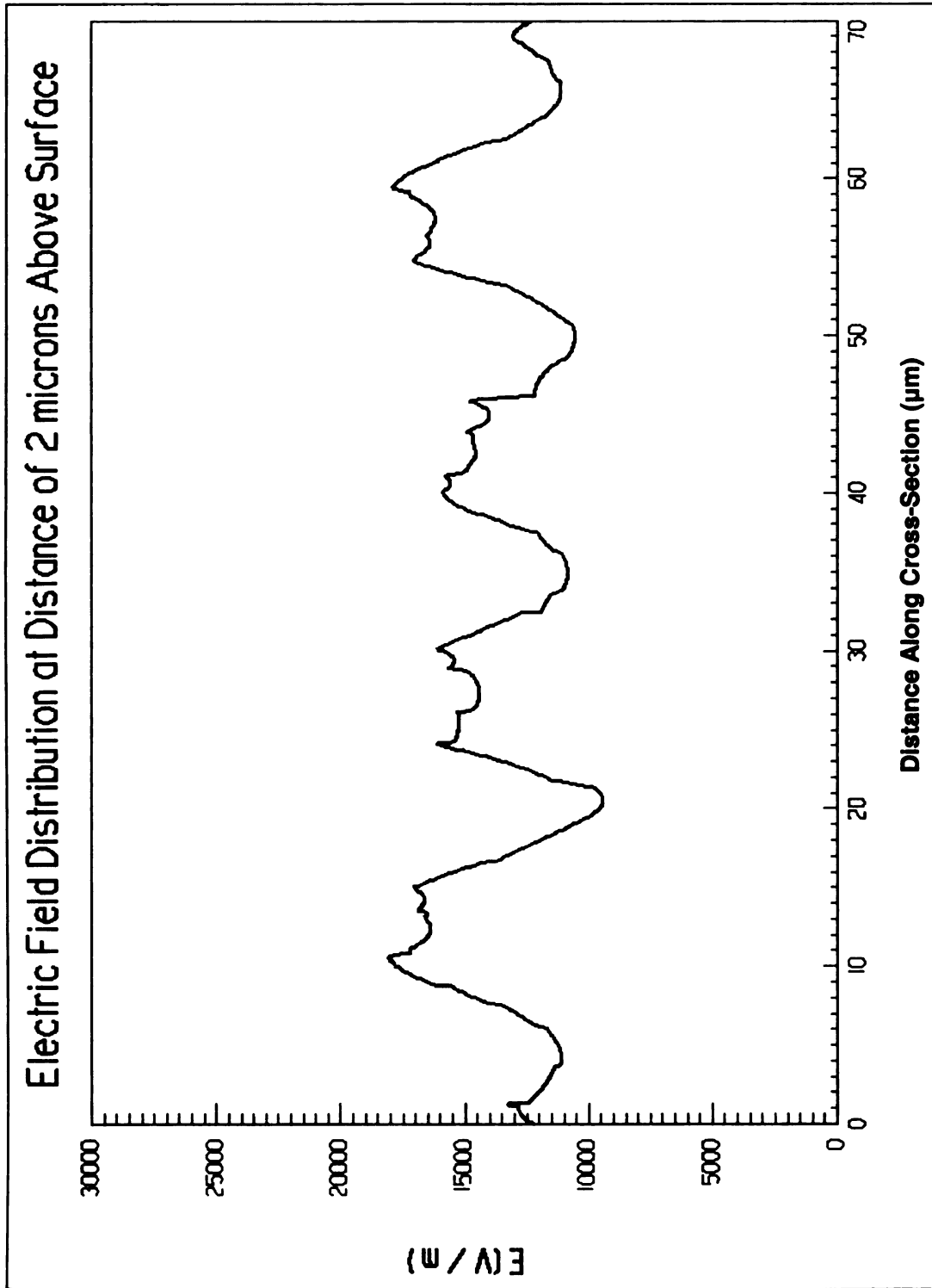


Figure C.6 Surface plot of the electric field distribution at a 2μm distance from a 5m x 10μm electrode array.

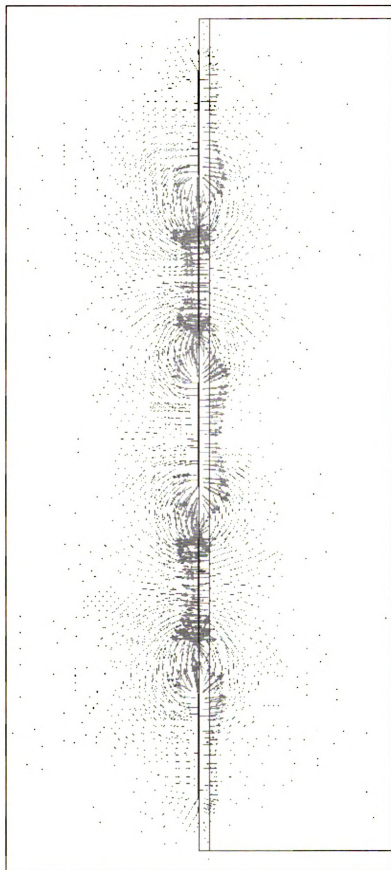


Figure C.7 Vector representation of electric field simulation of $6\mu\text{m} \times 6\mu\text{m}$ electrode array.

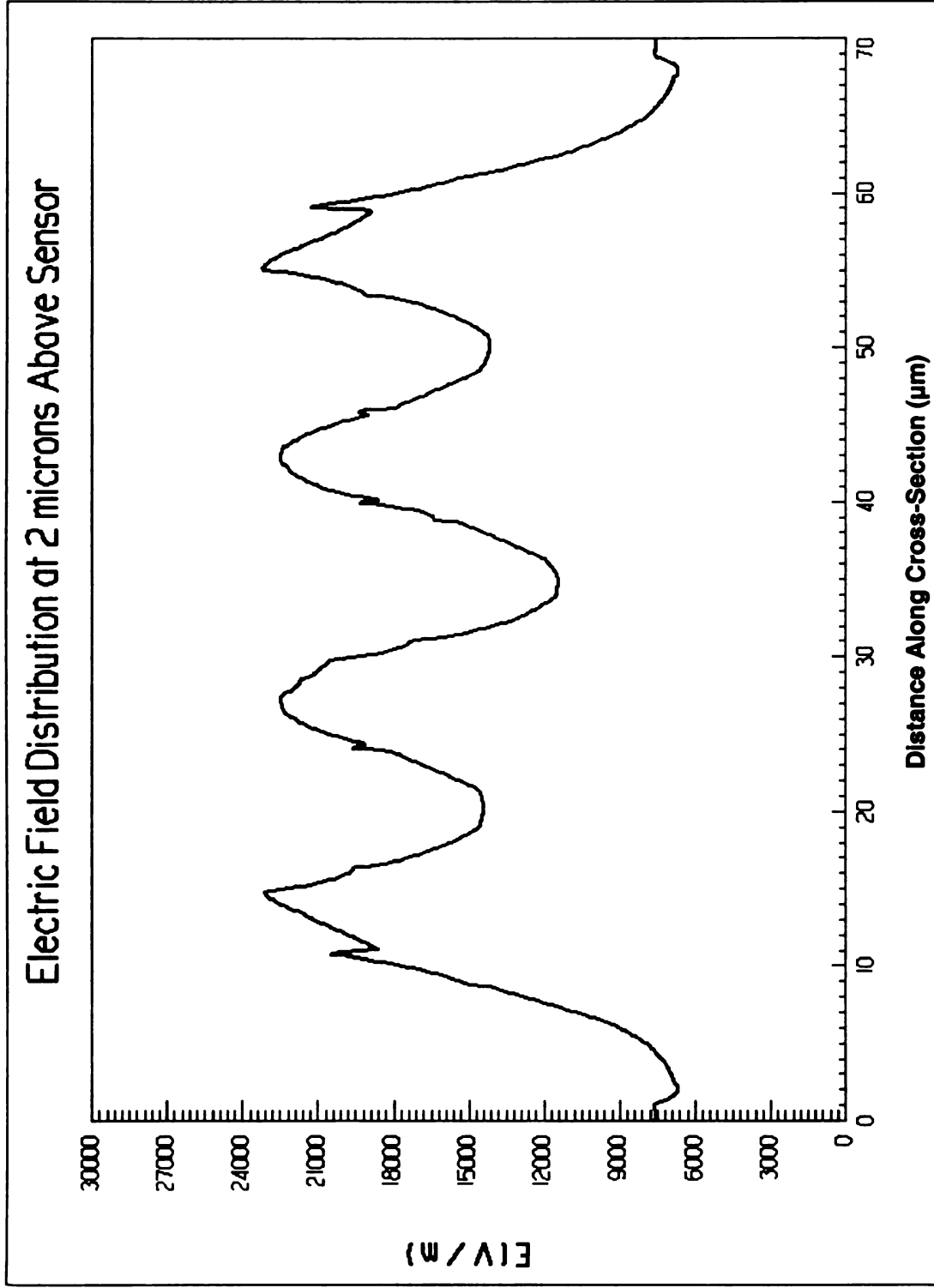


Figure C.8 Surface plot of the electric field distribution at a 2 μm distance from a 6 μm x 6 μm electrode array.

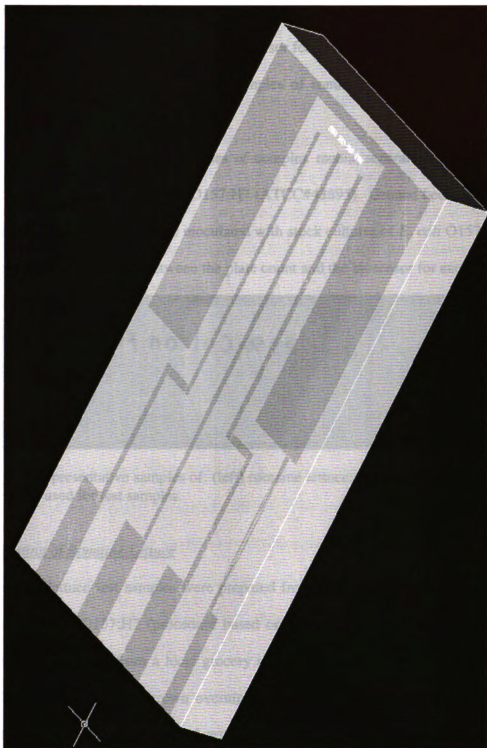


Figure C.9 3-D rendering of CAD layout file depicting biosensor.

APPENDIX D

D.1 Testing in Complex Media

Specific Aim 4 reads: To employ the biosensor for detecting *E. coli* O157:H7 bacteria extracted from artificially contaminated samples of romaine lettuce, ground beef, and bovine feces.

To validate the biosensor in samples of complex media, separate experiments were conducted using pathogenic *E. coli* O157:H7 (ATCC#43895). Ground beef, bovine feces and romaine lettuce samples were inoculated with stock cultures of *E. coli* O157:H7 cells and a comparison was made between the plate count and the biosensor for each sample.

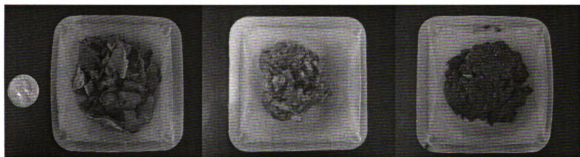


Figure D.1 Representative samples of: (left) romaine lettuce; (center) ground beef; (right) bovine feces used for test samples.

D.1.1 Testing of Romaine Lettuce

Romaine lettuce test samples were prepared from varying concentrations of a stock culture of *E. coli* O157:H7 (procedure based on Bennett and Beuchat, 2001). Lettuce samples were obtained from a local grocery store (Goodrich's Shop-Rite, East Lansing, MI). The pure culture was grown overnight in nutrient broth at 37°C. Samples were made by separating and weighing 3-gram samples of lettuce and placed into a sterile whirl pak bag (Nasco; Modesto, CA). Figure D.1 (left) is a representative sample of

romaine lettuce used in the experiments. The lettuce samples were inoculated with 1mL of serially diluted concentrations of *E. coli* O157:H7 and left for 60 minutes at room temperature. A volume of 30mL of 0.1% peptone water was added to each whirl pak bag to make a 1:10 dilution. The sample was processed by stomaching for 1 minute. Samples of 20mL were made from concentrations of 10^1 to 10^5 CFU/mL out of the processed samples. After sample preparation, biosensors were used to determine the presence of bacteria. Prior to inoculation, lettuce samples were tested for generic *E. coli* and *E. coli* O157:H7. The testing procedure, signal measurement and analysis were performed as described in Sections 3.3, 3.4 and 3.5. A detailed Bill of Process for sample preparation is included in Appendix B.

D.1.2 Testing of Ground Beef

Ground beef test samples were prepared from varying concentrations of a stock culture of *E. coli* O157:H7 (procedure based on FDA, 2001). The pure culture was grown overnight in nutrient broth at 37°C. Ground beef samples were obtained from a local grocery store (Kroger; Cincinnati, OH). Meat samples of 25g were separated, weighed and placed in a sterile whirl pak bag (Nasco; Modesto, CA). Figure D.1 (center) is a representative sample of ground beef used in the experiments. The ground beef was inoculated with 2mL of pure culture and left for 60 minutes under refrigerated conditions. A volume of 225ml of 0.1% peptone water was added to each whirl pak bag and processed by stomaching for 1-2 minutes. Samples of 20mL were made from concentrations of 10^1 to 10^6 CFU/mL out of the processed samples. After sample preparation, biosensors were used to determine the presence of the inoculants. Samples

were plated for confirmation. The testing procedure, signal measurement and analysis were conducted as described in Sections 3.3, 3.4 and 3.5.

D.1.3 Testing of Bovine Feces

Bovine feces (manure) test samples were prepared from varying concentrations of a stock culture of *E. coli* O157:H7 (procedure based on Sanderson et al., 1994). Manure samples were obtained from mature lactating dairy cows at the MSU Dairy Farm. Prior to inoculation with *E. coli* O157:H7, fecal samples were tested to confirm sample negativity for *E. coli* O157:H7. This was accomplished by weighing 1-gram samples of manure and incubating at 37°C for 24 hours in nutrient broth. The manure samples were then serially diluted and tested for *E. coli* O157:H7.

For sample preparation using the biosensor, manure samples of 20g were separated, weighed and placed in a sterile whirl pak bag (Nasco; Modesto, CA). Figure D.1 (right) is a representative sample of manure used in the experiments. The manure samples were inoculated with 1mL of serially diluted concentrations of *E. coli* O157:H7 and left for 60 minutes at room temperature. A volume of 50ml of 0.1% peptone water was added to each whirl pak bag and processed by stomaching for 1-minute. Samples of 20mL were made from concentrations of 10^1 to 10^5 CFU/mL out of the processed samples. After sample preparation, biosensors were used to measure the presence of the inoculants. The testing procedure, signal measurement and analysis used were as described in Sections 3.3, 3.4 and 3.5.

D.2 Results and Discussion of Testing in Complex Media

D.2.1 Results for Romaine Lettuce Testing

Romaine lettuce samples inoculated with *E. coli* O157:H7 exhibit a similar response to pure culture in that the change in impedance of the biosensor is proportional to the bacteria concentration. Figures D.2 and D.3 show the impedance for different concentrations of romaine lettuce samples inoculated with *E. coli* O157:H7. As with pure culture, the impedance is dependent on frequency and concentration. As frequency increases the presence of bacteria has a diminished effect on overall biosensor impedance, irrespective of concentration. High frequencies result in the near convergence of the impedance. For the lettuce wash water samples, low frequencies also show an increase in impedance with bacteria concentration, but the effect is less pronounced.

In proposing the specific aims for this study, one goal was to test the biosensors in samples having minimal sample processing requirements. Sample processing is time consuming since it often involves acquiring, separating and filtering of the sample. As described in the Methods and Materials section, the samples were not processed to reduce the amount of particulate in solution. For the inoculated lettuce, the sample solution was mainly free of particulates but the solution had a light green color, suggesting micro-sized particles and pigments of lettuce were present.

In addition to the effects of the double layer and parasitic capacitances, testing of the lettuce wash water yields reduced sensitivity due to the interference from food particulates in the liquid sample, and is one factor the microelectrodes were designed to

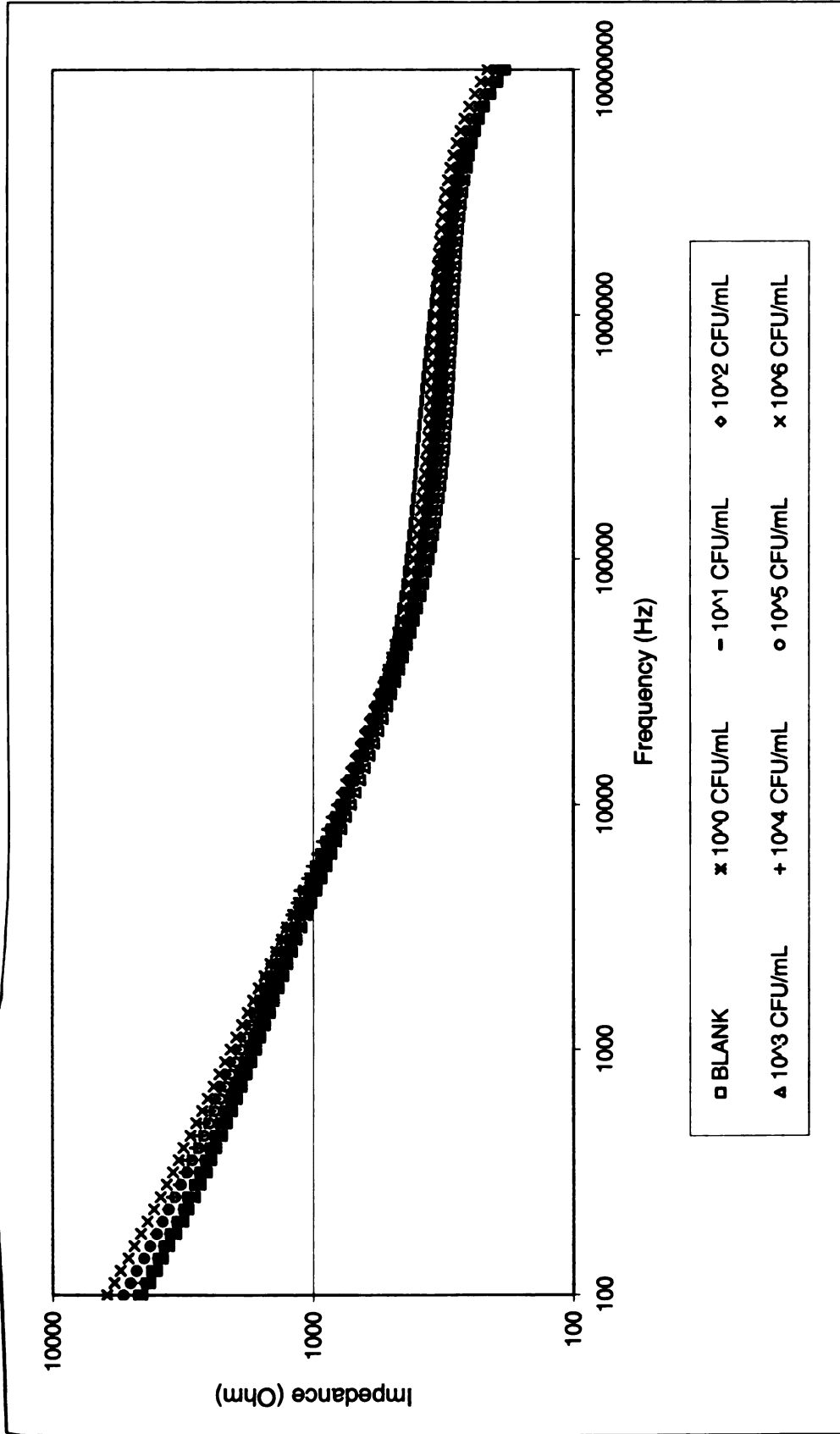


Figure D.2 Impedance for a frequency distribution from 100Hz -10MHz for romaine lettuce samples inoculated with *E. coli* O157:H7.

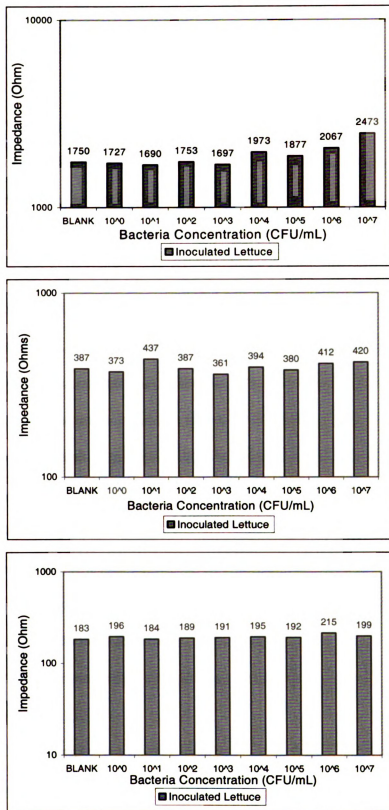


Figure D.3 Comparison of romaine lettuce samples inoculated with *E. coli* O157:H7 at selected frequencies: (top) 1kHz; (middle) 100kHz; (bottom) 10MHz.

minimize. The lower detection limit of *E. coli* O157:H7 in lettuce wash water is 10^7 CFU/mL.

D.2.2 Results for Ground Beef Testing

Ground beef samples inoculated with *E. coli* O157:H7 exhibit a similar response to romaine lettuce samples in that the change in impedance of the biosensor is proportional to the bacteria concentration, but less so than for samples in pure culture. Figures D.4 and D.5 show the impedance for different concentrations of ground beef samples inoculated with *E. coli* O157:H7.

At low frequencies, an increase in impedance is shown with bacteria concentration, but the effect is less pronounced than exhibited with pure culture. As with pure culture, the impedance is dependent on frequency and concentration but the ground beef samples behave differently for high frequencies. As frequency increases the presence of bacteria has a diminished effect on overall biosensor impedance, but the impedance between samples is considerably different. This could potentially be due to the effects of ground beef sample on the dielectric capacitance of the testing solution. High frequencies do still result in the convergence of the impedance, but there is more variability between sample concentrations. In addition to the effects of the double layer and parasitic capacitances, the ground beef samples has reduced sensitivity due potentially to the contribution of fats and proteins in the sample.

The ground beef samples were visibly full of fats, oils and proteins and had a light red color. The goal of the biosensor was to detect for bacteria in minimally processed samples. It is suspected that poor detachment of bacteria from the ground beef

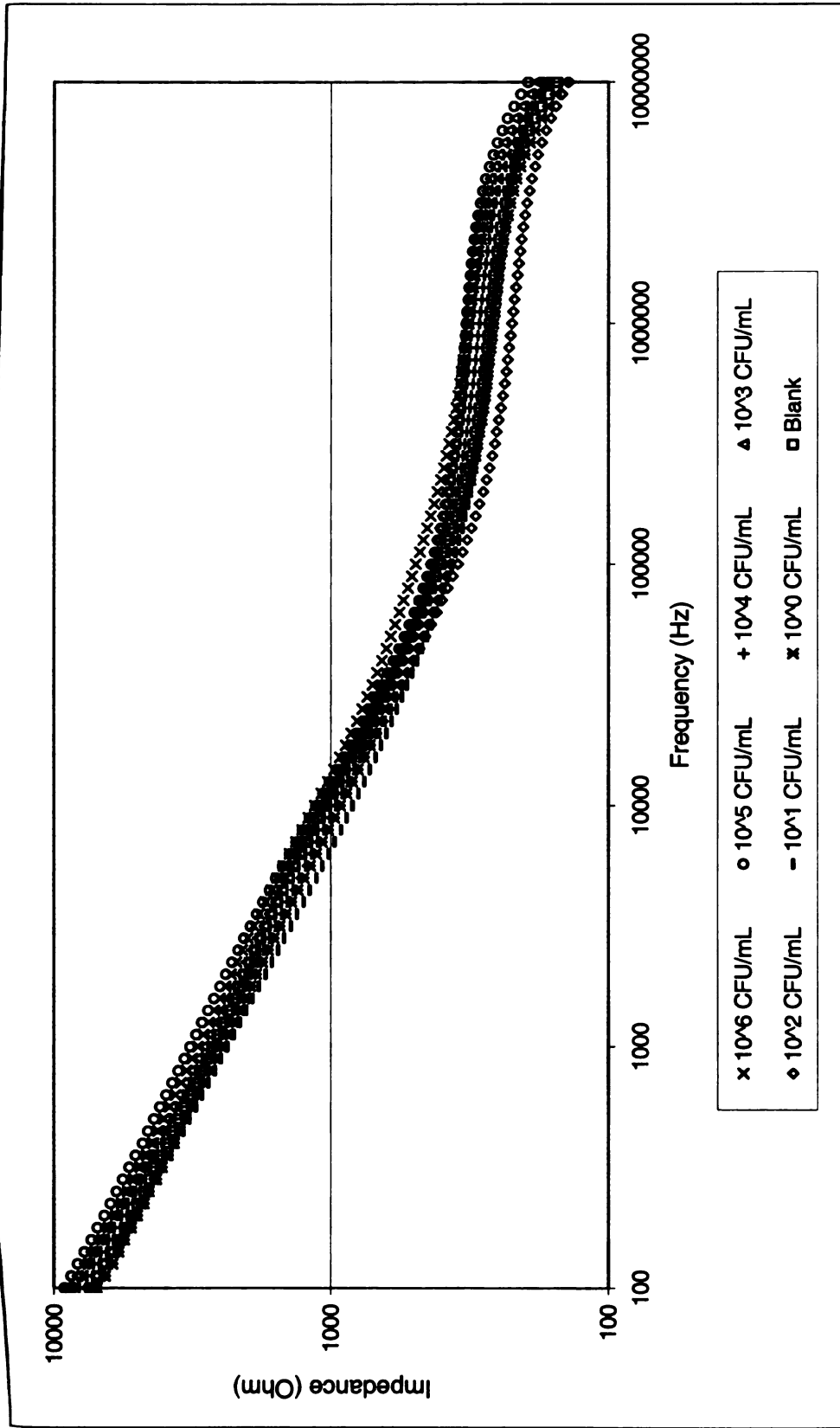


Figure D.4 Impedance for a frequency distribution from 100Hz - 10MHz for ground beef samples inoculated with *E. coli* O157:H7.

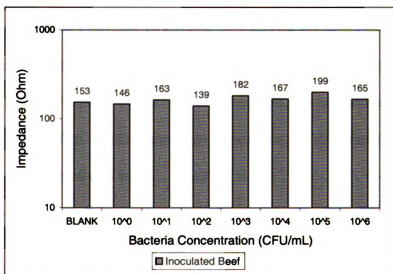
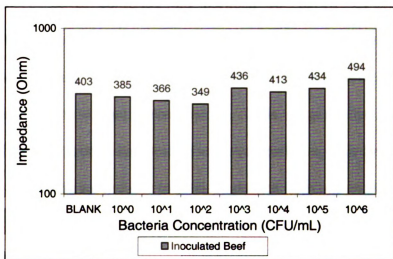
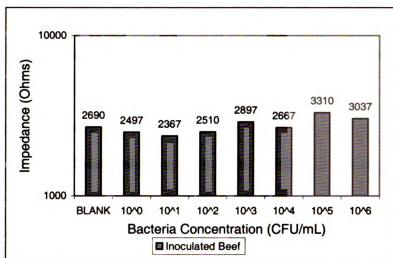


Figure D.5 Comparison of ground beef samples inoculated with *E. coli* O157:H7 at selected frequencies: (top) 1kHz; (middle) 100kHz; (bottom) 10MHz.

particulates resulted in fewer bacteria binding to the surface thereby further reducing the sensitivity. For ground beef, the sample matrix had a strong effect on the biosensor lower detection limit resulting in the inability of the biosensor to significantly distinguish between different bacteria concentrations.

The biosensor has a lower detection limit of 10^5 CFU/mL with respect to a sample concentration of 10^1 CFU/mL, however, all concentrations are insignificant with respect to the blank. In all data throughout this study, whether pure culture or complex media testing, the impedance of concentrations between 10^0 to 10^3 CFU/mL cannot be distinguished by the biosensor. Both 10^0 CFU/mL and blank measurements were insignificant due to a high degree of variability in impedance measurements due to the unreliable measurements at low concentrations. This suggests that the biosensor is "almost" significant for ground beef testing when comparing against the blank since low concentrations of bacteria are not able to be distinguished from one another.

D.2.3 Results for Bovine Feces Testing

Bovine feces (manure) samples inoculated with *E. coli* O157:H7 exhibited a similar response to ground beef and romaine lettuce samples in that the change in impedance of the biosensor is proportional to the bacteria concentration, but less so than for samples in pure culture. Figures D.6 and D.7 show the impedance for different concentrations of ground beef samples inoculated with *E. coli* O157:H7.

For the bovine feces, the samples were visibly full of partially digested fiber and organic matter and resulted in a dark brown, smelly sample. Bovine feces samples were dense with particulate in comparison to the lettuce and ground beef and were the most

challenging test for the biosensor. Also, the bovine feces samples contained a large amount of non-target *E. coli* bacteria. The sample concentrations used for the manure testing were 10^1 , 10^2 , 10^3 , 10^4 , and 10^5 CFU/mL, but were not able to be confirmed through plating due to the high concentration of *E. coli* O157:H7. Instead, the concentrations of the serially diluted pure culture used prior to inoculation are used to denote the concentration of *E. coli* used in the sample testing.

For the bovine feces samples, there is little uniformity between impedance measurements at high frequencies. The presence of bacteria still has a diminished effect on biosensor impedance at high frequencies, but the impedance between samples is considerably different due to the complexity sample matrix. The manure sample matrix also changes the dielectric capacitance of the testing solution, which is the dominant impedance element at high frequencies. At low frequencies, the impedance increases with increasing bacteria concentration. The data suggests the impedance is dependent on frequency and concentration as already discussed earlier. As with the lettuce and ground beef samples, it is suspected that poor detachment of bacteria from the manure particulates resulted in fewer target bacteria binding to the surface. It is also likely that there was non-specific binding due to the high numbers of non-target generic *E. coli* present in the sample.

For the manure testing, the biosensor was unable to significantly distinguish between different bacteria concentrations, as defined in the statistical analysis of the Methods and Materials. However, when lowering the significance level to 90% ($\alpha = 0.1$), the lower detection limit is 10^4 CFU/mL with respect to the blank.

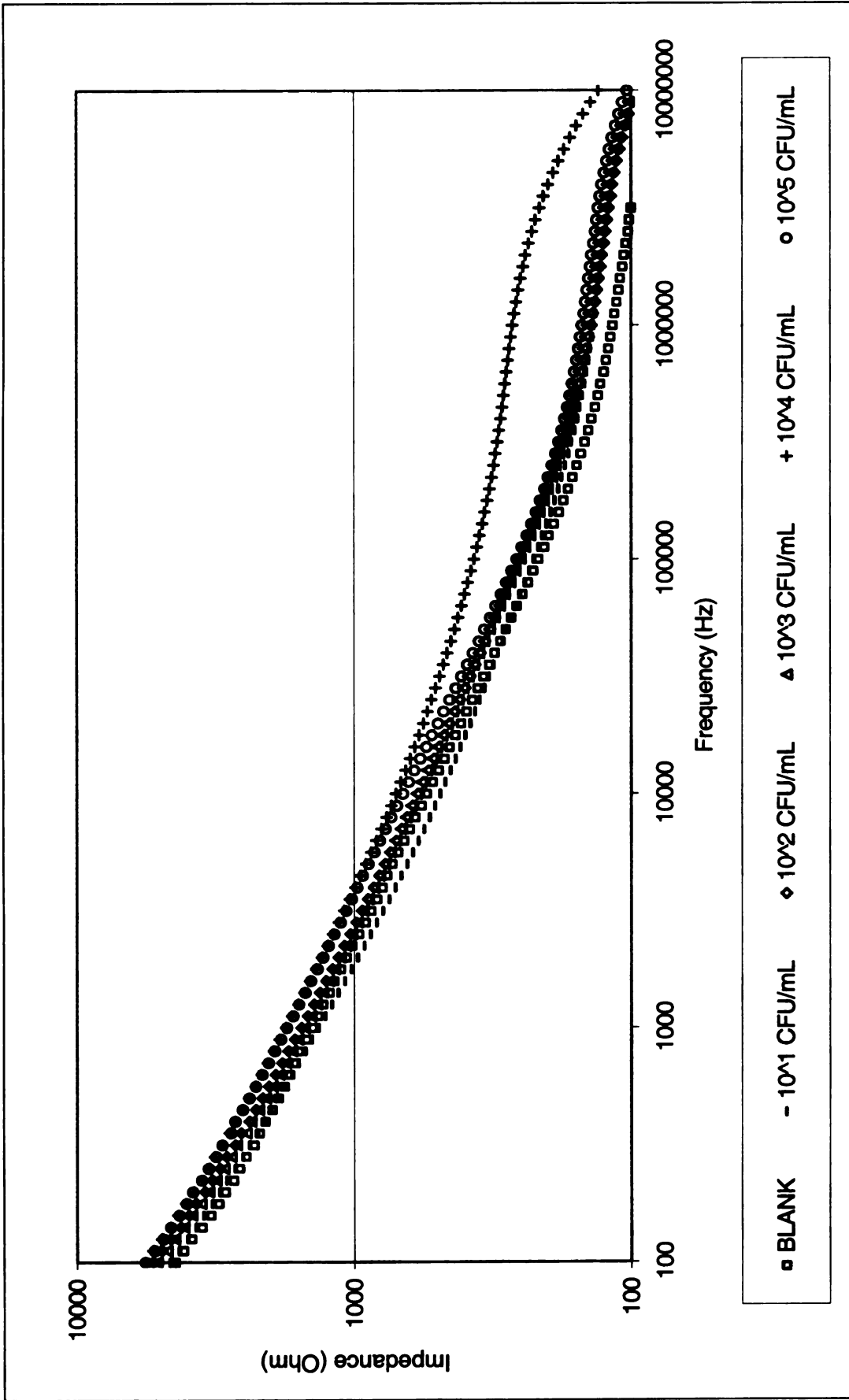


Figure D.6 Impedance for a frequency distribution from 100Hz - 10MHz for bovine feces samples inoculated with *E. coli* O157:H7.

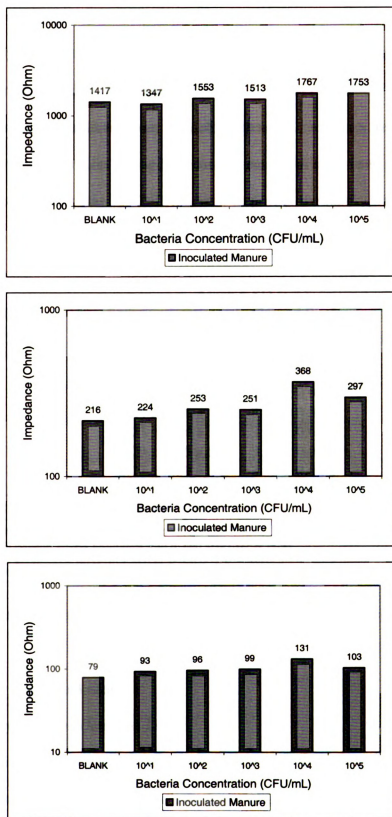


Figure D.7 Comparison of Bovine Feces samples inoculated with *E. coli* O157:H7 at selected frequencies: (top) 1kHz; (middle) 100kHz; (bottom) 10MHz.

For the complex media, the statistical analysis of romaine lettuce samples shows that the biosensor has a lower detection limit of 10^7 CFU/mL with respect to the blank (Figure D.8). Inoculated ground beef samples did not have a lower detection limit as samples were not statistically significant from each other, though there was a trend of increasing impedance with concentration among impedance means. For inoculated manure samples, the lower detection limit was 10^4 CFU/mL with respect to the blank (when lowering the significance level from 95% to 90%).

Concentration (CFU/mL)	Mean \pm SD and Significance ¹		
	Romaine Lettuce Impedance (log Ω) ²	Ground Beef Impedance (log Ω) ³	Bovine Feces Impedance (log Ω) ⁴
BLANK	3.24 \pm 0.04 a	3.43 \pm 0.05 a,b	3.14 \pm 0.09 a
1 x 10 ⁰	3.24 \pm 0.04 a	3.39 \pm 0.09 a,b	----
1 x 10 ¹	3.21 \pm 0.03 a	3.37 \pm 0.07 a	3.13 \pm 0.04 a
1 x 10 ²	3.24 \pm 0.06 a	3.40 \pm 0.06 a	3.19 \pm 0.09 a,b
1 x 10 ³	3.23 \pm 0.04 a	3.46 \pm 0.02 a,b	3.18 \pm 0.03 a,b
1 x 10 ⁴	3.29 \pm 0.05 a,b	3.42 \pm 0.06 a,b	3.25 \pm 0.04 b
1 x 10 ⁵	3.27 \pm 0.09 a,b	3.50 \pm 0.08 a	3.24 \pm 0.03 b
1 x 10 ⁶	3.31 \pm 0.03 a,b	3.48 \pm 0.05 b	----
1 x 10 ⁷	3.40 \pm 0.07 b	----	----

[1] Means with same letter are not significantly different ($p > 0.05$)

[2] Log transform of romaine lettuce inoculated with *E. coli* O157:H7 at 1kHz

[3] Log transform of ground beef inoculated with *E. coli* O157:H7 at 1kHz

[4] Log transform of bovine feces inoculated with *E. coli* O157:H7 at 1kHz ($p > 0.10$)

Figure D.8 Statistical significance of mean differences between concentrations for complex media study.

D.3 Summary and Conclusions

D.3.1 Summary of Lower Detection Limits

When testing the biosensor in complex sample media, the biosensor performance decreased. In testing for romaine lettuce, the lower detection limit was 10^7 CFU/mL. For ground beef, the sample media proved to cause too much variability in testing and as a

result, the biosensor is unable to distinguish between any concentration of bacteria with respect to the blank. (Though ground beef has a lower detection limit of 10^5 CFU/mL when compared to 10^1 CFU/mL.) Bovine feces was also affected by the sample matrix and had a lower detection limit of 10^5 CFU/mL with respect to the blank (with a significance of 90%).

In addressing the biosensor performance, it is noted that the presence of interferants (fats, oils, proteins and organic matter) changes the electrical properties of the sample media. It may be possible to improve signal processing to filter out the effects of the interferants on impedance. Though sample processing steps add time to the testing process, it might be interesting to try innovative sample processing techniques to reduce the presence of interferants in the sample. Perhaps the biosensor could be coupled in-line with a processing unit to provide real time data of filtered samples.

**APPENDIX E
(BUSINESS PLAN)**



AGEN BIOSENSE TEAM INFORMATION PAGE

TEAM ID#:
1051

BUSINESS CONCEPT NAME:
AGEN BIOSENSE

TEAM MEMBER INFORMATION:

DR. TODD ZAHN
zahnt@michigan.org
517.241.0368

MR. MAHENDRA RAMSINGHANI
ramsinghanim@michigan.org
517.241.4180

DR. EVANGELYN ALOCILJA
alocilja@egr.msu.edu
517.355.0083

MR. STEPHEN RADKE
steveradke@hotmail.com
517.485.3770

TABLE OF CONTENTS

<u>SECTION</u>	<u>PAGE NUMBER</u>
EXECUTIVE SUMMARY.....	121
AGEN BIOSENSE OFFERING.....	122
PRODUCT DEVELOPMENT.....	123
MARKET ANALYSIS.....	124
COMPETITIVE ANALYSIS.....	126
MARKETING.....	127
SALES.....	129
MANAGEMENT TEAM.....	131
GROWTH PLAN.....	135
RISKS AND COUNTERMEASURES.....	136
FUTURE GROWTH.....	137
FINANCIAL PLANNING.....	139



GREAT LAKES VENTURE QUEST-PHASE II BUSINESS PLAN

*This Business Concept Overview is prepared in response to the Great Lakes Venture Quest Phase II requirement and is submitted on behalf of Agen BioSense, Team #1051.

EXECUTIVE SUMMARY

PROBLEM STATEMENT

In the meat and food processing industry, undetected pathogens cause widespread diseases and lead to product recall. Pathogen testing is mandatory and regulated by USDA / FDA.

Public concern regarding food safety has increased markedly over the past decade. From farm to table, there are numerous opportunities for the pathogenic contamination of food, which results in food industry recalls, lost productivity, increased insurance costs, unnecessary illness and thousands of fatalities per year.

Escherichia coli are bacteria that naturally occur in the intestinal tracts of humans and warm-blooded animals to help the body synthesize vitamins. A particularly dangerous type is referred to as enterohemorrhagic *E. coli*, or EHEC. EHEC strains has been associated with foodborne outbreaks traced to undercooked meats, apple juice or cider, salad, salami, and milk. EHEC produces toxins that can cause anemia, stomach cramps and bloody diarrhea, and a serious complication called hemolytic uremic syndrome (HUS), which can lead to kidney failure. In North America, HUS is the most common cause of acute kidney failure in children, who are particularly susceptible to this complication.

The Centers for Disease Control and Prevention estimates that 76 million foodborne illnesses occur each year in the United States accounting for 325,000 hospitalizations and 5,000 deaths annually. The four major foodborne pathogens, *Salmonella*, *Listeria monocytogenes*, *Campylobacter*, and *Escherichia coli* O157:H7, are characterized in Table 1.

Pathogen	Number of Cases	Hospitalizations	Deaths
<i>Campylobacter</i>	1,963,141	10,539	99
<i>E. coli</i> O157:H7	62,458	1,843	52
<i>L. monocytogenes</i>	2,498	2,298	499
<i>Salmonella</i>	1,342,532	16,102	556

Table 1. Food Illnesses and Deaths in the United States Caused by Major Foodborne Pathogens in 1999. *Source: Centers for Disease Control and Prevention (Atlanta).*

According to the United States Department of Agriculture (USDA), medical costs and lost productivity resulting from food-borne illnesses is estimated to range between \$5 and \$6 billion annually. Due to the recent trend in Food & Drug Administration (FDA) and United States Department of Agriculture (USDA) regulations with the Hazard Analysis and Critical Control Point (HACCP) program, pathogen testing is mandatory in all meat processing, dairy, food, fruit and vegetable processing plants. Recent food security data indicates that cases of EHEC and other foodborne pathogen infections are rising in both the U.S. and in other nations.

SHORTCOMINGS OF EXISTING PATHOGEN DETECTION TECHNOLOGIES

The detection and identification of food borne pathogens continue to rely on conventional culturing techniques. These are very elaborate, time-consuming and expensive. Typical tests take a minimum of 24 hours for culture followed by 20 minutes of detection. The existing test methods are completed in a microbiology laboratory and are not suitable for on-site monitoring. As a result, the food and beverage industry needs real time pathogen detection sensors with higher sensitivity. According to The International Society of Optical Engineering (SPIE), existing pathogen detection methods, culture techniques and bioassays such as enzyme-linked

immunosorbent assay (ELISA) for determining pathogens in food are elaborate, time consuming and expensive.

AGEN BIOSENSE OFFERING

REAL-TIME PATHOGEN DETECTION WITH HIGHER SENSITIVITY

Agen BioSense has developed a patent protected, portable, real time pathogen detection biosensor. The sensors will enable the food processing industry to conduct real time microbial tests with higher sensitivity.

Company	Technologies	Sensitivity (cfu/mL)	Time
Neogen (Lansing, MI)	Lateral Flow	10,000	8 hours
Molecular Circuitry (King of Prussia, PA)	Immunobiosensor	100,000	24 hours
BioMerieux (France)	Immunoassay	100,000	25 hours
AGEN BIOSENSE	IMMUNOSENSOR	500	<5 min.

Table 2. Sensor Performance Comparison of Three Industry Leaders.

An estimated 25,000 US based food processors perform 144 million tests annually. Current pathogen detection tests conducted in the microbiology laboratory take an average of 8 ~ 25 hours. Delayed detection of pathogens has led to product recall resulting in losses of several million dollars for the meat processing industry.

Rapid, simple, and accurate on-site testing will provide considerable value to the food and beverage industry. Agen Biosense is developing user-friendly biological analysis systems that will be targeted at food processing lines and inventories. This is expected to be a significant advantage over existing testing methods conducted in the laboratory, which lead to production delays and product recalls.

VALUE PROPOSITION

Agen Biosense rapid pathogen detection will enable higher efficiencies in food industry by the following:

- Higher sensitivity ensures high product quality
- Faster on-site testing results in greater yields
- Reduction / Elimination of product recalls
- Reduced liability litigation cases

RAPID AND GROWING MARKET

Recent trends in FDA and USDA regulations suggest testing for pathogenic bacteria will be on the rise. Information extracted from Strategic Consulting, Keen Solutions and Business Communications Company data have estimated the 2001 pathogen testing market at over \$230 million (Table 2 in full plan). This represents approximately a 30% share of the total world market. The product design and manufacturing aspects of Agen’s technology are being accomplished with a low cost, high quality mindset to permit at least a 5% savings per test for our customers. This translates into an annual savings of \$7.2 million for the overall industry. Additionally, Agen Biosense believes that the versatile and easy to use pathogen detection biosensor will have first mover advantage into the home healthcare market of \$6.3B.

FINANCING REQUIREMENTS & RETURN ON INVESTMENT

	Year 1	Year 2	Year 4
Uses of Cash	Complete proto-type & third party testing	Hire CEO and sales team	Develop Sales & Dist. Channels
Capital Required	\$ 500,000	\$ 1.5 million	\$ 4 ~ \$5 million
Potential Sources	Founders, Grants (SBIR, MLSC)	Angel & Seed Stage Investors	Venture Cap.

Table 3. Finance Requirements.

Agen is in the final prototype development stages of the single test pathogen detection biosensor. Production of the first 5,000 units (estimate first year production capacity of 30,000 units) is anticipated by August of this year. Our initial capital outlay is estimated at \$500 K (Year 1 expenditures). The first \$100 K will be solely financed through founder investments, while the remaining \$400 K will be raised through federal and state granting programs and other external funding sources. Emphasis will be on research and development of new and improved product lines and will require an additional \$1 million (covers overhead R & D expenditures) infusion by the third quarter of this year. A final growth stage capital infusion is expected between year 4 and 5. Agen anticipates a breakeven in Year 3 and generate a healthy ROI via an acquisition after Year 5. Current acquisitions in the microbial testing sector are between 5X ~ 10X of actual revenues.

PRODUCT DEVELOPMENT

Agen has three biosensors in the product development pipeline: the single array, multiple array and a Microsystems based sensor. The single array biosensor (detects a specific pathogen at a time) is in the final prototype development stage and will be ready for production by September 2002. The biosensor consists of an electronic detection docking unit and disposable pathogen specific electrochemical cartridge. When the bacteria (pathogen) are present in a sample, a reaction occurs sending an electronic signal to a multi-meter that is used to quantify the bacterial count.

PRODUCT FUNCTIONALITY

Agen Biosensors are designed with the input and feedback from the end user. In 3 easy steps, detection of harmful pathogens can be achieved within 5 minutes. Additionally, the inexpensive disposable cartridges will minimize cross contamination and maximize results.

Steps

- 1) Place Pathogen Specific cartridge in Docking station
- 2) Apply liquefied sample (100 μ L) to application window and wait 5 minutes. Compare reading to the bacterial estimation chart on back of docking station (Indicates quantifiable presence of bacteria)
- 3) Remove and dispose of cartridge

The multiple array biosensor is anticipated to be completed by Q1 2003. As it is based on the same architecture and detection technology as the single test biosensor, thus will require less development time. It will offer the customers the ability to test several (~ 5-10) different pathogens per disposable card. Both the single and multiple arrays will use the same electronic docking display device.

	Year 1			Year 2				Year 3				Year 4	
	Q2	Q3	Q4	Q1	Q2	Q3	Q4	Q1	Q2	Q3	Q4	Q1	Q2
SINGLE PRODUCTION													
SINGLE PROTOTYPE													
MULTI PRODUCTION													
MULTI PROTOTYPE													
MULTI R&D													
Microsystems PRODUCTION													
Microsystems PROTOTYPE													
Microsystems R&D													

Figure 1. Product Development Timeline.

The Microsystems (MEMS) based biosensor is presently in the initial stages of R&D. It has the potential to offer the customer 1000s of tests all on a single silicon wafer. The MEMS test will not be disposable but it will be reusable. The customer would have to return the MEMS chip to Agen Biosense after use for chemical reapplication. The MEMS based biosensor is anticipated to be ready for production by late 2004.

There are two key technological points of interest that need to be considered: sensitivity and speed. The **sensitivity** refers to the concentration of bacteria present (colony forming units, cfu) in a sample needed for detection by the biosensor. Most biosensors being produced by research efforts have a sensitivity of 1000-10,000 cfu/mL. This is especially troubling since only 1 *E.coli* cell is necessary to cause an infection. **Speed** is the other critical technological variable. Culture based tests are sensitive, however, they take days to produce results. This is a problem since even a few hours is enough time for several people to be exposed to a contaminant. The current Agen biosensor is in the process of being validated by a third party with a sensitivity of 1-100 cfu/mL (10 fold decrease in sensitivity compared to competitor product lines) and a detection time of 5 minutes (closest competitor is 4 hours).

MARKET ANALYSIS

LARGE AND A GROWING MARKET

The overall food products testing industry is growing steadily. According to Business Communications Company, Inc., study titled *The Growing Food Testing Business: Pathogens, Pesticides, Genetically Modified Organisms (GMOs)*, sales in the U.S. for food-testing products will grow at an AAGR (average annual growth rate) of 9.9% between 1998 and 2005.

BCC also forecasts that the larger share (82%) of sales will be for tests to detect pathogens and will grow at an AAGR of 9.4%. (From \$122.6 million in 2000 to \$192.5 million in 2005.) BCC forecasts that sales for pesticide-residue tests will increase at an AAGR of 7.7% from \$8.9 million in 2000 to \$12.9 million in 2005

Companies in the pathogen detection and microbial testing industry are growing at a rate of 30 ~ 40 % in revenues each year with average Gross Profit margins in the range of 25- 50%. (Data obtained from Hoovers, Corp Tech, Dun & Bradstreet and Company Financial reports)

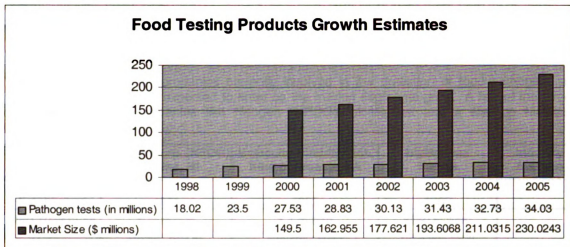


Figure 2. Food Testing Products Growth. *Source:* Business Communications Company, Inc., study titled *The Growing Food Testing Business: Pathogens, Pesticides, Genetically Modified Organisms (GMOs)*

NO CLEAR MARKET LEADER

While several companies are in the pathogen detection space, there is no single market leader in this industry. This has been validated by analysis from a study conducted by University of Michigan Business School Team.

INCREASED PATHOGEN TESTING

The Food and Drug Administration's Center for Food Safety and Applied Nutrition has adopted a food safety program known as Hazard Analysis and Critical Control Point, or HACCP. HACCP implementation is intended to be a proactive approach to prevent hazards that could cause food-borne illnesses. HACCP includes toxins, chemicals, and biological pathogens. Under the oversight of the USDA, all meat and poultry processing plants (~5,530) in the U.S. were required to comply with HACCP regulation effective January 2000. In 1995, the FDA established the HACCP regulation within the seafood industry that includes almost 4100 processing plants. Effective January 20th, 2004 all U.S. juice processing facilities are required to comply with HACCP standards that include pathogen testing prevention. The FDA is now considering developing regulations that would establish HACCP as the food safety standard throughout other areas of the food industry, including both domestic and imported food products.

BIOTERRORISM & NATIONAL SAFETY CONCERNS

Recent threats on national security and the events of September 11th have created an impetus for ensuring the protection of food and water supply. Companies involved in the food and beverage industries are aware of the possibilities for the biological contamination of their products and are evaluating low cost solutions that ensure their products are free of pathogenic material.

WORLD TRADE AND CORPORATE LIABILITY

The size of the food industry and the diversity of products and processes have grown tremendously in the amount of domestic food manufactured along with the number of foods imported. This trend has been associated with the increased number of new food pathogens and increased incidence of contamination. Not surprisingly, the FDA has noticed an increase in corporate liability settlements from food-borne illness cases. Reducing the litigation expenses incurred by food and beverage processing facilities is a primary objective for the industry leaders.

Technological advances in pathogen detection are being developed, and the companies that keep abreast of the technology and understand the value of such advances are positioning

themselves to increase consumer confidence, reduce corporate liability expenses, and build brand quality.

These trends are an indication that the pathogen testing market will continue to expand over the next few years.

COMPETITIVE ANALYSIS

There are a number of companies currently involved in the detection of food pathogens and several other entrants are expected to enter as the market segments grow. A few of the largest competitors include companies like Neogen (NEOG), bioMerieux and a start-up Molecular Circuitry.

	Neogen Corp. (NEOG) Lansing, MI	Molecular Circuitry, Inc. King of Prussia, PA	bioMerieux France	Industry Average
Year Established	1981	1992	1963	
2001 Revenues	\$23 million Public: NEOG	\$ 1 million Privately Held	\$560 million* Privately Held	
Gross Profit	54%	(Not shown profits yet)	N.A.	62.20%
Pre Tax Profit	14.52%	-	N.A.	4.65%
12 Month Revenue	38.80%	-	N.A.	49.50%
Sales / Employee	\$106,400		N.A.	\$120,000
Employees	230	48	4000	
Management	Established	Developing	Established	
Competitive Products	Reveal 8 & Alert	Detex System MC-18	VIDAS ECO	
Pricing	\$ 9.50 per test	\$ 10 per test	\$ 8 per test	
Market Segments	Food	Food	Food, Pharmaceuticals and Cosmetics	
Distribution	Direct Sales Follow sales conducted on phone	Direct Sales 2 Sales Managers for USA	Direct Sales 2 Sales Managers for USA	
Strengths	1) Market leader 2) Well established sales & marketing channels 3) Fiscal strength	1) Solid Board and executive team. 2) Product mature / tested	1) Well established in EU & International Markets 2) Strong R & D	
Weaknesses	1) No International presence 2) Limited R & D focus – acquisition approach	1) Losses for past eight years. 2) Poor market penetration	1) Limited presence in US	
Other Remarks	1) Acquisition related growth 2) About 25% Sales are from International Sales	1) 12 Employees laid off in 2001 2) Company has not shown profit yet.	1) 23% of Sales is from North America 2) 38% of total Sales revenues from immunoassays.	
Notes: 1) * bioMerieux Sales figures are for year 2000. 2) + Industry Average is based on Diagnostics Industry/Source: Hoovers Information. Other information is from annual reports.				

Table 4. Competitive Analysis of Three Industry Leaders.

MARKETING

MARKET STRATEGY

Agen's strategic marketing plan has been developed in detail to address the products, customers and the target market. Progress has been made on several of the following areas:

- **Market Research:** Agen has extensively evaluated data (annual financial reports of competitors, market research sources such as BBC, Hoovers, Dunn & Bradstreet) over the past five years to conclude that the market has been growing at a healthy rate. As indicated in the initial market analysis section, the market growth trends and size are healthy. The unit sales are growing at a CAGR of 9.9 % and the dollar sales are growing at a CAGR of 9.4%.
- **External & Internal audit:** After analyzing the tactics in distribution and pricing methods of various competitors, Agen has completed an extensive audit that assists in developing a market entry strategy. The strategy is explained in the following **Market Entry** section.
- **Customer Research:** A University of Michigan Business School team of five students is currently assisting Agen to conduct customer research. The research is targeted towards top dairy companies and top meat producers in North America. The survey focuses extensive interviews with target customers to gather data related to product performance, price, testing procedures, distribution channels. The findings will be available by end of Q1 2002.
- **Beta Testing and Initial product analysis:** Agen has contacted Kraft Foods to conduct beta tests of the product. The Agen team has had several discussions with Koegel Meat and is in the process of identifying meat processing sites for beta tests. The beta testing will be monitored closely by Agen. Results of the beta tests are expected to arrive by Q2 2002.

SEGMENTATION

The processed food sector accounts for the largest number of tests, with over 52.2 million performed annually (Table 5). This represents over 36% (Figure 3) of total tests performed, most likely driven by the larger number of plants (almost 38%). The dairy sector has the highest testing rate per plant, averaging over 630 tests per plant per week, while the beef and poultry sector performs the least number of tests per plant averaging 369 tests per plant per week. As a result, the beef and poultry sector accounts for only 22.3% of all testing in the industry. The fruit and vegetable sector is currently the smallest of the four sectors accounting for only 9.7% of testing. However, the fruit and vegetable sector is becoming more of a focus by the USDA food safety inspection service and is expected to result in a substantial increase in the next few years.

US Food Industry Sector Review			
Sector	Number of Plants	Total Tests	Average/Plant/week
Beef and Poultry	1,679	32,212,471	369
Dairy	1,388	45,887,576	636
Fruit/Veg	652	13,981,305	412
Processed foods	2,260	52,196,282	444
Total	5,979	144,277,634	464

Table 5. US Food Industry Sector Review. (Source: Strategic Consulting—Pathogen Testing in Food Industry, 1999)

The food testing industry is comprised of the following sectors (US figures):

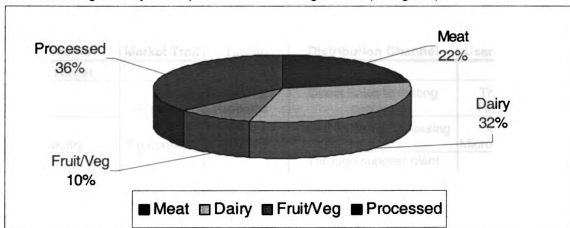


Figure 3. US Food Industry Tests per Sector.

MARKET ENTRY

Entry Methods & Launch timing: Agen expects to penetrate the dairy and meat processing market steadily by building relationships with key potential customers. The initial approach for year 1 will include leveraging upon the relationships of the Board members. After the product has been tested by a third party laboratory an aggressive market penetration strategy will be adopted. This is expected in year 2 and the low-cost approach will include the following:

- o Creating customer awareness by making presentations at key events such as the Association of Analytical Communities (AOAC) annual exposition held in September each year, the International Dairy Food Association (IDFA) worldwide expo held in October every year. A list of all target events and their impact has been developed by Agen.
- o Using a public relations strategy to generate media in key industry publications such as Food Quality, Food testing and Analysis and several other target publications.

Presence at exhibitions, collateral material development and full-blown campaign will be executed after initial funding in year 2.5 / year 3.

MARKETING MIX: THE FOUR P'S

PRODUCT PLAN: Agen's product will be positioned as a "Faster and Accurate" product with the ability to conduct tests for several pathogens on one strip.

PLACE: As most of the dairy companies are based in Midwest (primarily Wisconsin) along with several meat processing companies, the customer focus will remain in the Midwest region of North America during the beta testing and initial launch stages. The regional focus will shift to North America during the growth phase.

PROMOTIONAL PLAN: The company's promotion plan primarily focuses upon events (technical workshops, seminars) during year one with media strategy to broadcast the significant milestones. Development of an aggressive promotional plan, including development of collateral marketing material will be subsequent to third party testing of the product.

PRICING PLAN: Agen will follow the industry price levels of \$12 per test with sales emphasis upon speed and sensitivity. A discount structure for key customers has been developed depending upon the volumes of purchase.

Segments	Market Trait	Launch Timing	Distribution Channel	End User/Customer
Primary Target:				
Diary	Attractive	0 ~ 12 months	Direct Sales to testing centers	Third Party Testing Lab.
Beef & Poultry	Competitive	12~ 24 months	Direct Sales to processing center	In house Microbiology Lab.
Processed Foods	Fragmented	Year 2	Through supplier plant channels	Individual plants
Fruit & Vegetable	Emerging	Year 2-3	Direct sales to Testing labs	Processing plants
Secondary Target:				
Healthcare	Attractive	Year 2	Channel Sales	ICU / ER
Military	Competitive	Year 2	To Be Decided	
Env. Testing	Fragmented	Year 3	To Be Decided	
Vet. & Animal care	Fragmented	Year 4	To Be Decided	

Table 6. Marketing Entry Strategy for Targeted Industries.

BUDGET: The Marketing & Sales budget is expected to be as high as 45 ~ 50% of the revenues in first 2 years and will be driven down gradually to 35% by year 5.

SALES

IDENTIFYING THE CUSTOMER

- To determine the appropriate target customer within each sector, one must understand where pathogen testing is being performed. The market report, *Pathogen Testing in the U.S. Food Industry* (Strategic Consulting, 2000) analyzed where microbiological testing practices occurred most often, and discovered that testing took place in one of three areas:



Figure 4. Point of Pathogen Testing in Various Sectors. (Source: Keen Solutions, 1999 Report)

- o Processing plant – Microbiology Laboratory: Average 40% Tests
- o External / Third Party outside Reference laboratories: Average 41% Tests
- o Centralized corporate laboratories: Average 19% Tests

While aggressive sales are not expected to start till the end of year 1, a target customer list of the top 100 meat producers in North America has been acquired. Also, Agen is currently in advanced stages of gathering details of various laboratories in the Midwest that conduct pathogen testing for the dairy industry.

SALES STRATEGY: HOW TO GET THERE

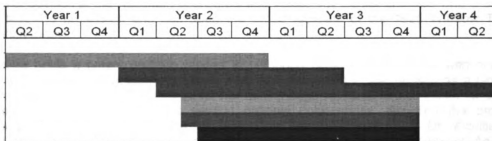


Figure 5. Sales Strategy and Yearly Milestones.

PROJECTED SALES & MARKET SHARE

Strategic Consulting, Keen solutions and Business Communications Company data anticipate a 2005 pathogen testing market estimate over \$230 million (Table 7), representing approximately 30% of the total world market. Not surprisingly, the processed foods sector represents the largest pathogen testing segment with total US consumable sales of \$75.9 million, representing 33% overall. The dairy sector comprises 29% (\$66.7million) of total US consumable sales in the pathogen testing market, while the beef and poultry sector accounts for 21% of total sales. The fruit and vegetable, and seafood sectors combine for the remaining 17% (9% and 8% respectively).

<i>Food Industry Market</i>	Seafood	Beef & Poultry	Dairy	Fruit & vegetable	Processed foods	Total
Consumable Sales (US) (million)	\$18.4M	\$ 48.3M	\$66.7M	\$ 20.7M	\$ 75.9M	\$230M
Overall Percentage	8%	21%	29%	9%	33%	100%
<u>Agen Market Share</u> *(5yr Min. Estimate= 10%Market share)	\$ 1.8M	\$7.24M	\$6.6M	\$1.65M	\$3.79M	\$21.08M
<u>Agen Market Share</u> *(5yr Max. Estimate= 20% Market share)	\$ 3.6M	\$ 14.48M	\$13.2M	\$3.3M	\$7.58M	\$42.16M

Table 7. Market Share Estimates and Target Sales Revenues from Food Industry Sectors.

Notes:

- 1) Agen Penetration is expected to be higher in Beef & Poultry (15%) with about 5% -10% in other markets.

2) Beef and poultry data was collected from only large 1,679 processing plants. Additional 3248 small plants are not included in the estimates.

3) HACCP pilot studies are currently being conducted in the fruit and vegetable sector. The expected date of HACCP implementation for this sector is January 20th, 2004, which could easily translate into a 3-5 fold increase in pathogen detection within this sector translating into potential returns of \$9-\$14 million for Agen Biosense.

MANAGEMENT TEAM

Dr. Evangelyn Alocilja, Ph.D.: Chief Scientific Advisor

Dr. Alocilja is a professor of Biosystems Engineering, Michigan State University. She also holds an adjunct position at the National Food Safety and Toxicology Center at MSU. She is dedicated to the teaching profession and has been the proud recipient of the 1995 Withrow Teaching Excellence award.

Dr. Alocilja holds a patent portfolio related to pathogen detection biosensors, with one patent issued and three currently pending. She is very well connected in the industry as a biosensors consultant and is nationally recognized for her cutting edge research in biosensors for pathogen detection. An invited speaker at several national conferences, including the prestigious Knowledge Foundation's conference on "Electronic Nose Technologies", Dr. Alocilja is the elected chair of the 2002 biosensors committee for the American Society of Agricultural Engineers. Dr. Alocilja will lead the efforts of scientific discovery & new product development.

Stephen Radke B.S.: Product Development

Mr. Radke will be an integral part of the biosensor product development team focusing on product improvements and quality control issues. Steve received his bachelor degree in engineering and is currently pursuing a doctorate in bio systems engineering from Michigan State University. His research focus is on biosensor development for rapid pathogen detection.

Mr. Radke is on leave from the General Motors Company as a product engineer where he was responsible for managing the design, build and installation of million dollar projects involving manufacturing integration equipment. Prior to this Steve was awarded a National Science Foundation fellowship at the Virginia Polytechnic Institute and State University where he focused on biosystems engineering and water quality research.

Todd Zahn Ph.D., MBA: Financial and Strategy

Dr. Zahn will be responsible for overseeing global corporate strategy and early stage corporate development. With his science and business background, Todd brings a unique perspective to the Agen team. He has a significant understanding of technology development and industry awareness. Additionally, he has overseen the activities for a \$1 billion fund dedicated to building the life sciences industry in the State of Michigan. As an integral part of a small team, Todd has contributed extensively to the strategic design and implementation of the Michigan life science corridor, which has become a benchmark and model for life science initiatives in other States including New York, Missouri, Pennsylvania, and Texas.

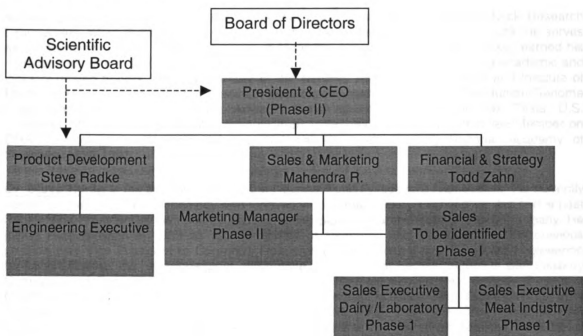
Prior to this, Todd was a corporate strategy consultant for a technology commercialization and licensing incubator that commercialized medical device technology discovered at Los Alamos National Labs. His research in anti-cancer agents led to the discovery of a handful of potent anti-tumor agents (patent pending) and provided useful insight into the mechanism of the most common link to human cancer. He was also successful in scaling up the manufacturing of anticancer agents that were sold to the largest chemical supply company in the U.S. Todd has published his research findings in highly respected international journals that include the Journal of the American Chemical Society and Journal of Medicinal Chemistry. Todd is an active member in the Society of Competitive Intelligence Professionals, and is a member and award recipient of the American Chemical Society.

Mahendra Ramsinghani, B.E., MBA: Sales & Marketing

Mr. Ramsinghani will lead sales and marketing efforts for Agen. Mahendra brings a wealth of resources and contacts to Agen, including a broad skill set in sales, marketing and business development. Currently, Mahendra serves as the Director of Venture Capital Initiatives for Michigan Economic Development Corporation and is responsible for the creation and utilization of incentives that help grow the venture capital resources. He has led development of a \$75 million venture capital incentive plan (under approval at legislature) expected to create upwards of \$ 300 million in venture capital for Michigan over time.

Mr. Ramsinghani received his MBA in 1996 from the University of Pune, India focusing on marketing and finance. Shortly thereafter, he led the growth & market penetration of Aluminum Company of America (ALCOA) in India. He successfully grew Alcoa's installation exceeding 150% of target goals in 18 months. In 1997, Mahendra was head for business development for Kemtec Technologies, Singapore where he led corporate sales & market growth from 0 to S\$ 2 million in 18 months. Subsequently, Kemtec Technologies went public in year 2000 (SGX:ISOFTEL).

ORGANIZATION CHART



Projected Staffing Needs					
	Year 1	Year 2	Year 3	Year 4	Year 5
Executive	1	2	4	6	6
Finance	0	1	2	2	2
Business Dev.	1	1	3	5	6
Marketing & Sales	2	4	14	28	37
Product Development	2	4	12	12	18
Technology Mgmt & Support	0	1	2	3	4
Total	6	13	36	56	73

Table 8. Projected Human Resources Requirements.

BOARD MEMBERS

We are currently in the process of recruiting five individuals to serve on the executive board. We have identified the following individuals to act as board members:

Dr. Michael H. Brodsky is President of Brodsky Consultants, in Thornhill, Ontario, Canada and is immediate past president of the Association of Analytical Communities (AOAC) INTERNATIONAL, the internationally recognized analytical test validation and approval agency for foods and agriculture. Mr. Brodsky began his career as a research scientist in environmental bacteriology, for the Laboratory Services Branch of the Ontario Ministry of Health. In 1982 he became Chief of Environmental Microbiology and Microbiological Support Services for the Ontario Ministry of Health, a position he held for 17 years. In 1999 Mr. Brodsky retired from the Ontario Ministry of Health and accepted a one-year appointment as General Manager of Silliker Laboratories of Canada, and subsequently founded his own consulting firm. In addition to his many years of service to AOAC as a training course instructor, Board member, and President, Mr. Brodsky serves as a Technical Assessor for ISO under the auspices of the Standards Council of Canada, and is active in a number of several professional associations.

Dr. Tom Caskey is chief executive officer and president of Cogene Biotech Ventures, Ltd, a private equity fund that focuses on intermediate stage and start-up biotech companies. He served as senior vice president, human genetics and vaccines discovery at Merck Research Laboratories, West Point, Pa. and president of the Merck Genome Research Institute. He serves as an adjunct professor at Baylor College of Medicine, Houston, Texas. Dr. Caskey earned his medical doctorate from Duke University, Durham, NC. He has received numerous academic and industry-related honors. He is a member of the National Academy of Sciences and Institute of Medicine. He is past president of American Society of Human Genetics and the Human Genome Organization. He served as Chair, Advisory Panel on Forensic Uses of DNA Tests, U.S. Congress Office of Technology Assessment from 1989-1990. He was a Committee Member on DNA Technology in Forensic Science, National Research Council, National Academy of Sciences, 1989-1991.

Dr. Steve Henig is the past president of the National Food Processors Association. He currently serves as Senior VP of Technology and Innovation for Ocean Spray Cranberries, Inc and is past Senior Vice President of Technology and Marketing Services for the Hunt-Wesson Company. He joined Hunt-Wesson in 1983 as Vice President of Research and Development. His previous position was Vice President of Corporate Research & Development and Corporate Engineering for Land O'Lakes, Inc., in Minneapolis, Minnesota. Prior to that he held positions with Pillsbury Company and General Foods Corporation. Dr. Henig received his Bachelor Science Degree in Chemical Engineering and a Master of Science Degree in Food and Biotechnology from Technion-Israel Institute of Technology. He earned his Ph.D. Degree in Food Science from Rutgers University, New Brunswick, New Jersey. Steve is a member of the Board of Directors for Bionutrics Inc. and served as director of LipoGenics from August 1992 until October 1996.

Dr. Paul Hall is on the Executive Board of the International Association for Food Protection. He serves as Vice President to the Kraft Foods Corporation. *We are waiting for an e-mail confirmation from him.*

MANAGERIAL RISKS / WEAKNESSES AND COUNTERMEASURES

- **Start-up Management and Growth Experience:** The basic team of four founders has minimal experience in the start-up environment.

Countermeasure in Phase1: While no founder has "started" a company, the team has identified two experienced business mentors. This will ensure that the first few steps in structuring the business and technology follow best practices.

Countermeasure in Phase 2: As soon as Agen completes building the product and beta tests, Agen will hire a seasoned sales and marketing expert with the necessary domain expertise. Agen will also actively seek the help of the Board to identify and recruit a Chief Executive Officer who can continue the rapid growth of the company by attracting customers and investors. Subsequent hiring of executives will be per the decision of the CEO.

OVERALL EXISTING MANAGERIAL STRENGTHS

- Strong technical and product development expertise
- Aggressive growth plan with milestones being executed per planned timelines
- Strong Board (5 Members)
- Strong Technical Advisory Board (7 Members)
- Extremely high motivation, drive, and determination of founders

BUSINESS SYSTEMS AND ORGANIZATION

Research and Development: The MEMS technology utilized in the Agen Biosensor is rapidly evolving. The research and development involved in further perfecting the speed, sensitivity, and selectivity are critical elements for the company and should be a source of competitive advantage. In addition to the technology, the development of biological material must be maintained as it is critical to have access to the latest antibodies. Agen believes that its current strengths are very strong in the research area.

Human Resources: Agen BioSense is focused on a high caliber of talent. As the company grows, focus will be on both the research and development team as well as the management team with the necessary skills to capture the company's market niche.

Marketing and Sales: Agen BioSense will employ a direct sales force to actively seek out new opportunities. We estimate that initially the company will employ 3 sales resources to focus on the target markets. Agen will focus the inbound logistics, manufacturing and outbound logistics subsequent to product development. In the initial phase, it is expected that all these activities will be outsourced.

Inbound Logistics of Supplies and Equipment: Inbound logistics of supplies and equipment is the process to obtain the raw materials from suppliers – electrical circuitry, cartridge housing, reader, and biological material. This process can range from creating contracts with suppliers and shipping companies to developing the inbound logistics in house.

Manufacturing: Manufacturing is the process of applying the antigen solution to the cartridge. This process is currently time consuming, but could be a source of competitive advantage in the future. The antigen solution is brushed on to the electrical circuitry board and then allowed to dry for 8 hours. Following the drying period, the coated circuit board is placed in the housing cartridge and set to outbound logistics.

Outbound Logistics: Outbound logistics will pair the cartridge housing and the number of requested detection readers and prepare them for shipping. Once packaged and ready to ship, options exist for Agen BioSense to outsource the activity or keep outbound logistics inhouse.

OVERALL GROWTH PLAN

Stage	Start-up	Growth	Rapid Growth	Continuous Growth
Phase	Phase 1	Phase 2	Phase 3	Phase 4
Timeline	0 ~ 2 years	2 ~ 4 years	4 ~ 6 years	Year 7 onwards
Goals	Develop Product	Drive Sales	Lead the market	Dominate the industry
Objectives				
Technical	-Complete Proof of concept -Complete 3rd party testing -Complete beta testing with customers	-Ensure consistent product performance -Complete multi-sensor -Identify IP for acquisition	-Complete MEMS prototype -Diversify product portfolio	-Prototype nanoscale sensors -Diversify product portfolio
Financial	-Raise Federal grants -Build relationships with angels & VCs -Finalize product-pricing	-Raise angel round and build strategic alliances. -Ensure revenues are per target. -Control Acc. Rec'ble.	-Raise VC rounds 1-3	-Target potential buyout or acquisition parent
Managerial	-Identify industrial partnerships -Develop manufacturing and testing vendors -Build R & D Group	-Attract CEO & VP, Sales -Add legal expertise -Build sales in dairy and meat markets -Add Additional R & D staff	-Continue building industry specific sales force in processed foods industry -Enter fruit and vegetable market	-Build on international sales force and product diversification team
Essential Resources Required	-Cash Required: \$ 100,000 -Existing team to support growth	-Capital Infusion: \$ 1.5M -Experienced sales and executive team.	-Capital Infusion:\$4-5M	-Human Resources, manufacturing, and managerial talent

Table 9. Growth Plan Milestones for Company Sectors.

INDUSTRIAL PARTNERSHIPS

Agem is in the process of identifying industrial partners to help with the manufacturing and testing of the Agem single test biosensor. We have initial interest from a well known manufacturing company who specializes in biosensor and MEMS based manufacturing. We are looking to form a partnership with them to increase the production scale-up of the single test biosensor. Additionally, we have received interest from the Kraft Foods corporate testing facility to help with our third party testing efforts and validation.

These deals are tentative and may involve equity, sublicense agreements, service contracts, or other financial arrangements in the final negotiations.

RISKS AND COUNTERMEASURES

EXTERNAL RISKS

- **Developing Technologies:** Several new technologies are being developed in the rapid pathogen detection space. Some of these include the use of fiber optics while other techniques use silicon / DNA based technologies.

Countermeasure: Agen will aggressively continue to develop the first product for *E. coli* testing, ensure that beta customers are lined up and the third party testing is completed quickly.

- **Entry of larger players / Better products from existing players:** Several companies like bioMerieux have been aggressively investing upwards of 12 to 15 % of their revenues in research and development. It is inevitable that large companies will come up with new and improved technologies.

Countermeasure: Agen will negotiate strategic alliances with the most appropriate partners to ensure that its products are accepted rapidly in the market place. Focus will be on leveraging our resources with others that have existing distribution and market channels. A significant emphasis will be on new product development as we attempt to continue the technological advantage our products currently offer.

- **Regulation:** The food industry is regulated by the Food & Drug Administration (FDA), which has implemented the Hazard Analysis and Critical Control Point (HACCP) guidelines. In 1998, the U.S. Department of Agriculture established HACCP for meat and poultry processing plants. Most of these establishments were required to start using HACCP by January 1999. Very small plants had until Jan. 25, 2000. (USDA regulates meat and poultry; FDA all other foods) FDA now is considering developing regulations that would establish HACCP as the food safety standard throughout other areas of the food industry, including both domestic and imported food products.

Countermeasure: While the FDA has established the HACCP guidelines, the food processing companies have lobbied extensively to ensure that the industry is not unduly regulated. Should the regulation change, Agen will have to react rapidly to ensure that its market position is not affected and product development strategy is in line with regulation.

INTERNAL RISKS

The success of the company depends on effective attraction and growth of financial, managerial and technical resources:

- **Financial / Funding:** In the initial product development stages, the progress of the company depends on availability of financial resources. Lack of funding can delay the implementation strategy and negatively affect our milestone achievements.

Countermeasure: Agen will pursue a multiple pronged strategy to attract federal and state grant funding in the early stages. Several such funding sources have been identified (SBIR/STTR, ATP, MLSC) and serious efforts are being made to maximize the probability of being funded through these programs. Additionally, as we meet our product manufacturing goals and obtain beta customers, we will be seeking Angel and VC investors to help us continue our aggressive growth potential.

- **Technical / Product Development:** The current sensor is in advanced stages of development and testing. Several risks exist at this stage in terms of stable product performance under severe test conditions. Third Party testing is essential for

validating the reliability of the tests. If the product fails to perform at any of the testing stages, design efforts will have to be revamped.

Countermeasure: Agen has confidence in the high profile scientific advisory board and believe we are allocating adequate financial and technical resources to ensure that product development is not compromised. However, we understand that validation testing does not always go as planned, thus we will continue product improvements and new product development to emphasize a solid product pipeline.

- **Managerial / Attraction of key personnel:** The existing team of Agen is in a position to grow the company to the beta test and initial market acceptance stage. However, it will be necessary to recruit highly experienced management talent when we begin an aggressive growth stage. In particular, we will need to attract a high profile marketing and sales professional as our current team is lacking the necessary skills.

Countermeasure: After crossing the initial milestones, the company will explore the possibility of hiring senior executives from the industry. Stock options, high growth industry and the challenge of the start-up environment may be some of the attraction tools. Most importantly, we believe the board of directors we are recruiting will help minimize the risk of failure and act as an incentive for recruiting executive talent.

FUTURE GROWTH

Agen's growth strategy will utilize a portfolio of technologies that would encompass the following:

- Pathogen Prevention Technologies
- Pathogen Detection
- Pathogen Elimination

The company will initially focus on their competitive strengths to market the pathogen detection biosensors product line. As significant progress is accomplished, efforts will be made to help offset the risk of competing companies and technologies. We will continue to improve existing biosensor technology and develop new biosensor capabilities until we have built significant brand awareness in this space. Ultimately we aim to offer products for the complete spectrum of pathogen specific needs.

FOOD SAFETY

The market potential for detection and identification of bacterial and viral pathogens in the food safety area is estimated at around \$100 million per year. Applications include detecting contaminants in food raw materials, food products, processing and assembly lines, and water supplies continue to rely on conventional culturing techniques. Currently, detection techniques typically require 2-3 days, and thus do not alert industrial producers to quality control problems until well after the fact. Real time testing will provide value to food producers through the elimination of product recalls and reduced treatment costs.

ENVIRONMENTAL QUALITY

Pathogens present in the environment is becoming crucial to a wide range of industries, including food, pulp and paper, cosmetics, metals, plastics, petrochemical and power generation. With greater pressure to recycle water, minimize the use of antibacterial agents, and maintain quality discharges, manufacturers in a wide variety of industries are seeking technologies to rapidly identify contamination problems at the source.

For example, *Cryptosporidium parvum* is a waterborne pathogen infective at a dose of a single organism. It is responsible for frequent widespread outbreaks of intestinal disease that can be life-threatening for individuals with compromised immune systems. To detect the presence of such organisms, there is a need for rapid biological testing systems that can concentrate the

organisms from several gallons of water. Real time, on-site testing systems will play an important role in further enabling the detection of environmental pathogens.

BIODEFENSE

As the threat of domestic and international bioterrorism continues to grow, so does the need for rapid, automated, field-based tests for pathogenic agents, as well as faster, more specific laboratory bioanalysis and detection systems. Military units facing an enemy with the potential for an arsenal of biological weapons require the ability to monitor the environment and provide at-risk troops with the means to rapidly identify contaminated air, water, food, and equipment. Testing may also be helpful in guiding cleanup after an attack with spore-forming agents such as anthrax, which can persist in the environment for years.

Field-ready systems are being deployed to enable environmental surveillance because the biological agents most likely to be used in a terrorist attack do not immediately produce effects. Currently, samples taken from the environment, such as soil and water, and most clinical samples must be cultured for reliable identification, typically requiring 4—48 hours before a result is available. Real time, highly sensitive on-site testing systems will play an important role in enabling timely detection of these types of pathogens.

FINANCIAL PLANNING & FINANCING**Agen BioSense****Income Statement (\$)**

	2002	2003	2004	2005	2006
Revenue					
All Cartridges	\$300,000	\$2,400,000	\$13,440,000	\$16,406,000	\$21,089,900
Base unit	\$2,500	\$72,500	\$103,675	\$134,778	\$191,139
Total Revenue	\$302,500	\$2,472,500	\$13,543,675	\$16,540,778	\$21,281,039
Cost of Goods Sold					
	\$56,250	\$612,875	\$2,510,176	\$3,264,860	\$4,496,729
Gross Margin					
	\$246,250	\$1,859,625	\$11,033,499	\$13,275,917	\$16,784,310
% of Revenue	81%	75%	81%	80%	79%
Operating Expenses					
Engineering	\$117,600	\$400,949	\$856,910	\$1,039,787	\$1,081,607
% of Revenue	39%	16%	6%	6%	5%
Marketing/Sales	\$196,253	\$1,145,366	\$4,986,861	\$6,175,866	\$7,377,540
% of Revenue	65%	46%	37%	37%	35%
Administration	\$89,288	\$313,783	\$685,535	\$839,287	\$988,742
% of Revenue	30%	13%	5%	5%	5%
Total Operating Expenses	\$403,141	\$1,860,097	\$6,529,306	\$8,054,941	\$9,447,889
% of Revenue	133%	75%	48%	49%	44%
Income Before Int & Taxes					
	(\$156,891)	(\$472)	\$4,504,193	\$5,220,977	\$7,336,421
% of Revenue	-52%	0%	33%	32%	34%
Income Before Taxes					
	(\$156,891)	(\$472)	\$4,504,193	\$5,220,977	\$7,336,421
Tax Exp	\$0	\$0	\$1,735,714	\$2,088,391	\$2,934,568
Net Income					
	(\$156,891)	(\$472)	\$2,768,480	\$3,132,586	\$4,401,853
% of Revenue	-52%	0%	20%	19%	21%

Agen BioSense**Balance Sheet (\$)**

	2002	2003	2004	2005	2006
ASSETS					
Current Assets					
Cash	(\$385,674)	(\$310,323)	\$2,042,885	\$5,067,686	\$9,372,121
Net Accounts Rec	\$299,475	\$210,375	\$1,117,353	\$1,364,614	\$1,755,686
Inventory (15 days)	\$22,500	\$101,082	\$132,428	\$183,653	\$237,099
					\$11,364,90
Total Current Assets	(\$63,699)	\$1,135	\$3,292,666	\$6,615,953	6
Gross Fixed Assets					
Gross Fixed Assets	\$32,500	\$88,500	\$142,500	\$179,500	\$174,000
Less Accum Depreciation	\$5,750	\$25,458	\$72,958	\$121,958	\$150,458
Net Fixed Assets	\$26,750	\$63,042	\$69,542	\$57,542	\$23,542
					\$11,388,44
TOTAL ASSETS	(\$36,949)	\$64,176	\$3,362,208	\$6,673,495	8
LIABILITIES					
Short Term Liabilities					
Accounts Payable (30 days)	\$95,150	\$173,257	\$246,293	\$321,158	\$423,044
Salaries Payable (15 days)	\$14,792	\$38,282	\$60,869	\$76,536	\$76,206
Taxes Payable (90 days)	\$0	\$0	\$433,928	\$522,098	\$733,642
Line of Credit (10% of net A/R)	\$0	\$0	\$0	\$0	\$0
Current Portion of Capital					
Equipment Lease	\$0	\$0	\$0	\$0	\$0
Current Portion of Long Term					
Debt	\$0	\$0	\$0	\$0	\$0
Total Short Term Liabilities	\$109,942	\$211,539	\$741,091	\$919,792	\$1,232,892
TOTAL LIABILITIES	\$109,942	\$211,539	\$741,091	\$919,792	\$1,232,892

Agen BioSense**Statement of Sources & Uses (\$)**

	2002	2003	2004	2005	2006
BEGINNING CASH	\$10,000	(\$385,674)	(\$310,323)	\$2,042,885	\$5,067,686
Sources of Cash					
Net Income	(\$156,891)	(\$472)	\$2,768,480	\$3,132,586	\$4,401,853
Add Depr/Amort	\$5,750	\$19,708	\$47,500	\$49,000	\$28,500
Plus Changes In:					
Accounts Payable (30 days)	\$95,150	\$78,107	\$73,036	\$74,865	\$101,886
Salaries Payable (15 days)	\$14,792	\$23,490	\$22,587	\$15,667	(\$330)
Taxes Payable (90 days)	\$0	\$0	\$433,928	\$88,169	\$211,544
Total Sources of Cash	(\$41,199)	\$120,834	\$3,345,532	\$3,360,287	\$4,743,453
Uses of Cash					
Less Changes In:					
Net Accounts Rec	\$299,475	(\$89,100)	\$906,978	\$247,261	\$391,072
Inventory (15 days)	\$22,500	\$78,582	\$31,346	\$51,225	\$53,446
Gross Fixed Assets	\$32,500	\$56,000	\$54,000	\$37,000	(\$5,500)
Total Uses	\$354,475	\$45,482	\$992,324	\$335,486	\$439,017
CHANGES IN CASH	(\$395,674)	\$75,351	\$2,353,208	\$3,024,801	\$4,304,435
ENDING CASH	(\$385,674)	(\$310,323)	\$2,042,885	\$5,067,686	\$9,372,121

BIBLIOGRAPHY

References

1. **Abdel-Hamid, I., Ivnitski, D., Atanasov, P., Wilkins, E., 1998.** Flow-through immunofiltration assay system for rapid detection of *E. coli* O157:H7. *Biosensors and Bioelectronics* 14:3:309-316.
2. **Alocilja, E., and Radke S., 2003.** Market analysis of biosensors for food safety. *Biosensors and Bioelectronics* 18:841-846.
3. **Bao, L., Deng, L., Nie, L., Yao, S., Wei, W., 1996.** Determination of microorganisms with a quartz crystal microbalance sensor. *Analytical Chemistry Acta* 319:97-101.
4. **Bard, A.J. and Faulkner, L. R., 1980.** *Electrochemical Methods: Fundamentals and Applications.* J. Wiley, New York, NY USA.
5. **Bhatia, S., Shriver-Lake, L., Prior, K., Georger, J., Calvert, J., Bredehorst, R., Ligler, F., 1989.** Use of thiol-terminal silanes and heterobifunctional crosslinkers for immobilization of antibodies on silica surfaces. *Analytical Biochemistry* 178:408-413.
6. **Binns, K. and Lawrenson, P., 1973.** Analysis and computation of electric and magnetic field problems. Pergamon (Oxford), 25-29 and 151-187.
7. **Bockris, J. and Reddy, A., 1970.** *Modern Electrochemistry.* Plenum Press, New York, NY USA.
8. **Borkholder, D., 1998.** Cell based biosensors using microelectrodes. Dissertation. Stanford University, Stanford, CA, USA.
9. **Brooks, J., Mirhabibollahi, B., Kroll, R., 1992.** Experimental enzyme linked amperometric immunosensors for the detection of *Salmonella* in foods. *Journal of Applied Bacteriology* 73:189-196.
10. **Burnett, A., Beuchat, L., 2001.** Comparison of sample preparation methods for recovering *Salmonella* from raw fruits, vegetables, and herbs. *Journal of Food Protection* 64:10:1459-1465.
11. **Buzby, J., Roberts, T., Lin, C., MacDonald, J., 1996.** Bacterial foodborne disease: medical costs and productivity losses. *Agricultural Economics Report No. 741:100.* USDA Economic Research Service. Washington DC USA.

12. **CDC-Centers for Disease Control and Prevention, 2002.** Report on the Decline of Foodborne Illness. Atlanta, GA.
13. **CDC-Centers for Disease Control and Prevention, 2001.** Outbreaks caused by Shiga toxin-producing *Escherichia coli*, Summary of 2000 Surveillance Data. Atlanta, GA.
14. **CDC-Centers for Disease Control and Prevention, 2004.** Bioterrorism agents/diseases, <http://www.bt.cdc.gov/agent/agentlist-category.asp>.
15. **Che, Y., Li, Y., Slavik, M., Paul, D., 2000.** Rapid detection of *Salmonella* Typhimurium in chicken carcass wash water using an immunoelectrochemical method. *Journal of Food Protection* 13:8:1043-1048.
16. **Cohn, G.E., 1998.** Systems and Technologies for Clinical Diagnostics and Drug Discovery. SPIE Proceedings Vol. 3259. Bellingham, WA: The International Society for Optical Engineering.
17. **Ciureanu, M., Levadoux, W., Goldstein, S., 1997.** Electrical impedance studies on a culture of a newly discovered strain of *Streptomyces*. *Enzyme and Microbial Technology* 21:441-449.
18. **DeMarco, D. and Lim, D., 2002.** Detection of *Escherichia coli* O157:H7 in 10- and 25-gram ground beef samples with an evanescent-wave biosensor with silica and polystyrene waveguides. *Journal of Food Protection* 65:4:596-602.
19. **Doyle, M.P., Zhao, T., Meng, J., Zhao, S., 1997.** *Escherichia coli* O157:H7. In *Food Microbiology Fundamentals and Frontiers*, 171-191. M. Doyle, L. Beuchat, T. Montville eds. Washington, D.C.: American Society for Microbiology.
20. **D'Souza, S., 2001.** Microbial biosensors. *Biosensors and Bioelectronics* 16:337-353.
21. **Diniz, F., Ueta, R., Pedrosa, A., Areias, M., Pereira, V., Silva, E., da Silva, J., Ferreira, A., Gomes, Y., 2003.** Impedimetric evaluation for diagnosis of Chaga's disease: antigen-antibody interaction on metallic electrodes. *Biosensors and Bioelectronics* 19:79-84.
22. **Dutra, R., Castro, C., Azevedo, C., Vinhas, E., Malagueno, E., Melo, E., Lima-Filho, J., Kennedy, J., 2000.** Immobilization of pneumococcal polysaccharide vaccine on silicon oxide wafer for an acoustical biosensor. *Biosensors and Bioelectronics* 15:511-514.
23. **Ehret, R., Baumann, W., Brishwein, M., Schwinde, A., Stegbauer, K., Wolf, B., 1997.** Monitoring of cellular behavior by impedance measurements on interdigitated electrode structures. *Biosensors and Bioelectronics* 12:1:29-41.

- 24. FDA-Food and Drug Administration, 1998.** FDA/CFSAN Bad Bug Book. Rockville, MD USA.
- 25. FDA-Food and Drug Administration, 2001.** Bacteriological Analytical Manual. Rockville, MD USA.
- 26. Food Manufacturing Coalition, 1997.** Real Time Monitoring of Foodborne Pathogens: State-of-the-Art Report, P.O. Box 741, Great Falls, Virginia 22066.
- 27. Fratamico, P., Strobaugh, T., Medina, M., Gehring, A., 1998.** Detection of *Escherichia coli* O157:H7 using a surface plasmon resonance biosensor. *Biotechnology Techniques* 12:7:571-576.
- 28. Gau, J., Lan, E., Dunn, B., Ho, C., Woo, J., 2001.** A MEMS based amperometric detector for *E. coli* bacteria using self-assembled monolayers. *Biosensors and Bioelectronics* 16: 745-755.
- 29. Gomez, R., Bashir, R., Sarikaya, A., Ladisch, M., Sturgis, J., Robinson, T., Geng, A., Bhunia, H. Apple, 2003.** Microfluidic biochip for impedance spectroscopy of biological species. *Biomedical Microdevices* 3:201-209.
- 30. Gorschlüter, A., Sundermeier, C., Rob, B., Knoll, M., 2002.** Microparticle detector for biosensor applications. *Sensors and Actuators B*, 85:158-165.
- 31. Ghindilis, A., Atanasov, P., Wilkins, M., Wilkins, E., 1998.** Immunosensors: electrochemical sensing and other engineering approaches. *Biosensors and Bioelectronics* 13:113-131.
- 32. Gimsa, J., Muller, T., Schnelle T., Fuhr, G., 1996.** Dielectric spectroscopy of single human erythrocytes at physiological ionic strength: dispersion of the cytoplasm. *Biophysics Journal* 71:495-506.
- 33. Grimes, C., Kouzoudis, D., Ong, K., Crump, R., 1999.** Thin-film magnetoelastic microsensors for remote query biomedical monitoring. *Biomedical Microdevices* 2:1:51-60.
- 34. HHS-US Department of Health and Human Services, 2000.** HHS Fact Sheet: HHS Initiative to Reduce Foodborne Illness. March 16, 2000. Washington, D.C. Available at <http://www.hhs.gov/news/press/2000pres/20000316a.html>
- 35. Hoyle, B. 2001.** High-tech biosensor speeds bacteria detection. *ASM News* 67:9:434-435.

- 36. Jacobs, P., Varlan, A., Sansen, W., 1995.** Design optimization of planar electrolytic conductivity sensors. *Medical Biological Engineering Computation* 33:802-810.
- 37. Jung, A., Stemmler, I., Brecht, A., Gauglitz, G., 2001.** Covalent strategy for immobilization of DNA-microspots suitable for microarrays with label-free and time-resolved optical detection of hybridization. *Fresenius Journal of Analytical Chemistry* 371:128-136.
- 38. Keene, W.E., McAnulty, J.M., Hoesly, F.C., Williams, L.P., Hedberg, K., Oxman, G.L., Barrett, T.J., Pfaller, M.A., Fleming, D.W., 1994.** A swimming associated outbreak of hemorrhagic colitis caused by *Escherichia coli* O157:H7 and *Shigella sonnei*. *New England Journal of Medicine* 331:579-584.
- 39. KPL-Kirkegaard and Perry Laboratories, Inc., 1992.** Polyclonal affinity purified goat antibody to *E. coli* O157:H7 product sheet. Gaithersburg, MD USA.
- 40. Kohnen, A. 2000.** Responding to the threat of agroterrorism: specific recommendations for the USDA. BCSIA Discussion Paper 2000-29, ESDP Discussion Paper ESDP-2000-04, John F. Kennedy School of Government, Harvard University.
- 41. Koppes, L., Woldringh, C., Nanninga, N., 1978.** Size variations and correlation of different cell cycle events in slow-growing *Escherichia coli*. *Journal of Bacteriology* 134:423-433.
- 42. Kovacs, G, 1998.** Micromachined transducers sourcebook. McGraw Hill, New York, NY, USA.
- 43. Liu, Y., Ye, J., Li, Y., 2003.** Rapid detection of *Escherichia coli* O157:H7 inoculated in ground beef, chicken carcass and lettuce samples with an immunomagnetic chemiluminescence fiber optic biosensor. *Journal of Food Protection* 66:3:512-517.
- 44. Madigan, M., Martinko, J., Parker, J., 1997.** Brock Biology of Microorganisms, 8th edition. Upper Saddle River, NJ: Viacom.
- 45. Madou, M., 2002.** Fundamentals of microfabrication: the science of miniaturization, 2nd edition. CRC Press, Boca Raton, FL, USA.
- 46. Markx, G. and Davey, C., 1999.** The dielectric properties of biological cells at radiofrequencies: Applications in biotechnology. *Enzyme and Microbial Technology* 25:161-171.
- 47. Mathew, F., Alagesan, D., Alocilja, E., 2004.** Chemiluminescence detection of *Escherichia coli* in fresh produce obtained from different sources. *Luminescence*

19:4:193-198.

48. **McAdams, E., Lackermeier, A., McLaughlin, J., Macken, D., 1995.** The linear and non-linear properties of the electro-electrolyte interface. *Biosensors and Bioelectronics* 10:67-74.
49. **McClelland, R. and Pinder, A., 1994.** Detection of *Salmonella typhimurium* in dairy products with flow cytometry and monoclonal antibodies. *Applied Environmental Microbiology* 60:4255-4262.
50. **Mead, P.S., Slutsker, L., Dietz, V., McCaig, L., Bresee, J., Shapiro, Griffin, P., and Tauxe, R., 1999.** Food-related illness and death in the United States. *Emerging Infectious Diseases* 5:607-625.
51. **Meng, J., Zhao, S., Doyle, M., Kresovich, S., 1996.** Polymerase chain reaction for detection *E. coli* O157:H7. *International Journal of Food Microbiology* 32:1-2:103-113.
52. **Meeusen, C., Alocilja, E.C., Osburn, W., 2001.** "Detection of *E. coli* O157:H7 using a surface plasmon resonance biosensor," *Transactions of the ASAE*, (submitted for review 2003).
53. **MSU-Michigan State University, 1998.** Biosafety Manual. Office of Radiation, Chemical, and Biological Safety (ORCBS).
54. **Muhammad-Tahir, Z. and Alocilja, E., 2003.** A conductometric immunosensor for biosecurity. *Biosensors and Bioelectronics* 18:813-819.
55. **Muhammad-Tahir, Z and Alocilja, E., 2003.** Fabrication of a disposable biosensor for *Escherichia coli* O157:H7 detection. *IEEE Sensors Journal* 3:4:345-351.
56. **NIAID-National Institute of Allergy and Infectious Disease, 2004.** *NIAID Category A, B & C Priority Pathogens*, http://www.niaid.nih.gov/biodefense/bandc_priority.htm.
57. **Nilsson, J. and Riedel, S., 1996.** *Electric circuits*, 5th Edition. Addison-Wesley Publishing Company, Reading, MA, USA.
58. **Ong, K., Bitler, J., Grimes, C., Puckett, L., Bachas, L., 2002.** Remote query resonant-circuit sensors for monitoring of bacteria growth: application to food quality control. *Sensors* 2:219-232.
59. **Radke, S., and Alocilja, E., 2004.** Design and Fabrication of an Impedimetric Biosensor. *IEEE Sensors Journal* 4:434-440.

60. Rishpon, J., Ivnitski, D., 1997. An amperometric enzyme-channeling immunosensor. *Biosensors and Bioelectronics* 12:3:195-204.
61. Ruan, C., Wang, H., Li, Y., 2002. A bienzyme electrochemical biosensor coupled with immunomagnetic separation for rapid detection of *E. coli* O157:H7 in food samples. *Transactions of the ASAE*, 45:249-255.
62. Sanderson, M., Gay, J., Hancock, D., Gay, C., Fox, L., Besser, T., 1994. Sensitivity of bacteriologic culture for detection of *Escherichia coli* O157:H7 in bovine feces. *Journal of Clinical Microbiology* 33:10:2616-2619.
63. Seo, K.H., Brackett, R.E., Hartman, N.F., Campbell, D.P., 1999. Development of a rapid response biosensor for detection of *Salmonella* Typhimurium. *Journal of Food Protection* 62:5:431-437.
64. Sergeyeva, T., Piletskii, S.A., Rachkov, A.E., El'Skaya, A.V., 1996. Polyaniline label-based conductometric sensor for IgG detection. *Sensors and Actuators B* 34:283-288.
65. Sheppard, N., Mears, D., Guiseppi-Elie, A., 1996. Model of an immobilized enzyme conductimetric urea biosensor. *Biosensors and Bioelectronics* 11:10:967-979.
66. Shriver-Lake, L., Donner, B., Edelstein, R., Breslin, K., Bhatia, S., Ligler, F., 1997. Antibody immobilization using heterobifunctional crosslinkers. *Biosensors and Bioelectronics* 12:11:1101-1106.
67. Sperveslage, J., Stackebrandt, E., Lembke, F., Koch, C., 1996. Detection of bacterial contamination, including bacillus spores, in dry growth media and in milk by identification of their 16S RDNA by polymerase chain reaction. *Journal of Microbiolog. Methods* 26:3:219-224.
68. Suehiro, J., Hamada, R., Noutomi, D., Shutou, M., Hara, M., 2003. Selective detection of viable bacteria using dielectrophoretic impedance measurement method. *Journal of Electrostatics* 57:157-168.
69. Taylor, R. and Schultz, J., 1996. Handbook of chemical and biological sensors. IOP Publishing, London, UK.
70. Tien, H. and Ottova-Leitmannova, A., 2000. Membrane biophysics as viewed from experimental bilayer lipid membranes. Elsevier Science, Amsterdam, The Netherlands.
71. Turner, A.P.F., Karurbe, I., Wilson, G.S. (Eds.), 1987. *Biosensors Fundamentals and Applications*. Oxford University Press, Oxford, UK.

- 72. Van Gerwen, P., Laureyn, W., Laureys, W., Huyberechts, G., De Beeck, M., Baert, K., Suls, J., Sansen, W., Jacobs, P., Hermans, L., Mertens, R., 1998.** Nanoscaled interdigitated electrode arrays for biochemical sensors. *Sensors and Actuators B* 49:73-80.
- 73. Van Zant, P., 2000.** Microchip fabrication. McGraw Hill, New York, NY, USA.
- 74. Venable, R., Brooks, B., Pastor, R., 2000.** Molecular dynamics simulations of gel (L-beta-I) phase lipid bilayers in constant pressure and constant surface area ensembles. *Journal of Chemical Physics* 112:10:4822-4832.
- 75. WHO-World Health Organisation, 2002.** Terrorist threats to food: guidance for establishing and strengthening prevention and response systems. Geneva, Switzerland.
- 76. Wiegand, G., Arribas-Layton, N., Hillebrandt, H., Sackmann, E., Wagner, P., 2002.** Electrical properties of supported bilayer membranes. *Journal of Physical Chemistry B* 106:4245-4254.
- 77. Yang, L., Li, Y., Griffis, C., Johnson, M., 2004.** Interdigital microelectrode (IME) impedance sensor for the detection of viable *Salmonella* Typhimurium. *Biosensors and Bioelectronics* 19:1139-1147.

MICHIGAN STATE UNIVERSITY LIBRARIES



3 1293 02504 0506